



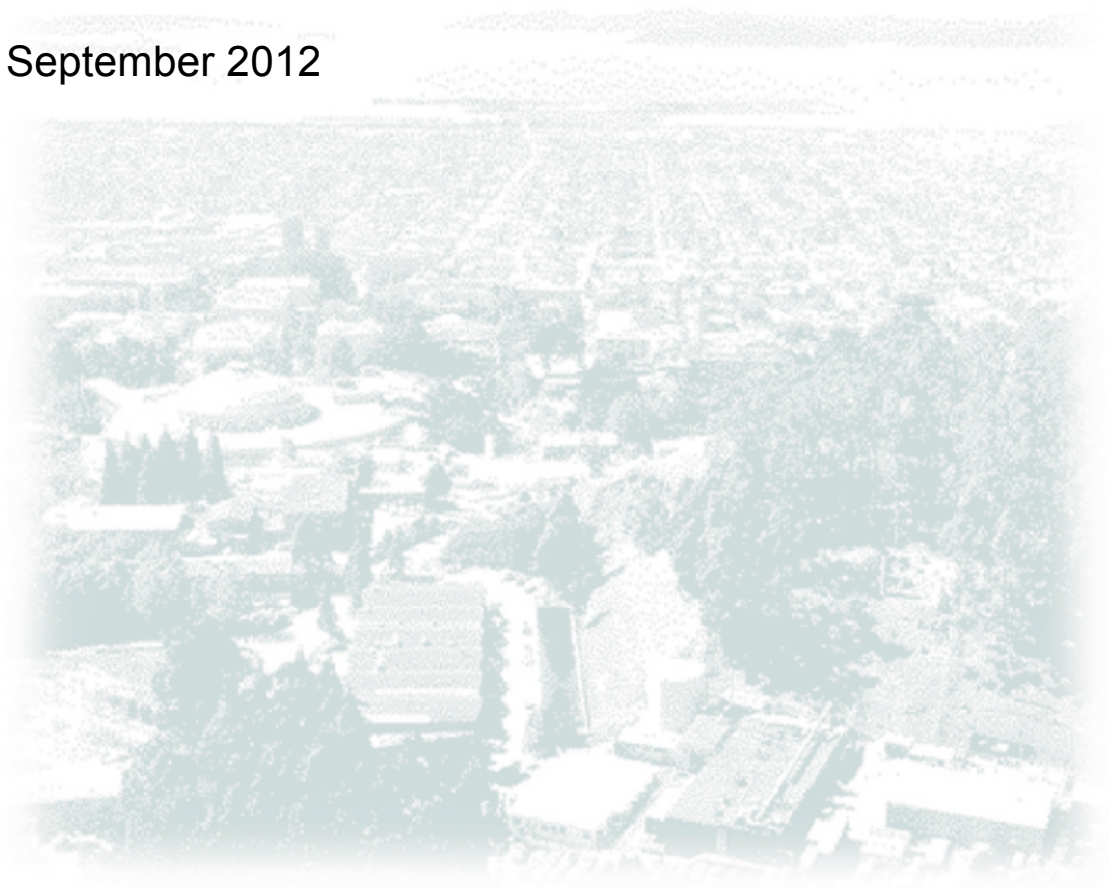
ERNEST ORLANDO LAWRENCE BERKELEY NATIONAL LABORATORY

Measurement Methods to Determine Air Leakage Between Adjacent Zones

Erin L. Hult, Darryl J. Dickerhoff, Phillip N. Price

Environmental Energy Technologies Division

September 2012



Disclaimer

This document was prepared as an account of work sponsored by the United States Government. While this document is believed to contain correct information, neither the United States Government nor any agency thereof, nor the Regents of the University of California, nor any of their employees, makes any warranty, express or implied, or assumes any legal responsibility for the accuracy, completeness, or usefulness of any information, apparatus, product, or process disclosed, or represents that its use would not infringe privately owned rights. Reference herein to any specific commercial product, process, or service by its trade name, trademark, manufacturer, or otherwise, does not necessarily constitute or imply its endorsement, recommendation, or favoring by the United States Government or any agency thereof, or the Regents of the University of California. The views and opinions of authors expressed herein do not necessarily state or reflect those of the United States Government or any agency thereof or the Regents of the University of California.

Acknowledgments

The work described in this report funded by the California Energy Commission (Energy Commission), Public Interest Energy Research (PIER) Program, under Work for Others Contract No. 500-08-061, and by the U.S. Department of Energy under Contract No. DE-AC02-05CH11231.

Table of Contents

Abstract	v
Executive Summary	1
Introduction.....	3
Background	4
Single Zone	4
Multi-zone leakage testing.....	5
Previous work	7
Study Objective:	12
Methods	13
Metrics	13
Single pressure station test method.....	15
Multiple pressure station, parameter fitting method	16
Measurement uncertainty.....	21
Simulated data.....	23
Single Zone Leakage Results.....	25
Inter-zone Leakage Results	28
Three Single Zone Method Results.....	28
Pairs of single blower door configuration tests	30
What limits the accuracy of these methods?.....	39
How do test methods fail?	40
Number of pressure stations	41
Two blower door results.....	42
Pressure balancing method	42
Summary of synthesized data analysis.....	50
Field Testing and Evaluation	51
Procedure	52
Analysis.....	53
Expected vs. Observed variability in test results.....	60
Two Blower Door Field Tests.....	61

Limitations and future work.....68

References.....68

Appendices.....72

 Appendix A: Uncertainty in pressure and flow rate measurements.....72

 Appendix B: Optimization Function.....77

 Appendix C: Bias associated with least squares fitting in a non-linear system.....79

 Appendix D: Leakage testing in Under-Floor Air Distribution Systems.....82

Abstract

Air leakage between adjacent zones of a building can lead to indoor air quality and energy efficiency concerns, however there is no existing standard for measuring inter-zonal leakage. In this study, synthesized data and field measurements are analyzed in order to explore the uncertainty associated with different methods for collecting and analyzing fan pressurization measurements to calculate inter-zone leakage. The best of the measurement and analysis methods was a method that uses two blower doors simultaneously based on the methods of Herrlin and Modera (1988) to determine the inter-zone leakage to within 16% of the inter-zone leakage flow at 4Pa, over the range of expected conditions for a house and attached garage. Methods were also identified that use a single blower door to determine the inter-zone leakage to within 30% of its value. The test configuration selected can have a large impact on the uncertainty of the results and there are testing configurations and methods that should definitely be avoided. The most rigorous calculation method identified assumes a fixed value for the pressure exponent for the interface between the two zones (rather than determining the interface pressure exponent from the measured data) and then uses an optimization routine to fit a single set of air leakage coefficients and pressure exponents for each of three wall interfaces using both pressurization and depressurization data. Multiple pressure station tests have much less uncertainty than single pressure station approaches. Analyses of field data sets confirm a similar level of variation between test methods as was expected from the analysis of synthesized data sets and confirm the selection of specific test methods to reduce experimental uncertainty.

Key Words: Residential ventilation, infiltration, leakage

Executive Summary

Inter-zone leakage can have a negative impact on indoor air quality, through chemical transport from an attached garage to a house or between units in multi-family housing. Inter-zone leakage testing methods are also used for energy efficiency objectives to identify leakage paths in multi-family homes or single-family homes with adjacent attic or basement zones. While a number of strategies have been used to determine inter-zone leakage, currently no standard exists for this measurement.

Objective: To identify the most accurate methods to obtain the inter-zone leakage using fan-pressurization testing.

Methods: Various data collection and analysis methods were compared using both synthesized data sets as well as field data. Synthesized data analysis using Monte Carlo simulations allowed for comparison of different methods under a wide range of conditions. Conditions of the testing that were varied include:

- The relative magnitude of the leakage area in different wall segments.
- The magnitude of fluctuations in the 'measured' pressure and flow rate quantities.

Aspects of the testing methodology that were explored include:

- Using single pressure station testing versus multiple pressure stations, as well as the number of pressure stations used.
- Using test configurations with different blower door placement and with windows or doors in zone interfaces either open or closed.
- Using either a single blower door or two blower doors simultaneously.
- Varying the pressure station pairs used for two blower door tests.
- Fitting leakage parameters for pressurization and depressurization conditions data jointly or separately.
- Specifying a fixed pressure exponent for the inter-zone leakage.

The synthesized data analysis to test the methods and conditions described above involved first generating the 'exact' leakage parameters for a two-zone leakage case. Then measurement noise and bias was added to the 'exact' solution to get a synthesized 'measured' dataset. Various analysis methods were then applied to the 'measured' dataset to determine how accurately the 'exact' parameters could be determined. Because certain quantities in the generation of the 'measured' dataset are randomly selected, this process was repeated for a large number of iterations to determine not only the median result, but also the result one standard deviation above and below the median result, to describe the distribution of the uncertainty resulting from different methods.

In addition to the synthesized data analysis used to compare different methods that have been developed to determine inter-zone leakage, a set of field data was collected and analyzed to determine the leakage between a single family house and an attached garage. Data for 6 homes was collected in a variety of test configurations using one or two blower doors. The field data was analyzed using the same methods as in the synthesized data analysis section.

Key Results:

The best of the measurement and analysis methods was the method developed by Herrlin and Modera (1988) which used two blower doors simultaneously to determine the inter-zone leakage to within 16%, over the range of expected conditions.

While some two blower door methods consistently obtained accurate results, many did not give accurate results. Care should be taken to follow recommended testing procedures.

The best single blower door methods included testing the two adjacent zones and the combined zone with three single zone tests by opening particular doors. The best single blower door methods were used to determine the inter-zone leakage to within 30% of its value.

Some sets of testing configurations performed very poorly and should definitely be avoided. For example, certain single blower door methods outperformed a commonly used test when the leakage area of the second zone was large ($C_{GO}/C_{HO}>1$).

The choice of analysis method can reduce uncertainty in the calculation of house-garage leakage significantly. Making the assumption that the pressure exponent for the inter-zone wall is 0.65 was better than fitting for that pressure exponent, regardless of how many pressure stations were used. Additionally, the uncertainty was reduced by fitting a single set of parameters to both pressurization and depressurization data.

The single pressure station approach could not reliably be used to determine inter-zone leakage due to uncertainty in measured quantities and the pressure exponents in the different interfaces. If the objective is simply to identify which inter-zone partitions may have high leakage flows for air-sealing purposes, using single point testing may be sufficient (Blasnik and Fitzgerald 1992).

Analysis of field datasets confirmed a similar level of variation between test methods as was expected from the analysis of synthesized data sets. Field data analysis also confirmed the assertion that some test pairs provide more consistent results than others.

Introduction

The objective of this study is to identify the best test procedure for determining the air leakage between two adjacent zones of a building using fan pressurization (blower door) tests. This study focuses on leakage between homes and attached garages because this is an important air leakage path for automotive and stored chemical emissions to impact indoor air quality (Thomas et al. 1993, Tsai and Weisel 2000, Moore and Kaluza 2002, Graham et al. 2004). The measurement procedures and analysis apply to inter-zonal leakage paths in general, including air leakage between adjacent units in multi-family housing. Air leakage across the party wall separating adjacent townhouses can be significant, leading to cigarette smoke and sound transmission between units (Love and Passmore 1985). Building mechanical codes and IAQ standards (such as ASHRAE 62.2) have requirements for limiting the air leakage of this interface using prescriptive requirements, but little is known about the effectiveness of these requirements. From the perspective of providing performance paths to compliance for standards, and understanding the effectiveness of current prescriptive requirements, a test method is required. The procedures for determining air leakage for an entire house are well established in ASTM test methods (E1827-11, E779-10) and by training and rating organizations (BPI 2010, RESNET 2011). For two adjacent spaces such as a house and an attached garage or two attached houses, standardized procedures are not well established and currently popular methods (ALA 2006, Offerman 2009) may not be the best approach, as we will show.

There are multiple strategies to determine the air leakage between two adjacent zones using one or more blower doors. For a house with an attached garage, blower door tests may be conducted with the blower door in an exterior doorway of a house, or in the doorway between the house and the garage, or in a doorway between the garage and the outdoors. Tests may be conducted with doors and windows between the house and outdoors open or closed, with the large garage door open or closed, and with the door between the house and garage open or closed. We call each combination of the blower door location and the open/closed state of windows or doors a "configuration". Different combinations of configurations can be used to determine the inter-zone leakage. Due to measurement noise, some sets of test configurations provide much more accurate results than others. Uncertainty in this type of testing stems from the combination of fluctuations in measured pressures and flows due to the effects of wind during testing and the nature of the analyses where the quantity of interest is often a small value found by determining the difference between two much larger values. Relatively small errors in the larger values translate into significant errors in their difference. In this report, data analysis methods and best test configuration choices are presented, based on analysis using synthesized data and measured field test results. Because not all residences have doors in each interface, and either 1 or 2 blower doors may be available for testing, best options are provided for a range of conditions.

The key questions addressed by this study are:

Which test configurations are the most robust?

What measurements should be taken and how should they be analyzed?

What is the uncertainty in the results?

These questions will be investigated by using simulated data where we know the correct answer, and then the analyses are applied to measurements from six houses.

Background

To determine the air leakage between two adjacent zones, fan pressurization techniques can be used to quantify the leakage flow through a wall segment at a certain pressure difference across the wall segment. The continuity equation is applied to each zone, with the flow supplied by blower door fans balanced by air leakage through the surrounding walls. The determination of inter-zone leakage builds on the protocol to determine the leakage through the envelope of a single zone. To orient the reader, a brief review of single zone air leakage testing using fan pressurization is provided here.

Single Zone

For a single zone, the flow rate through cracks and openings in the building envelope follows the form:

$$Q = CP^n \quad (1)$$

where Q is the flow rate through the blower door, the pressure difference: $P=P_{\text{indoor}}-P_{\text{outdoor}}$, C is the flow coefficient and n is the pressure exponent. If flow through a single opening is considered, the pressure exponent has a theoretical upper bound of $n=1$ in the case of fully laminar flow and a lower bound of $n=0.5$ in the case of fully turbulent flow (Sherman 1992). A building envelope will have cracks of a variety of sizes, shapes and flow regimes, and Equation (1) provides a reasonable model for flow through a network of cracks, with an example of measured data shown in Figure 1.

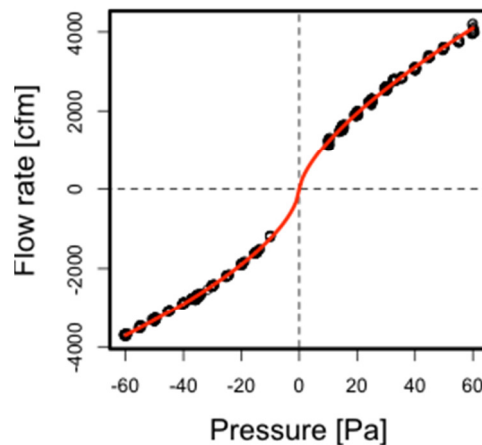


Figure 1: An example of single zone, fan pressurization data: flow rate, Q , and pressure P , taken in Home 7 (see field data section below). The curve is fitted in the form of Equation (1), with pressurization and depressurization data fitted separately.

Analysis of about 7000 single family homes in the US in LBNL's Residential Diagnostic Database suggests the pressure exponent for leakage through the envelope of the whole house is approximately normally distributed with a mean value of $n=0.646$ and a standard deviation of 0.057 (Walker et al. 2012). Previous analysis by Orme et al. (1994) also found a mean value of $n=0.65$. The coefficient, C , is equal to the flow rate when the indoor—outdoor pressure difference is $P=1\text{Pa}$. In this analysis, the uncertainty in Q_4 , the leakage flow at a reference pressure of 4 Pa, is used as a metric. While the flow

rate at 50Pa (Q_{50}) is an oft-used metric of envelope air leakage, the uncertainty in Q_{50} is not a primary metric in this analysis. Different analysis methods can accurately resolve Q_{50} but do not accurately resolve leakage flow at the indoor-outdoor pressure differences of less than 5Pa typically observed (CMHC 2004).

There are a number of methods used to determine the envelope air leakage:

Method 1: The simplest method is to pressurize (or depressurize) the house to $P=\pm 50\text{Pa}$ and measure Q_{50} . From Q_{50} , the flow rate Q_4 can be extrapolated using Equation (1) if the value of n is specified:

$$Q_4 = Q_{50} \left(\frac{4}{50} \right)^n \quad (2)$$

Method 2: Rather than collecting pressure and flow rate measurements at a single pressure, measurements can be taken at a range of pressure stations, as required in ASTM E779-10. Then pressure exponent, n , can be calculated as well as the flow coefficient C . In this analysis, Equation (1) can be written in the form:

$$\log(|Q|) = n\log(|P|) + \log(C) \quad (3)$$

where pressurization data ($p>0$) and depressurization data ($p<0$) can be fitted together to find n and C (Method 2A) or separately to find $n+$, $n-$, $C+$ and $C-$ (Method 2B). Because in practice, often only one test is performed, the case when the depressurization test is conducted and the leakage is assumed to be the same under pressurization conditions is also considered (Method 2C).

Table 1: Methods to calculate leakage through a single zone using fan pressurization.

Method	Pressure stations	Parameters fit (i.e., to get Q_4)	Notes:
Method 1	50Pa	$C+$, $C-$	$n=0.65$ assumed
Method 2A	Multiple	C , n	C and n fit to both press and depress data
Method 2B	Multiple	$C+$, $C-$, $n+$, $n-$	
Method 2C	Multiple	$C-$, $n-$	C and n fit just to depressurization data

Multi-zone leakage testing

To determine the leakage through the interface between two adjacent, control volume analysis including infiltration and fan flow is applied to the each adjacent zone and to the composite volume. The wall segment between the house and outdoors is assumed to have different leakage parameters than the wall segment between the garage and outside and the wall segment between the house and garage. There are three air leakage flow paths that are determined in the test: house to outside, garage to outside and house to garage.

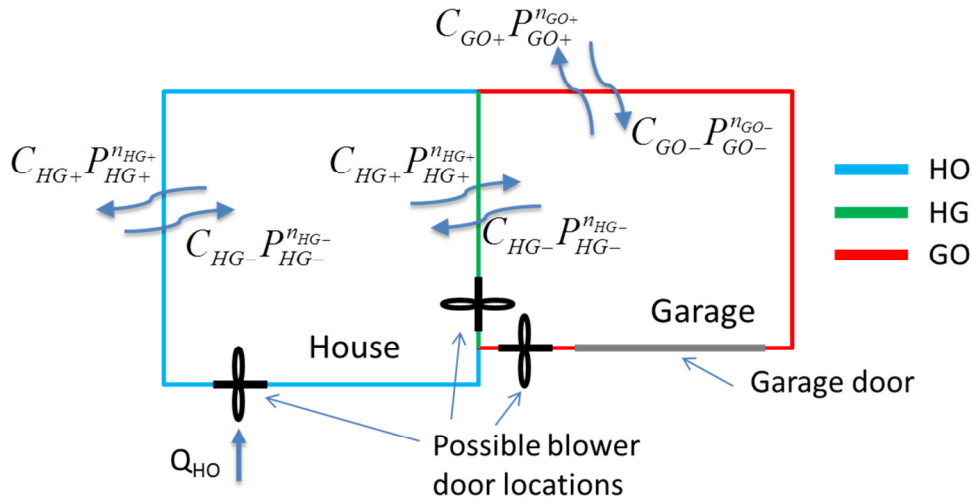


Figure 2: Schematic for testing air leakage between adjacent zones, illustrated here as a house and attached garage. Here, doorways exist in the HG and GO interface, but this may not be the case in all scenarios.

As shown in Figure 2, the air leakage through each wall segment can be modeled by the product of a coefficient, C_{ij} , and the pressure difference across the wall segment raised to a pressure exponent, $P_{ij}^{n_{ij}}$. Before discussing the challenges in measuring interfacial leakage rates and the previous methods that have been developed, it is helpful to introduce the notation used in this report. The indices refer to: HO = house to outside, HG = house to garage, and GO = garage to outside. P_{ij} is the pressure in zone i relative to the pressure in zone j . Q is the flow through the blower door in the interface noted by the index, where flow is from the second index to the first. For instance, P_{HG} is the pressure difference between the house and the garage and is positive if the house is at a higher pressure. The flow coefficient, C_{ij} , and the pressure exponent, n_{ij} , use the same indices. The + and - in the coefficient and exponent indicate pressurization and depressurization conditions.

There are many configurations in which the system in Figure 2 can be tested using fan pressurization. The blower door can be placed in any of three locations: house door, garage door and the door between the house and garage. Optionally, a second blower can be used simultaneously in a second interface. Finally, the house to outside, garage to outside and house to garage interfaces may all have doors that can be opened to minimize the pressure drop to the outside or between the zones. In this study, the configuration is specified with a three digit number, where the first digit corresponds to the house-outside interface, the second corresponds to the house-garage interface, and the third corresponds with the garage-outside interface. A 1 or 2 indicates the 1st or 2nd blower door is in this interface. Zero indicates there are large openings in this interface, such as open doors, windows or the garage door to minimize the pressure drop across this interface. 9 indicates all doors, windows and other operable vents are closed in this interface. For example, the configuration 109 indicates the blower door is between the house and the outside, the door between the house and garage is open and the doors between the garage and outside are closed. The information available from this test is equivalent to configuration 901 assuming the opening between the house and the garage is large enough not to

introduce a significant resistance ($P_{HG} = 0$). There are other pairs of equivalent configurations such as 019 and 091.

As in the single zone system, there are a number of approaches to determine the leakage flows through the inter-zone (HG) interface at the reference pressure, as well as through the HO and GO interfaces. These approaches include:

- Assuming a fixed value for pressure exponents, n_{ij} to reduce the number of parameters.
- Taking measurements at multiple pressure stations to increase the number of equations.
- Testing the system in additional configurations to increase the number of equations.

Additional concerns in the development of a testing procedure include:

- The strength of the signal relative to fluctuations in the pressure and flow rate measurements.
- The uncertainty associated with extrapolation to a reference pressure.
- The location of doorways available for blower door placement.
- The time required to complete testing (number of blower door locations, pressure stations).
- The complexity of required calculations.
- The equipment available (1 or 2 blower doors).

This study will explore the uncertainty associated with various testing and analysis methods available to determine the inter-zone leakage, in order to determine the most robust procedure.

Previous work

A number of studies have developed methods to determine leakage between adjacent zones (some focusing specifically on the house and attached garage scenario), but there is no existing standard for how to make this measurement. The American Lung Association (2006) specifications for a Health House require that the house-garage pressure coupling be below a certain level, however this metric is not considered to be robust (Offerman 2009). According to the ALA requirement, the house to outside pressure is depressurized to $P_{HO} = -50\text{Pa}$, at which time the house to garage pressure should not be less than 1Pa below this pressure ($P_{HG} < -49\text{Pa}$). The specifications note that mechanical ventilation can be used to decrease the garage pressure relative to the house pressure. Offerman (2009) performed this test in 107 new homes in California, and found that in 65% of homes, there was more than 1Pa difference between P_{HO} and P_{HG} so this standard was not met. Whether additional garage ventilation was used during the test was not reported. This pressure coupling can provide valuable information: the magnitude of P_{HG} compared to P_{GO} indicates how leaky the House-Garage interface is relative to the Garage-Outside interface. When P_{HO} is held at 50Pa , if the HG interface is very tight relative to the GO interface, then P_{HG} will approach 50Pa (Blasnik and Fitzgerald 1992). It is the absolute leakage between the House and Garage, however, that is most important to air quality if the objective is to limit air exchange between the zones, not the relative leakiness of the HG interface compared with the GO interface. Thus is not clear that this pressure coupling standard defined by the ALA Health House Guidelines can be used to identify potentially hazardous conditions. Parallels exist between inter-zone leakage methods and ASTM test methods for measuring duct leakage (E1554-07) which also include

methods to distinguish leakage to the outside from total leakage and employ more than one pressurization device.

A number of strategies have been explored to use a single blower door to test inter-zone leakage in buildings with two or more zones. One strategy to quantify air leakage between attached row houses is to assume leakage parameters are consistent for a row of homes and then while pressurizing one home, measure the pressure differential to adjacent homes (Nylund 1981, Love and Passmore 1987). This strategy is limited to symmetric arrangements of similar homes, however. The following section outlines methods that have been developed to determine inter-zone leakage.

Three Single Zone Method:

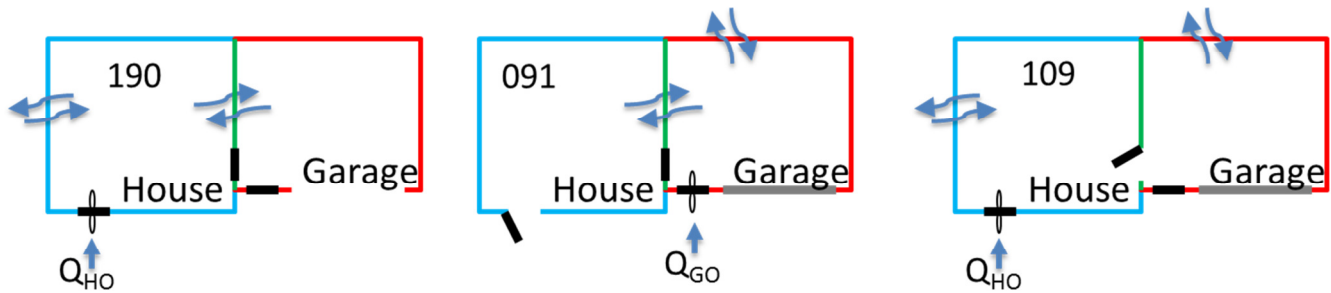


Figure 3: Three single zone method: test configurations 190, 091 and 109.

Emmerich et al. (2003) used results from 3 configurations (190, 091 and 109) to calculate inter-zone leakage, as illustrated in Figure 3. This is equivalent to performing three single zone tests, where the single zone contains the HO+HG interface, the GO+HG interface, and then the HO+GO interface:

$$Q_{HO,190} = C_{HO}P_{HO,190}^{n_{HO}} + C_{HG}P_{HG,190}^{n_{HG}} \quad (4)$$

$$Q_{GO,091} = C_{GO}P_{GO,091}^{n_{GO}} + C_{HG}P_{GO,091}^{n_{HG}} \quad (5)$$

$$Q_{HO,109} = C_{HO}P_{HO,109}^{n_{HO}} + C_{GO}P_{GO,109}^{n_{GO}} \quad (6)$$

Similarly to in the single zone analysis, this system can be solved for the coefficients C_{HO} , C_{GO} and C_{HG} using measurements at a single pressure station if the pressure exponent is assumed, or alternately the parameters C_{ij} and n_{ij} can be determined explicitly if measurements are taken at multiple pressure stations. Emmerich et al. (2003) took measurements at 4 to 7 pressure stations for 4 houses with attached garages. Using a slightly different formulation of the equations above, they determined a value of n and C for each single zone control volume using linear regression, from which the leakage flow through each interface could be determined. Emmerich et al. report uncertainty of 8% to 109% of the Effective Leakage Area (ELA) through the HG interface at 4Pa, based on error propagation at the 95% confidence interval using methods outlined in ASTM E779-99 for the single zone test. Of these 4 homes, the uncertainty in the HG leakage area was particularly high when the Garage leakage area was large (uncertainty of 67% to 109% of ELA at 4Pa).

Pairs of single blower door tests:

There are many possible strategies to use two single blower door tests to determine the leakage between two adjacent zones. Wouters et al. (1988) used a single blower door to test the leakage between two adjacent zones by altering boundary conditions to generate different configuration pairs (109 and 199, 199 and 190). An NYSERDA report goes further, outlining strategies to test inter-zone leakage for the many zone interfaces within a multi-family building (NYSERDA 1995). Blasnik and Fitzgerald (1992) provide an accessible overview to the benefits of inter-zone leakage testing to facilitate air sealing and describe several strategies to determine the leakage between adjacent zones using different single blower door tests. For determining house-garage leakage, Blasnik and Fitzgerald recommend completing a pair of tests with the blower door in the house-outside interface and the garage door closed. In the first test, the door between the house and garage is closed (199), and then in the second test the door between the house and garage is opened (109). Blasnik and Fitzgerald outlined the test at a single pressure ($P=50$ Pa), but the house zone pressure can also be increased over a range of pressure stations (Offerman 2009).

While the 109/199 pair of tests configurations is convenient because it does not require moving the blower door location, other test configuration pairs are also possible and are listed later in Table 2. Other test pairs can be analyzed in the same manner using the appropriate formulations of the control volume equations, but the test pair 199/109 is used here to illustrate how parameters are determined. The following equations govern the air leakage in the 199 test:

$$Q_{HO,199} = C_{HO}P_{HO,199}^{n_{HO}} + C_{HG}P_{HG,199}^{n_{HG}} \quad (7)$$

$$C_{GO}P_{GO,199}^{n_{GO}} = C_{HG}P_{HG,199}^{n_{HG}}, \quad (8)$$

and in the second test where the door between the house and garage is open (109):

$$Q_{HO,109} = C_{HO}P_{HO,109}^{n_{HO}} + C_{GO}P_{GO,109}^{n_{GO}}. \quad (9)$$

As in the three single zone case, this system of equations can be solved either using measurements at a single test pressure, P_{HO} , or using measurements at a range of pressure station values for P_{HO} . For single pressure station testing we need to assume a pressure exponent, n , and we can solve for the flow coefficient, C_{HG} :

$$C_{HG} = \frac{Q_{HO,199} - \left(\frac{P_{HO,199}}{P_{HO,109}}\right)^n Q_{HO,109}}{P_{HG,199}^n \left(1 - \left(\frac{P_{GO,109}}{P_{GO,199}}\right)^n\right)} \quad (10)$$

If n is not assumed, the system has 3 equations and 6 unknowns. To fit pressurization and depressurization coefficients and exponents separately, there are then 6 equations and 12 unknowns.

Test Combinations

Given that the blower door can be in each of the three interface locations (HO, HG, and GO), and the remaining interfaces can each be either open or closed, there are 21 test pair configurations that can be used to determine the house-garage air leakage (see Table 2). The 3 Single Zone Method will also be studied. Many configuration pairs produce equivalent information and we have defined four groups that show these relationships. Some test pair configurations cannot be used to determine the house-garage leakage, (such as 190/091), so test configuration pairs not included in Table 2 should definitely be avoided. While there are 21 pairs, some pairs are equivalent from an error analysis perspective, such as 3A and 3C, because the only difference is that the total leakage (HO plus GO) was measured with the blower door in the house in one case and in the garage in the other. In practice one may chose a test pair from column C or D over A or B because of the location of available doorways for mounting the blower door in a given house. Also, in practice, the HG doorway can provide significant resistance to flow in the total leakage (house plus garage) configuration so 109 or 901 should be avoided. If it is necessary to use one of these configurations and the garage is very leaky, 901 should be used rather than 109 so that the pressure in the house and garage zones is comparable.

Changing the blower door location from the house-outside interface to the garage-outside interface (or vice-versa) for the test pairs in column A leads to the test pairs in column B. In the particular case where the leakage area in the house and garage are equal, test pairs in column A and B should have the same accuracy in the calculation of the house-garage leakage flow. In practice, however, this is not often the case, and test pair 4A or 4B for example may lead to a more accurate measurement of the house-garage leakage depending on whether the leakage area of the house or garage is leakier. Thus, analysis in this study considers test configuration pairs from column A and column B.

Table 2: Table of possible pairs of blower door configurations that can be used to determine house-garage leakage.

Group\version	A	B (mirror of A)	C (equivalent to A)	D (equivalent to B)
1	109/199	991/901	901/199	991/109
2	109/919		901/919	
3	199/091	991/190	199/019	991/910
4	199/190	991/091	199/910	991/019
5	199/919	991/919		
6	199/991			
7	910/919	019/919	190/919	091/919

Two Blower Door Methods

Two blower doors can be used simultaneously rather than using a single blower door in multiple configurations to determine the leakage between house and garage zones. If two blower doors are available, three configurations can be used to determine the house-garage leakage: 192, 129, and 912, where 2 indicates the location of the second blower door. The most commonly used 2 blower door method is referred to as the ‘pressure-masking’ or ‘pressure-balancing’ method, but other techniques are also possible. In the pressure-balancing method, the goal is to isolate the leakage through a portion of a zone’s envelope by using additional fan pressurization devices to minimize the pressure difference and thus the leakage across other portions of the envelope (Shaw 1980, Reardon et al. 1987). This method can be used in multi-unit buildings to determine the leakage area of different interior partition walls, but can require a large number of blower doors (Modera et al. 1986, Finch et al. 2009). For the house-garage case, the leakage through just the HO interface can be determined by using one fan to pressurize the house and a second to hold the garage at the same pressure, or, equivalently, maintaining zero pressure across the HG interface. To determine the leakage across the HG interface, first a 199 test is run and then the same test pressures, P_{HO} , are established in the 192 configuration with the second blower door reducing the pressure difference across the HG interface to zero. Thus, the difference in the flow rate into the house zone (Q_{HO}) between the two tests is equivalent to the leakage flow through the HG interface.

This method has the advantage of being computationally very simple—once the test is run at multiple test pressures, P_{HO} , the values of C_{HG} and n_{HG} can be determined using a linear least squares fit where $x = \log(P_{HG})$ and $y = \log(Q_{HO,199} - Q_{HO,192})$. Although the single zone leakage testing standard E779 requires the flow rate to be measured to within 6%, the inaccuracy in Q as described by the standard is associated with calibration bias. Because the both flow rates in the difference: $Q_{HG} = Q_{HO,199} - Q_{HO,192}$ are measured with the same blower door (#1), calibration bias will have minimal impact on the uncertainty in the house-garage leakage Q_{HG} . However, there will still be precision and accuracy errors. The pressure-balancing approach was used to test House-garage leakage in a survey of Canadian homes (CMHC 2004).

In practice, the pressure-balancing method can require a lot of equipment and it can be difficult to match pressures between zones exactly. Feustel (1990) compared the pressure-balancing method to an alternate technique to use two blower doors to isolate the leakage through an interior partition wall in a multi-zone building without matching pressures exactly in adjacent zone, and the alternate method seemed to provide more consistent results than the pressure-balancing. Herrlin and Modera (1988) presented a method to determine inter-zone leakage by holding the pressure of one zone at 50Pa while varying the pressure across the interface between the zones from 0 to 50Pa using a second blower door to control the pressure of the second zone. This leads to the mass balance equation for the first zone:

$$Q = C_1 + C_{HG} P_{HG}^{n_{HG}} \quad (11)$$

Where $Q = Q_{HO}$ in the 192 configuration. C_1 is a constant since P_{HO} is held constant for this test method. Thus, the constants C_1 , C_{HG} and n_{HG} can be fit to the measured data Q and P_{HG} . While it is possible to complete this test in the 129 configuration as well where $Q = Q_{HO} + Q_{HG}$, in practice this requires very high flow rates. This method does not determine the leakage parameters for the HO and GO interfaces, only

the inter-zone leakage parameters (HG). For the case when a garage zone is intentionally vented to the outdoors, the garage leakage is not necessarily of interest. Herrlin and Modera found using simulations that using this method, only 10% of the uncertainty was related to wind fluctuations but uncertainty in the measured flow rates and pressures lead to 40% uncertainty in the leakage quantities. Since the Herrlin and Modera study, the uncertainty in fan pressurization devices has been reduced substantially. This method was tested in the current study and was found to determine the inter-zone leakage to within 20% under a range of conditions.

Proskiw and Parekh (2001) proposed a perturbation method similar to the pressure-balancing approach, but which does not require the inter-zone pressure to be exactly equalized. The method proposed is to place the blower door in a doorway in the HG interface, and then use two test configurations at several test pressures to determine the flow coefficient and pressure exponent for the interface. Specifically, the 919 configuration is tested and the flow into one zone, Q_{HO} , is determined. Then the leakiness of the GO interface is altered (by opening windows or using an additional fan or blower door), and then the 910 configuration or 912 configuration is tested. In the Master's thesis of Proskiw (2007), laboratory experiments are used to explore the accuracy of this test method in a controlled environment (i.e., no wind), and it is found that the interface leakage can be determined to within 2% when a blower door is used to alter the pressure in the second zone using a 192 test configuration, but detailed information is not provided on the accuracy of this method in field settings. While the testing method described by Proskiw and Parekh (2001) has promise, their calculation technique used data from only one or two pressure stations to determine the inter-zone leakage. This method may be more accurate if data from a range of pressure stations are used to determine the parameters in an over-determined system of equations. These methods will be discussed below with other possible other possible configurations.

Study Objective:

As discussed in *Previous Work*, there are many possible approaches to determining the air leakage between two adjacent zones. The objective of this study was to determine the simplest test that will reliably deliver accurate results. This study used simulations to compare different test methods including:

- Single pressure station tests (i.e., Q50 test).

- Multiple pressure station tests, including pairs of single blower door tests, three single zone tests, and using two blower doors simultaneously.

- Pressurization and/or depressurization tests.

Sensitivity to conditions was explored including:

- Fluctuations in pressure and flow rate measurements

- The leakage of the inter-zone interface relative to the house leakage: C_{HG}/C_{HO}

- The relative leakage in the two zones: C_{GO}/C_{HO} .

The analysis used to determine the leakage flow from the data collected was also considered in this study. Specifically, analysis methods included:

Fitting all C_{ij} and n_{ij} values for pressurization and depressurization (12 parameter fitting method).

Fitting all C_{ij} and n_{ij} except for n_{HG+} and n_{HG-} (10 parameter method).

Fitting all C_{ij} and n_{ij} but assuming parameters for pressurization and depressurization are equal (6 parameter method).

Fitting C_{ij} and n_{ij} except for n_{HG} and assuming pressurization and depressurization parameters are equal (5 parameter method).

Fitting C_{ij} but assuming a fixed n (3 parameter method).

First, the methods used to generate and analyze the synthesized data are presented. A discussion of the results of the synthesized data analysis follows. Then, the results are presented from the application of the analysis to field data collected in a variety of configurations in order to examine the consistency of different techniques in practice. Finally, conclusions from the study are presented along with some discussion on how to select a testing method.

Methods

To assess the best measurement and analysis methods to determine inter-zone leakage, synthesized datasets were generated, varying parameters over the range of conditions expected in practice. First, 'exact' datasets of pressure and flow rate measurements were generated from a specified set of envelope leakage parameters. Then, noise was added to the exact measurements to replicate measured data. The leakage parameters C_{ij} and n_{ij} were calculated from these noisy datasets and compared with the exact values specified initially to provide an estimate of the uncertainty associated with the measurement and analysis method. Using Monte-Carlo techniques, this process was then repeated to generate hundreds of iterations to determine the distribution of results, given that some input parameters were selected from probability distributions. This synthesized data approach allowed different measurement and analysis strategies to be compared for the same conditions. Field data were also collected using a range of test configurations and the analysis of this set of field tests provided additional insight into the uncertainty associated with different methods. The methods used for field data collection are presented later in the *Field Testing and Evaluation* section.

The analysis procedure for the single pressure station test method and the multiple pressure station (MPS) parameter fitting methods are described below. First, the parameter fitting processes are described for single pressure station data and for multiple pressure station data. For multiple pressure station data, several options are presented (12, 10, 6, and 5 parameter models), depending on whether pressurization and depressurization data are fit separately and whether a pressure exponent, n_{HG} , is assumed in the modeling of the inter-zone leakage. The process for specifying the 'exact' data and for synthesizing 'measured' data is then described.

Metrics

Many metrics are used to quantify air leakage through a building envelope (see Sherman and Chan (2003) for an in depth discussion on air leakage metrics). Although contractors may prefer to report the leakage flow rate at a high pressure where the pressure induced by the blower door fan is large relative

to any fluctuations (e.g., Q at 50Pa), the typical pressure difference across the envelope under normal operating conditions is likely to be much lower: perhaps on the order of 0 to 2Pa. As discussed in the *Background* section above, the leakage flow rate in the operating range is typically determined by measuring at high pressures or over a range of pressures and then extrapolating to lower pressures. Here, the metric used to assess the accuracy of different measurement and analysis methods is the inter-zone air leakage flow rate at a reference pressure of 4Pa. This reference flow across the HG interface will be referred to as Q_{HG4} . Although typical pressure differences between two zones may be less than 4Pa, this reference pressure is used to be consistent with ASTM E779-10.

For a given set of conditions, a number of iterations were simulated and the uncertainty in Q_{HG4} was calculated by comparing the leakage flow calculated from the parameters fit to the data against the original 'exact' parameters from which the synthesized 'measured' quantities were generated. For each iteration, the difference between the 'exact' and measured values of Q_{HG4} was computed and then scaled by either itself or the total house leakage:

$$Q_{HT4} = Q_{HG4.X} + Q_{HO4.X} \quad (12)$$

$$Q_{GT4} = Q_{HG4.X} + Q_{GO4.X} \quad (13)$$

where $Q_{HG4.X}$, $Q_{HO4.X}$ and $Q_{GO4.X}$ are the exact leakage quantities through the HG, HO and GO interfaces, respectively. Because the leakage area of the HG interface is often small relative to the total house leakage, sometimes it was helpful to interpret the uncertainty in the HG leakage as a fraction of the total house leakage. However, the uncertainty in a number of methods turned out to be a constant fraction of the inter-zonal leakage itself, so both quantities were provided. The accuracy with which different tests could determine the total house leakage and the total garage leakage (the garage leakage is of less interest typically) was also of interest, so these quantities are also presented in the *Results* Section. The uncertainty metrics are presented in Table 3.

Table 3: Uncertainty metrics for inter-zone air leakage.

Description	Notation in the text	Calculation method
Uncertainty in the leakage through the HG interface scaled by itself	$u(Q_{HG4})/Q_{HG4}$	median value from all iterations of $((Q_{HG4+} - Q_{HG4.X+})^2 + (Q_{HG4-} - Q_{HG4.X-})^2)^{1/2}/Q_{HG4.X}$
Uncertainty in the leakage through the HG interface scaled by the total house leakage	$u(Q_{HG4})/Q_{HT4}$	median value from all iterations of $((Q_{HG4+} - Q_{HG4.X+})^2 + (Q_{HG4-} - Q_{HG4.X-})^2)^{1/2}/Q_{HT4}$
Uncertainty in the house to outside (HO) leakage scaled by the total house leakage (HO +HG)	$u(Q_{HO4})/Q_{HT4}$	median value from all iterations of $((Q_{HO4+} - Q_{HO4.X+})^2 + (Q_{HO4-} - Q_{HO4.X-})^2)^{1/2}/Q_{HT4}$
Uncertainty in the garage to outside (GO) leakage scaled by the total garage leakage (GO+HG)	$u(Q_{GO4})/Q_{GT4}$	median value from all iterations of $((Q_{GO4+} - Q_{GO4.X+})^2 + (Q_{GO4-} - Q_{GO4.X-})^2)^{1/2}/Q_{GT4}$

Single pressure station test method

For each set of test data, if a pressure exponent, n , is assumed, the system of mass balance equations as illustrated earlier for test configuration pair 199/190 can be solved to determine C_{HG} as well as C_{HO} and C_{GO} . The test data can be comprised of tests at a single pressure in multiple configurations using a single blower door or from a single configuration using two blower doors to vary the two zone pressures. In this study, the system of linear equations was solved in R, a free statistical computing program. For test pairs where 4 system equations were available to solve for the 3 flow coefficients, least-squares regression was used to determine the parameters.

The Single Pressure Station test method was designed to be fast to complete and straightforward to calculate the result. Typically, the coefficients, C_{HO} , C_{HG} , and C_{GO} are not calculated separately for pressurization and depressurization conditions in this analysis. A contractor may only perform a single test (either pressurization or depressurization). For test pairs 109/199 and 199/190, it is straightforward to calculate C^+ and C^- separately, because the governing equations are decoupled (i.e., the pressure drop across all interface sections has the same sign). For the remaining test pairs, the sign of one pressure drop is different from the sign of the other two. While it is possible to solve the system of equations for C^+ and C^- for each of HO, HG and GO, provided a test is completed at a positive and negative test pressure for each of the test configurations, it requires solving a system of 6 (or 8) equations for the 6 variables. In this study, it was assumed that in a single pressure station test to determine the interfacial leakage, only one test was performed (pressurization or depressurization but

not both). In calculation of the uncertainty resulting from this method, the leakage flow at 4Pa was extrapolated from the value of C_{HG} calculated from the 'measured' data and compared with the exact values Q_{HG4+} and Q_{HG4-} .

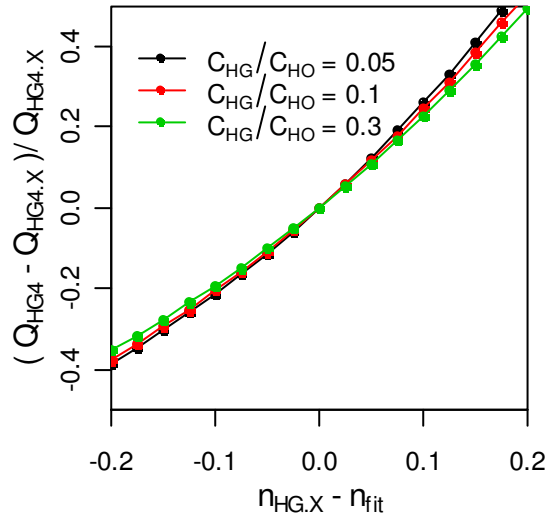


Figure 4: Error in Q_{HG4} caused by offset in choice of pressure exponent n_{HG} when there are no other sources of error. If the exact pressure exponent is higher or lower than the assumed pressure exponent, n_{fit} , this increases the error in the interface leakage, Q_{HG4} . $C_{GO}/C_{HO}=0.7$, but these results are not sensitive to this parameter.

Assuming a fixed value for n_{HG} can stabilize the process of parameter fitting, but it is important to consider the error introduced by this assumption. Assuming the leakage through the HG interface behaves according to the form $Q=CP^n$, then for a given interface, there is an exact pressure exponent that relates the pressure and flow rate, $n_{HG,X}$. It is expected that the pressure exponent for the interface between zones will vary between homes, depending on the shape and size of the leaks present. The error introduced by assuming a value for n_{fit} that differed from the exact value is shown in Figure 4. When the value of $n_{HG,X}$ fell below or above the value of n_{fit} , the error in the leakage, Q_{HG4} increased for all test configuration pairs. In this example, only n_{HG} was varied from the n_{fit} . Figure 4 indicates that assuming a pressure exponent n_{HG} that was off by 0.05 led to error in Q_{HG4} of 15-20%, which was approximately 0.5- 1% of Q_{HO4} . This was the error introduced from the model choice only and did not include the measurement error. To reduce the uncertainty introduced by assuming a pressure exponent, the pressure exponent can be fitted directly by collecting measurements at multiple pressure stations as described in the next section.

Multiple pressure station, parameter fitting method

Alternatively, pressure and flow rate measurements can be taken at a range of pressures and then the parameters, C_{HO} , C_{HG} , C_{GO} , n_{HO} , n_{HG} , and n_{GO} can be fit for both pressurization and depressurization. The 12 parameters in total from the system of mass balance equations (see Equations (7), (8) and (9) for example) can be found using optimization. In this study, the parameters were optimized by minimizing the expression:

$$\sum_{i=1}^N (Q_{m,i} - Q_{c,i})^2 \quad (14)$$

for N observations where Q_m is the measured flow rate through the blower door, and Q_c is the flow rate calculated from each mass balance equation for the configuration specified. Thus, the difference between the measured and calculated flow rate was minimized. In this analysis, the optimization was done using the optimization routine 'nlminb' within the open source statistical analysis package, R. This routine determined the value for the parameters that lead to the minimum value of Expression (14), using a quasi-Newton solver with box constraints on each parameter. The flow coefficients, C_{ij} , were constrained to be between 0.01 and 4000, and pressure exponents, n_{ij} , were constrained to be between 0.4 and 1.2. While the physical limits of the pressure exponents are 0.5 and 1, the statistical distributions of parameters assumed in this study led to some 'exact' values of the pressure exponent falling slightly out of this range. Additionally, whether a parameter was fit to the boundary constraint value was used as an indicator of whether or not a good fit was found to the data, so it was helpful to set the boundary constraints beyond the range of the 'exact' values expected. Appendix B contains additional information on the fitting algorithm. While the fitting algorithm was much faster when run using R, a worksheet was also developed to run the same optimization in Excel using the solver tool to fit the specified parameters. The worksheet was not validated as extensively as the R methods, but did replicate results from the R methods in limited testing.

For example, consider fitting all 12 parameters n_{ij} and C_{ij} in configurations 109 and 199, as described by the system in Equations (7), (8), and (9). First, an initial guess is made for the 12 parameters, which is used to calculate Q_c for each of the 6 pressures tested (at both pressurization and depressurization) leading to 18 values of Q_c . The 12 parameters are then varied to minimize the sum of the differences between the measured flow rates, Q_m , at each pressure, and the calculated flow rate Q_c for the current parameter values. Through this iterative method, the values of the parameters C_{ij} and n_{ij} are determined to minimize the difference between the control volume model and the observations.

Within the analysis of multiple pressure station data, two options were explored:

- 1) Whether n_{HG} was fitted or specified
- 2) Whether pressurization and depressurization data were fit separately or jointly.

This led to analysis methods where all 12 parameters were fit, 10 parameters were fit (and n_{HG} was specified), 6 parameters were fit (pressurization and depressurization data were fit jointly) 5 parameters were fit (pressurization and depressurization data fit jointly and n_{HG} specified). These methods are summarized Table 4, along with the 3 parameter fitting method from single pressure station data. The final method listed in Table 4 is the method proposed by Herrlin & Modera (1988), which uses two blower doors simultaneously to fit only the inter-zone leakage parameters, not the HO or GO parameters.

Table 4: Multiple pressure station methods for inter-zone leakage testing.

	12 Parameter	10 Parameter	6 Parameter	5 Parameter	3 Parameter	Herrlin & Modera (1988)		
C _{HO+}	Fitted	Fitted	C _{HO} fitted to + & -	C _{HO} fitted to +	C _{HO} fitted to +	Not fitted		
C _{HO-}	Fitted	Fitted		& -	or -			
C _{HG+}	Fitted	Fitted	C _{HG} fitted to + & -	C _{HG} fitted to +	C _{HG} fitted to +	C _{HG} fitted to + & -		
C _{HG-}	Fitted	Fitted		& -	or -			
C _{GO+}	Fitted	Fitted	C _{GO} fitted to + & -	C _{GO} fitted to +	C _{GO} fitted to +	Not fitted		
C _{GO-}	Fitted	Fitted		& -	or -			
n _{HO+}	Fitted	Fitted	n _{HO} fitted to + & -	n _{HO} fitted to +	n = 0.65	Not fitted		
n _{HO-}	Fitted	Fitted		& -			& -	
n _{HG+}	Fitted	n _{HG+} = 0.65	n _{HG} fitted to + & -	n _{HG} = 0.65		n = 0.65	n _{HG} fitted to + & -	
n _{HG-}	Fitted	n _{HG-} = 0.65						& -
n _{GO+}	Fitted	Fitted	n _{GO} fitted to + & -	n _{GO} fitted to +			n = 0.65	Not fitted
n _{GO-}	Fitted	Fitted		& -				

Repeated field observations suggest that envelope leakage test results are often different under pressurization and depressurization conditions. Asymmetric leakage can be caused by valving of moveable components or by asymmetric geometries in cracks and holes. Any door, window, hatch or damper can exhibit this effect by opening when the pressure difference across is in one direction and closing when it is in the other direction. Observations suggest that in US climates, both pressurization and depressurization across the house-garage interface may occur (CMHC 2001). Thus, testing both pressurization and depressurization conditions can characterize the system in more detail. One advantage to fitting pressurization and depressurization data jointly is that the impact of certain sources of uncertainty, including a consistent pressure offset across a wall segment, can be reduced substantially by averaging pressurization and depressurization test results.

Pressure exponents reported for the testing of leakage through the envelope of single family houses were approximately normally distributed: analysis of approximately 7000 single family homes in the LBNL Residential Diagnostics Database led to a mean pressure exponent $n_{\text{mean}}=0.646$ with a standard deviation of 0.057 (Walker et al., 2012), consistent with previous analysis of smaller datasets where $n_{\text{mean}}=0.66$ with a standard deviation of about 0.05 (Orme et al. 1994). While it has been suggested that some of the observed variability in pressure exponents at different houses is due to wind fluctuations during testing, the data of Walker et al. (2012) suggest there is significant variability in the pressure exponent between houses, regardless of wind conditions. Walker et al. found that when low wind tests

were compared to tests at all wind speeds at a set test houses, the variability in the pressure exponent was lower for the low wind tests but not much lower: for low speed tests, $n=0.697\pm0.115$ and for all tests $n=0.723\pm0.141$. The variability resulting from multiple tests on the same house in the same configuration was also of interest in this analysis, but no source was found for this information.

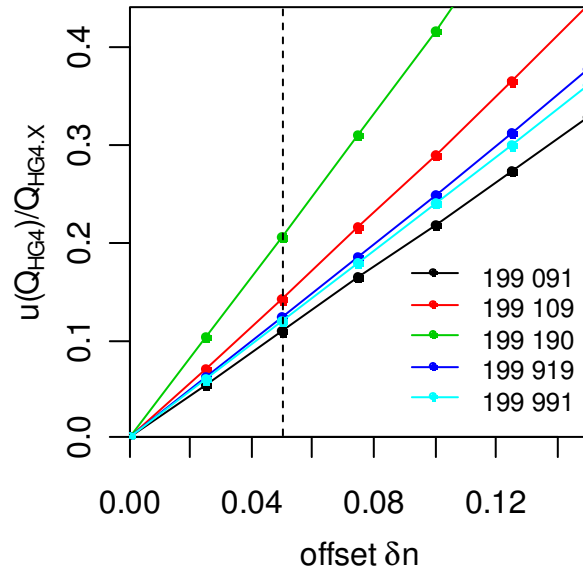


Figure 5: Baseline error in Q_{HG4} introduced by varying the difference between the exact pressure exponent n_{HG} and the fitted pressure exponent ($n_{fit}=0.65$). The error indicated is the mean of the uncertainty resulting from using a positive and negative offset of magnitude δn . No other sources of error were included. The dashed line indicates the value assumed in this study: $\delta n=0.05$. The 5 parameter fitting method was used.

Some of the fitting methods (5 parameter, 10 parameter) involved assuming a fixed pressure exponent, n_{HG} rather than fitting this parameter from the data. In order to quantify the impact of this assumption, we had to consider the distribution of values of n_{HG} . Because it is unlikely that the mean pressure exponent for the HO, HG or GO interface in a set of homes will be known precisely, in this analysis it was assumed that $n_{fit} = 0.65$, and that for each interface HO, HG and GO, $n_{exact} = 0.65 + \epsilon_n + \delta n$. Here, ϵ_n was a random perturbation with zero mean and standard deviation of 0.05, and $\delta n = \pm 0.05$ was an offset with randomly selected sign, chosen conservatively to include the effect of the uncertainty in the actual distribution of n_{HO} , n_{HG} , and n_{GO} . The error introduced by including an offset δn in n_{HG} established the baseline uncertainty for the 5 and 10 parameter fitting methods beneath which the total uncertainty in Q_{HG4} cannot be reduced. Figure 5 illustrates the magnitude of this baseline uncertainty based on the value of δn that was included in the synthesized data. For most test configuration pairs, the inclusion of $\delta n=0.05$ led to a baseline uncertainty of 12-15% of Q_{HG4} . There was increased uncertainty for cases where the blower door remained in one location (e.g., 199/190, 199/109).

The impact on the uncertainty resulting from fitting pressurization and depressurization conditions jointly depended on how different the pressurization and depressurization parameters were. From previous analysis of the Residential Diagnostics Database (Sherman and Dickerhoff 1998), when both pressurization and depressurization tests were performed on 280 single family homes, the normalized leakage was 2% higher for pressurization tests with a standard deviation of 11 percentage points.

Pressurization and Depressurization tests taken as part of the 2010 California New Home Energy Survey also indicated that leakage flows at 50Pa were within 5% (Proctor et al. 2011). From the field data collected as part of this study, fitted values of n and C for pressurization and depressurization conditions were analyzed to determine the extent to which this difference between the leakage during pressurization and depressurization was caused by changes in n or C . Analysis of the field data suggested that the $2\% \pm 11\%$ difference between pressurization and depressurization leakage area was caused by $(n_{\text{press}} - n_{\text{depress}}) / n_{\text{mean}} = -3\% \pm 6\%$, and $(C_{\text{press}} - C_{\text{depress}}) / C_{\text{mean}} = 5\% \pm 10\%$ (these offsets had opposing effects on the leakage flow Q). Some of the observed difference between pressurization and depressurization was likely due to measurement uncertainty in the test, but for this study these distributions were used. This allowed the accuracy of methods fitting pressurization and depressurization parameters separately to be compared with those that calculated parameters jointly.

Table 5: ‘Exact’ parameters specified

Parameter	‘exact’ value	Min (or 5%)	Max (or 95%)
$C_{\text{HO}+}$	200	NA	NA
$C_{\text{HO}-}$	$C_{\text{HO}+} + \epsilon_C$, $\epsilon_C = N(\mu = -0.05C_{\text{HO}+}, \sigma^2 = (0.1C_{\text{HO}+})^2)$	$0.75C_{\text{HO}+}$	$1.15C_{\text{HO}+}$
$C_{\text{HG}+}$	$(C_{\text{HG}}/C_{\text{HO}})C_{\text{HO}+}$	4	60
$C_{\text{HG}-}$	$C_{\text{HG}+} + \epsilon_C$, $\epsilon_C = N(\mu = -0.05C_{\text{HG}+}, \sigma^2 = (0.1C_{\text{HG}+})^2)$	$0.75C_{\text{HG}+}$	$1.15C_{\text{HG}+}$
$C_{\text{GO}+}$	$(C_{\text{GO}}/C_{\text{HO}})C_{\text{HO}+}$	40	1600
$C_{\text{GO}-}$	$C_{\text{GO}+} + \epsilon_C$, $\epsilon_C = N(\mu = -0.05C_{\text{GO}+}, \sigma^2 = (0.1C_{\text{GO}+})^2)$	$0.75C_{\text{GO}+}$	$1.15C_{\text{GO}+}$
$n_{\text{HO}+}$	$0.65 + \epsilon_n + \delta n$, $\epsilon_n = N(\mu = 0, \sigma^2 = 0.05^2)$, $\delta n = \pm 0.05$	0.54	0.76
$n_{\text{HO}-}$	$n_{\text{HO}+} + \epsilon_{n2}$, $\epsilon_{n2} = N(\mu = 0.03n_{\text{mean}}, \sigma^2 = (0.06 n_{\text{mean}})^2)$	0.54	0.80
$n_{\text{HG}+}$	$0.65 + \epsilon_n + \delta n$, $\epsilon_n = N(\mu = 0, \sigma^2 = 0.05^2)$, $\delta n = \pm 0.05$	0.54	0.76
$n_{\text{HG}-}$	$n_{\text{HG}+} + \epsilon_{n2}$, $\epsilon_{n2} = N(\mu = 0.03n_{\text{mean}}, \sigma^2 = (0.06 n_{\text{mean}})^2)$	0.54	0.80
$n_{\text{GO}+}$	$0.65 + \epsilon_n + \delta n$, $\epsilon_n = N(\mu = 0, \sigma^2 = 0.05^2)$, $\delta n = \pm 0.05$	0.54	0.76
$n_{\text{GO}-}$	$n_{\text{GO}+} + \epsilon_{n2}$, $\epsilon_{n2} = N(\mu = 0.03n_{\text{mean}}, \sigma^2 = (0.06 n_{\text{mean}})^2)$	0.54	0.80

The calculation methods used to generate the ‘exact’ parameters used in the synthesized data analysis are shown in Table 5. In Figure 6, the distributions of values generated for pressure exponents n_{ij+} and n_{ij-} are shown. Each synthesized ‘measured’ dataset started from a set of parameters determined as specified in Table 5, and then simulated fluctuations and bias were added to generate the ‘measured’ data points P_{ij} and Q_{ij} . The fluctuations and bias are discussed in the following subsection.

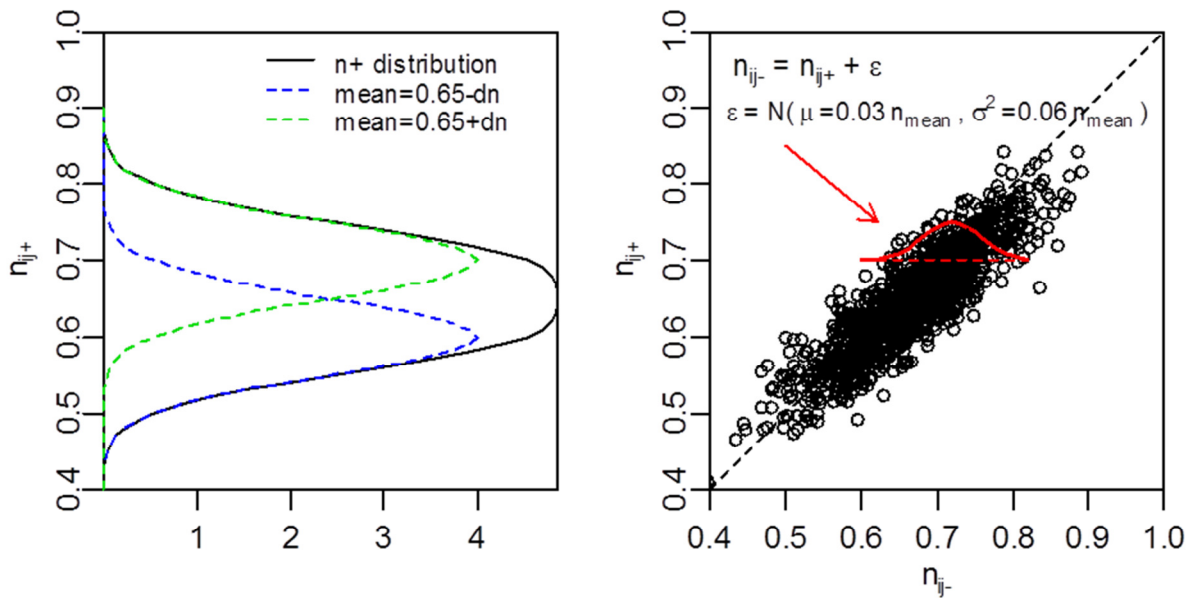


Figure 6: Distribution of pressure exponents used in the generation of synthesized data (left). The right plot shows the distribution of n_{ij-} given a particular value of n_{ij+} (inset red solid line), along with example pairs of the ‘exact’ values of n_{ij+} and n_{ij-} generated in 1000 iterations. The equations for n_{ij+} and n_{ij-} are in Table 5.

While a number of factors were included in the generation of the ‘exact’ parameters including the variation in observed pressure exponents and the difference between pressurization and depressurization conditions, additional modelization errors can exist. For example, we assumed that the leakage flow is related to the pressure in the form: $Q=CP^n$, but in practice this is not always the case. A classic problem is that some leaks change geometry with pressure difference and airflow so that C and n are not independent of pressure and flow. This can lead to measured exponents <0.5 or > 1 , or to curves where the best fit exponent depends on the pressure range.

Another factor that was not considered in the synthesized data analysis is the impact of pressure offsets. Typically, when fan pressurization testing is done, the mean pressure offset for each pressure (P_{HO} , P_{HG} , P_{GO}) is measured before (and sometimes after) a test is completed, and the mean offset is subtracted from each measured pressure. Here, it was assumed there was no pressure offset in the ‘exact’ or ‘measured’ data. If there were a pressure offset in measured data that had not been removed, this would likely increase the uncertainty of all methods, but some methods may be more sensitive to such offsets.

Measurement uncertainty

Measurement uncertainty estimates were made in two ways:

1. An analysis based on synthesized data to systematically adjust the relevant parameters over a range to represent their uncertainty, and

2. Comparison of the results of different field test approaches covering most of the combinations in Table 2 together with multi-blower door approaches.

There are a number of ways in which uncertainty can be introduced into the calculation of the air leakage between two adjacent zones. There is some uncertainty in the measurement values themselves, but perhaps more importantly is the degree to which the measurements taken represent the quantities of interest in the problem. It is the pressure difference across a crack that drives air leakage, but this may not be the pressure difference that is measured. Wind and temperature variation can cause fluctuations in the local pressure that can vary across the building envelope. If the outdoor pressure is measured at a single location, how well does the measured indoor-outdoor pressure difference represent the actual indoor-outdoor pressure difference across each crack? Similarly, when using a blower door to calculate the flow through the door, how well does the pressure difference measured between the blower door and a reference location represent the actual pressure difference across the blower door's flow sensing element? First, uncertainty in the measurement devices themselves will be addressed, followed by the uncertainty associated with what these measurements represent.

In a blower door test, the flow rate is calculated from the measured pressure drop across the flow sensing element in the blower door (typically one or more orifices or nozzles). Standard E779 requires the flow rate measurements to be accurate to within 6% of the mean reading. Although the blower doors from The Energy Conservatory used in this study have a stated accuracy of 3%, thus (in the absence of other sources of uncertainty) we assume that the calibration error in the flow rate calculated from blower door data is no larger than 3%. For example, if the two blower door flows are reported as 50 and 100cfm, these flows are assumed to be 50 ± 1.5 cfm and 100 ± 3 cfm. However if Q_1 and Q_2 are measured with the same device, the uncertainty in the ratio of $Q_1/Q_2 = 50/100$ will be less than 3%, as in this case the calibration errors bias each measurement similarly. According to ASTM E779, the pressure measurement device must be accurate to 2.5Pa for testing the total envelope leakage using the fan pressurization method. However the DG700 digital manometer used in this study was much more accurate, with an uncertainty of 1% of the pressure measurement or 0.2 Pa, whichever is greater.

Field data were analyzed to determine the typical range of the magnitude of fluctuations in the measurements of pressure and flow rate. Pressure and flow rate data from fan pressurization tests conducted at the field sites discussed later in this report were fitted to a curve in the form: $Q=CP^n$, and the deviation from the fitted curve was used to estimate the expected fluctuation in fitted flow coefficient and pressure exponent. Further details of this analysis are provided in Appendix A. From this analysis, fluctuations in the measured pressure were typically between 0.25Pa for the most calm conditions observed and 1.2Pa for the windiest conditions. From the field data in this study, it was estimated that 2/3 of the observed variability was due to fluctuations in P and 1/3 to fluctuations in Q, so the standard deviation of flow measurements, $u(Q)$, was approximately 1/2 of the standard deviation of pressure measurements, $u(P)$. However, it turned out that the overall uncertainty in the inter-zone leakage was not very sensitive to the magnitude of $u(Q)$, as shown in Appendix A, Figure 44. Repeated measurements of P and Q may reduce the uncertainty, provided the interval between measurements is long relative to the correlation time scale of the wind. The pressure data collected in this study suggests that measurements every 15s could be considered independent. However, the longer the full test takes to complete, the more likely it is that there will be longer term (rather than fluctuation around a mean) changes in the wind speed and/or direction. Because a change in the mean wind speed can introduce

additional uncertainty, increasing sampling time is unlikely to significantly reduce the overall uncertainty.

The same uncertainty was assumed for each pressure differential regardless of the interface. I.e., it was assumed that fluctuations in P_{HO} , P_{HG} and P_{GO} were of the same magnitude but uncorrelated. Although the pressure difference P_{HG} was not exposed to the outdoors and so one might expect it to be more sheltered from the effects of wind, the field measurements suggested this was not always true. Figure 41 in Appendix A shows how the pressure in the house and garage zones sometimes varied together and sometimes did not. Thus, it was conservatively assumed that the magnitude of noise was the same for P_{HO} and P_{HG} . The impact of using correlated versus uncorrelated fluctuations was not explored in this study.

Simulated data

Synthesizing datasets can be an inexpensive and flexible alternative to taking field measurements, but in order for the results to be meaningful, the synthesized data must have a grounding in reality. This includes choosing appropriate 'exact' values as well as including reasonable quantities of noise and bias. The range of leakage values simulated in this study reflected observations of house-garage leakage in previous field studies (CMHC 2001; Emmerich et al. 2003; Batterman et al. 2007; Offerman 2009), with the Offerman study of new, single-family California Homes being the most extensive study to make this type of measurement. Values from these studies are listed in Table 6. Typically, the garage envelope leakage area is of roughly the same magnitude as the house envelope leakage area ($C_{GO}/C_{HO} \sim 1$), but some homes have garages with large leakage area relative to that of the house, perhaps due to intentional venting of the garage space. Ideally, the recommended measurement and analysis strategy would be sufficiently robust to be able to test the full range of possible conditions.

In this study, the capacity of the fan pressurization device to deliver the necessary flow rate to reach the pressures indicated was not considered. I.e., for some of the simulated cases, a blower door that can provide up to 5000 cfm would not be able to generate the pressure difference listed here.

Table 6: Range of house-garage leakage parameters found in field studies. Values listed are the median (if N<10) or mean otherwise, +/- one standard deviation.

	C_{HG}/C_{HO}	$C_{HG}/(C_{GO}+C_{HO})$	C_{GO}/C_{HO}
This study N=6	0.05+/-0.16 Min=0.02, max = 0.45	0.03+/-0.02 Min=0.01, max = 0.06	0.7+/-3 Min=0.20, max = 8.5
Emmerich et al. (2003) N=5	0.14+/-0.17 Min=0.04, max = 0.49	0.10+/-0.07 Min=0.02, max = 0.21	1.4+/-1.5 Min=0.13, max = 3.7
Offerman (2009) N=105		0.055+/-0.035 Min = 0, max = 0.18	
CMHC (2001) N=25	0.14 Min = 0.01, max = 0.43		
Batterman et al. (2007)		0.065+/-0.053 (fraction of house air from garage from PFT study)	

The analysis of synthesized data that follows assumed for the flow rate a calibration error of 3% and normally distributed fluctuations with zero mean and standard deviation of 0.5%. For the synthesized pressure measurements, a bias error of 1% was assumed plus normally distributed fluctuations with zero mean and standard deviation between 0 and 1.5Pa. Table 7 outlines the generation of synthesized data used in this study.

Table 7: Summary of synthesized pressure and flow rate measurements including bias and noise fluctuations.

Synthesized measurement	Base value	Bias	Noise fluctuation (standard dev.)	Example
Pressure (P_{HO} , P_{HG} , P_{GO})	Pressure difference for interface with blower door: Single pressure station: 50Pa MPS (single blower door): 12.5, 25, 37.5, 50, 62.5, 75Pa Remaining pressure differences: as determined by P above, testing configuration and leakage parameters.	$\pm 1\%$	$u(P)$ varied 0-1.5Pa	$P_{meas} = (50+N(0,u(P)^2))*(1 \pm 0.01)$
Flow rate (Q_{HO} , Q_{HG} , Q_{GO})	as determined by P, testing configuration & leakage parameters	$\pm 3\%$	$u(Q) = u(P) \times 0.5 \times dQ/dP$	$Q_{meas} = (Q+N(0,u(Q)^2))*(1 \pm 0.03)$

While these conditions may not correspond exactly to the uncertainty in all field tests, the goal was to provide a framework to compare test configurations and analysis methods for typical conditions. Even if the magnitude of the uncertainty calculated here was not exactly correct, the performance of an individual test configuration relative to other configurations was, for the most part, independent of the magnitude of the assumed errors, so the choice of the most robust test configurations is unlikely to change. I.e., the best test when $u(P) = 0.5\text{Pa}$ is likely to still be a top method if $u(P)$ is actually 0.2Pa or 1Pa . It is possible that if the uncertainty associated with different behavior for pressurization and depressurization was much greater than was assumed here, then the 10 or 12 parameter method would perform better than the 5 or 6 parameter method. Additionally, if the inter-zone leakage is a large fraction of the total zone leakage, then assuming a pressure exponent for the inter-zone leakage may not be beneficial.

The procedure for generating the synthesized data was:

1. Select the testing configurations (e.g., 199 and 109)
2. Select a set of chosen 'exact' values for the parameters n_{ij} and C_{ij} (see Table 5).
3. Set the pressure difference across envelope walls containing the blower door(s) at specified pressure station values.
4. Calculate the remaining pressure differences and flow rates using the governing control volume equations for the testing configuration as well as $P_{HO}=P_{GO}+P_{HG}$.
5. To obtain 'measured' pressures, add randomly sampled noise as well as bias to Q_{ij} , $P_{HO,exact}$ and $P_{HG,exact}$ (See Table 7). Recalculate P_{GO} as $P_{HO}-P_{HG}$, as it would typically be in the field.
6. Repeat for each iteration (typically 400-1000 iterations were completed under each set of conditions).

When two blower doors are used simultaneously, there are many possible sets of pressure differences across the two interfaces containing the blower doors that could be tested. Strategies explored in this study included holding P_{HO} at a fixed pressure and varying P_{GO} , and holding P_{HG} at a fixed pressure (0 or otherwise) and varying P_{HO} and P_{GO} .

A similar procedure for generating synthesized data was applied for the single zone leakage analysis except the single zone control volume was used instead of the control volume equations for two adjacent zone control volumes.

Single Zone Leakage Results

To orient the reader to the methods, a brief summary of results is provided on measuring the air leakage through a single, isolated zone. The assumptions followed those described for the inter-zone leakage case except there was only a single zone. For example, the pressure exponent was sampled from the same distribution resulting from the sum of normal distributions centered at $n=0.7$ and $n=0.6$, each with standard deviation of 0.05. The variability between 'exact' parameters for pressurization and depressurization was assumed to be the same: $C_- = C_+ + \epsilon_C$, where $\epsilon_C = N(\mu=-0.05C_+, \sigma^2=(0.1C_+)^2)$; $n_- = n_+ + \epsilon_{n2}$ where $\epsilon_{n2} = N(\mu=0.03n_{mean}, \sigma^2=(0.06 n_{mean})^2)$. Also, the uncertainty in the flow rate measurements was related to $u(P)$ as described in Table 7.

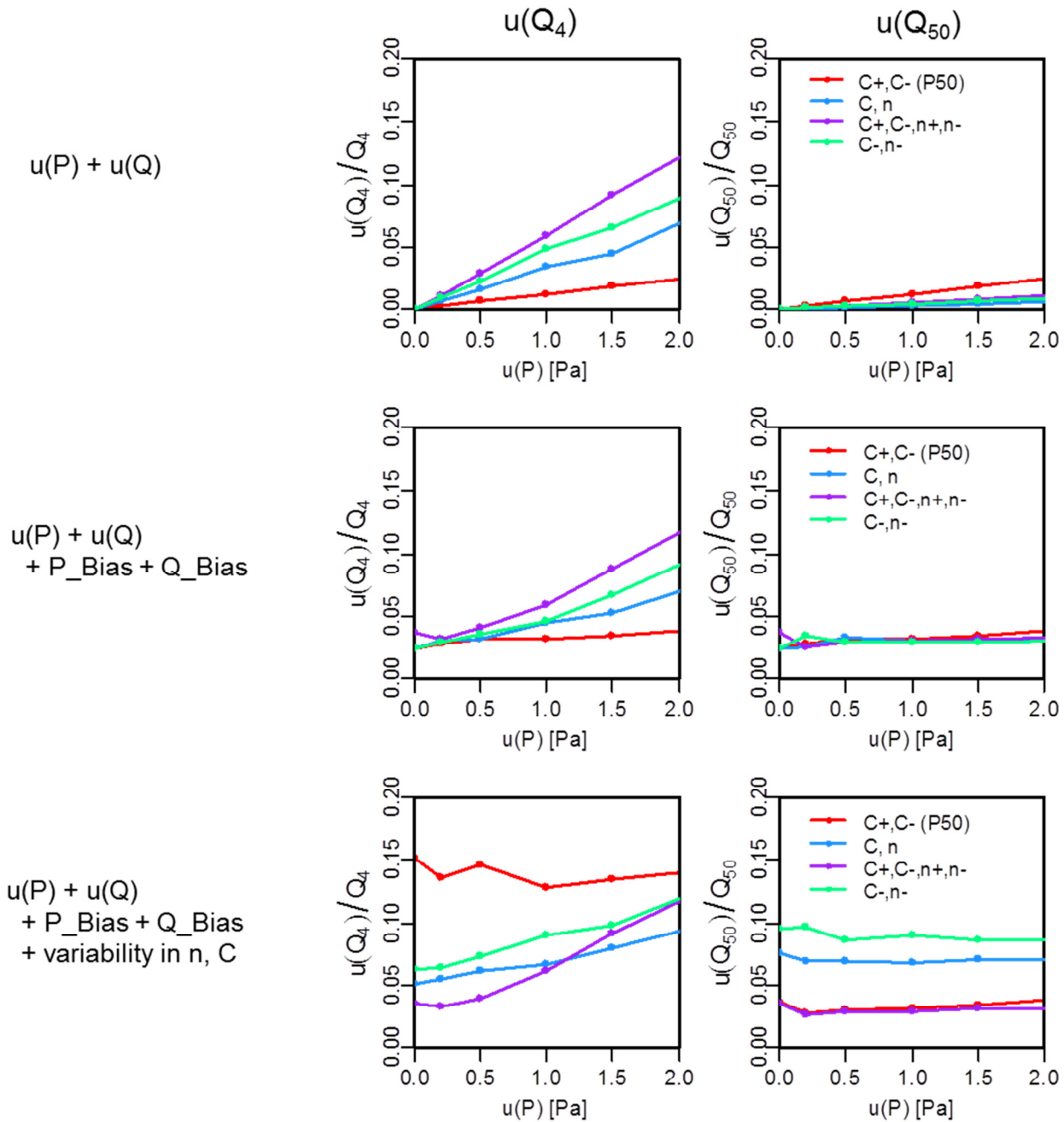


Figure 7: Uncertainty in Q_4 leakage flow at 4 Pa reference pressure, and Q_{50} (the leakage flow at 50 Pa test pressure). The uncertainty shown is the median uncertainty. Testing methods listed in Table 1 are shown in each figure: Method 1 (red), Method 2A (blue), 2B (purple), and 2C (green). The biases assumed were the same as for the inter-zone leakage case: $\pm 1\%$ for pressure measurements and $\pm 3\%$ for flow rate measurements. In the top two rows, $n_{\text{exact}}=0.65$ and $C+=C-$, whereas in the bottom panel, the same assumptions about the distribution of n and variation between pressurization and depressurization conditions were made as listed in Table 5.

Results from analysis of synthesized data simulating fan pressurization tests of a single zone are shown in Figure 7. In this figure and in the rest of the study, the median uncertainty is shown rather than the mean in order to show the uncertainty above and below which one half of the cases tested fell. Because a good fit to the data is not found in some cases (particularly for inter-zone leakage), it is difficult to select a meaningful value to include in the calculation of the 'mean' uncertainty. Tests with poor fits may predict very low or very high leakage values. So when a value of 100% (or near 100%) median uncertainty is reported, the test method is not likely to be reliable under those testing conditions.

The top row in Figure 7 shows the uncertainty in Q_4 and Q_{50} assuming that the fitted pressure exponent was exactly equal to the 'exact' pressure exponent of the envelope, and that the exact leakage parameters were the same under pressurization and depressurization conditions. Under these circumstances, the uncertainty in all 4 methods listed increased linearly as the uncertainty in the measured quantities increased indicated by $u(P)$. The single pressure station method was particularly effective here, because measurements are only made at $P=50\text{Pa}$, where the pressure signal due the fan was large relative to any fluctuations introduced ($50\text{Pa} \gg u(P)$). In the limit when $u(P)$ was small, the uncertainty in all methods approached zero.

When measurement bias in the instrument was also included in the middle panel of Figure 7, the effect was to increase the uncertainty in Q_4 and Q_{50} by 2-3 percentage points for all methods, with larger increases when $u(P)$ was small. Given that typical fluctuations $u(P)$ due to light wind are on the order of 0.5Pa , the increase in uncertainty due bias in the measurement devices was of the same magnitude of uncertainty due to wind fluctuations. The relative performance of the different methods was similar to in the top row.

In the bottom row, variation in the exact pressure exponent as well as variation between pressurization and depressurization conditions were included, as well as fluctuations and bias in the measured quantities. Including variation in the pressure exponent changed the relative performance of methods dramatically. This was because n_{exact} was no longer necessarily the same as the value assumed in a fixed- n model, such as Method 1. Some key points are:

When the actual pressure exponent was not necessarily equal to the assumed pressure exponent, this increased the uncertainty in Q_4 obtained with single pressure station tests (Q_{50} test), by a factor of 5.

Using multiple pressure stations reduced the uncertainty in Q_4 by a factor of 3 below the single point test for typical noise level $u(P)=0.5\text{Pa}$: Method 1 had 14.9% uncertainty in Q_4 versus 4.2% using Method 2B.

Although sampling a single pressure station for a longer period of time reduced the uncertainty in the mean pressure and flow rate, this effect was minimal compared with the uncertainty introduced by assuming a specific pressure exponent n (i.e., the difference between Method 1 and Method 2A,B or C.).

The uncertainty in Q_{50} is also plotted in Figure 7 to show the extent to which the Q_{50} metric was impacted by various sources of uncertainty. Variation between pressurization and depressurization conditions led to uncertainty in Q_{50} if parameters were not fit to each separately. The variability in the pressure exponent n had no impact on Q_{50} , because the flow rate was measured at the pressure of interest. The impact of measurement uncertainty on Q_{50} was also very small. Even though Q_{50} can be determined consistently by taking a measurement only at 50Pa , this does not mean that reference flow rates calculated by extrapolating to lower pressures will give a similarly consistent value. In the single

zone case, the uncertainty in Q_4 obtained using a single pressure station measurement at 50Pa was approximately 15%, even if $u(P)$ was increased to 2Pa, which corresponds to quite windy conditions. 15% uncertainty may be acceptable for the estimation of the leakage through an entire zone. The situation becomes more complex when trying to calculate the inter-zone leakage, given that the interface area between two zones can be small relative to the entire surface area of the zones.

Inter-zone Leakage Results

This section outlines results from using Monte Carlo simulations to assess the accuracy of measurement strategies. Following the analysis of the Monte Carlo simulation results, the same methods were applied to analyze field blower door test data.

Three Single Zone Method Results

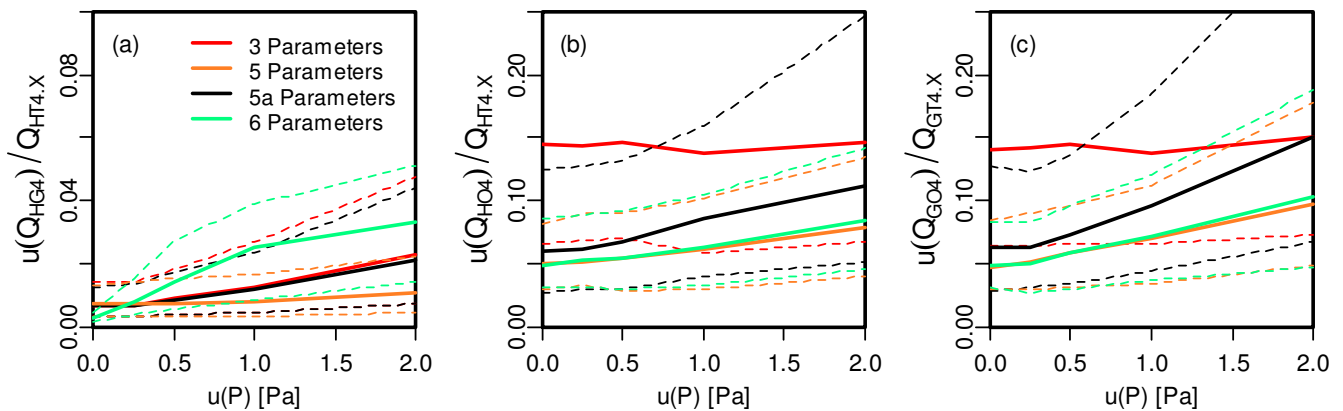


Figure 8: For 3 single zone method (configurations 190, 091, and 109). Uncertainty in Q_{HG4} (a), Q_{HO4} (b) and Q_{GO4} (c), comparing the 3 parameter fit (red), 5 parameter fit w/ simple calculation (black), 5 parameter fit (orange) and 6 parameter fit (green). Solid lines are the median uncertainties and the dashed lines show one standard deviation above and below the median (84% and 16% quantiles). The x-axis shows the magnitude of the noise added to pressures (P_{HO} and P_{HG}) (see Table 7). $C_{HG}/C_{HO} = 0.05$, $C_{GO}/C_{HO} = 0.7$, 1000 iterations.

Figure 8 shows the results when three single zone tests were used to determine the air leakage at the reference pressure across the House-Outside, House-Garage and Garage-Outside interfaces (Q_{HO4} , Q_{HG4} , and Q_{GO4}). Both the 3 parameter fit using a single pressure station and the multiple pressure station methods (5 parameter fit and 6 parameter) resolved Q_{HG4} to within 1% of Q_{HO4} when $u(P)=0.5Pa$. Fitting the pressure exponent, n , made a much larger difference in the uncertainty in Q_{HO4} and Q_{GO4} . The uncertainty in Q_{HO4} and Q_{GO4} was 3 times greater using the 3 parameter method compared with the 5 or 6 parameter methods when $u(P)=0.5Pa$. When the uncertainty in the pressure $u(P)$ was increased, the advantage of using additional pressure stations decreased, however it is unlikely this test would be performed when $u(P)>1.5$. In addition to the 5 and 6 parameter fitting methods, an alternate method 5a (black) shows the results when n_{HG} was assumed to be equal to the pressure exponent for the remainder of the zone (i.e. $n_{HG}=n_{HO}$ in 190, $n_{HG}=n_{GO}$ in 091). The 5a method allowed for the calculation of

the 5 parameters by linear fitting of $\log(P)$ vs. $\log(Q)$ data, which is advantageous because this calculation method is similar to the method already used for single zone, multi-pressure station tests. The 5a parameter fit with simplified calculation gave similar results to the 5 parameter fit method, particularly when $u(P) < 0.5$. The 10 and 12 parameter methods were not applied to the three single zone test data. Because of the nature of the system of conservation equations resulting from the 190, 109 and 091 tests, it is difficult to determine a unique solution for the system using the 10 or 12 parameter method.

While the three single zone method was used with a single pressure station measurement to determine the inter-zone leakage Q_{HG4} with reasonably high accuracy, multiple pressure station measurements are recommended in order to improve the accuracy of the house and garage zone leakage and to give more consistent results for the inter-zone leakage when the noise level is high.

Pairs of single blower door configuration tests

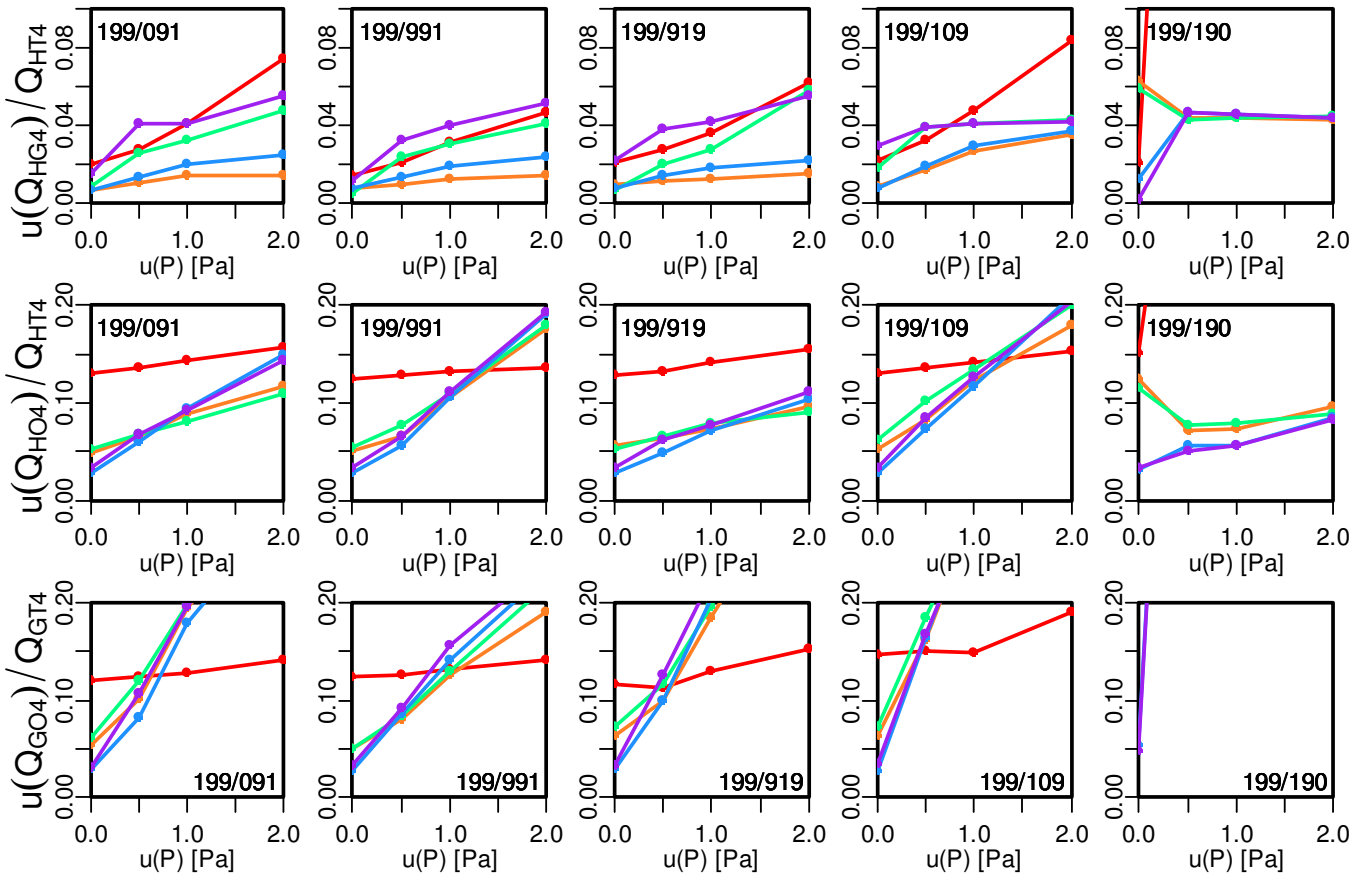


Figure 9: Uncertainty in Q_4 using pairs of single blower door test configurations. Each plot shows the median uncertainty as $u(P)$ is varied for the following methods: 12 parameter fit (purple), 10 parameter fit (blue), 6 parameter fit (green), 5 parameter fit (orange) and 3 parameter fit (red). The top row shows the uncertainty in Q_{HG4} scaled by the total house zone leakage Q_{HT4} , the middle row shows the uncertainty in Q_{HO4} scaled by Q_{HT4} , and the bottom row the uncertainty in Q_{GO4} scaled by the total Garage zone leakage Q_{GT4} . The 84% and 16% quantiles were omitted here for clarity. $C_{GO}/C_{HO}=0.7$, 400 iterations. Since $C_{HG}/C_{HO}=0.05$ here, $u(Q_{HG4})/Q_{HT4}=0.05$ corresponds to 100% uncertainty as a fraction of Q_{HG4} .

Rather than performing three single zone tests, the air leakage through the HO, HG and GO interfaces can also be determined using pairs of single blower door configurations. Results are shown in Figure 9 for 5 pairs of test configurations. While additional test pairs are possible (see Table 9), pairs shown here contain the test configuration typically done to determine the house leakage (199). Even with no fluctuations in the ‘measured’ quantities ($u(P)=0$), there was some uncertainty in the inter-zone leakage due to the assumptions of bias in the measurement devices. Although this uncertainty was often small compared with the total house leakage ($<4\%$), this uncertainty was relatively large compared with magnitude of Q_{HG4} itself when $C_{HG}/C_{HO}=0.05$. When the noise level $u(P)$ was increased in the synthesized data, it became increasingly difficult to recover the initial, ‘exact’ parameters used to generate the synthesized dataset. For the 5 parameter fit, test pairs 199/091, 199/991 and 199/919 were

capable of determining Q_{HG4} to within 1% of the total house zone leakage in the expected range of noise level for testing ($u(P)<1$), for $C_{HG}/C_{HO}=0.05$.

From the top row, it is clear that the 5 parameter fit consistently gave the most accurate results for determining Q_{HG4} , followed by the 10 parameter fit. Thus, the uncertainty from assuming $n_{HG}=0.65$ was outweighed by the benefit of this assumption in stabilizing the fitting of C_{HG} . In the middle and bottom rows showing the uncertainty in the house to outside and garage to outside leakage, the uncertainties associated with the 5,6,10 and 12 parameter methods were within a few percent for the top 4 test pairs shown. Using the 3 parameter, single pressure station method at $u(P)=0.5\text{Pa}$ increased the uncertainty in Q_{HG4} , Q_{HO4} and Q_{GO4} by a factor of two above the multi-pressure station methods.

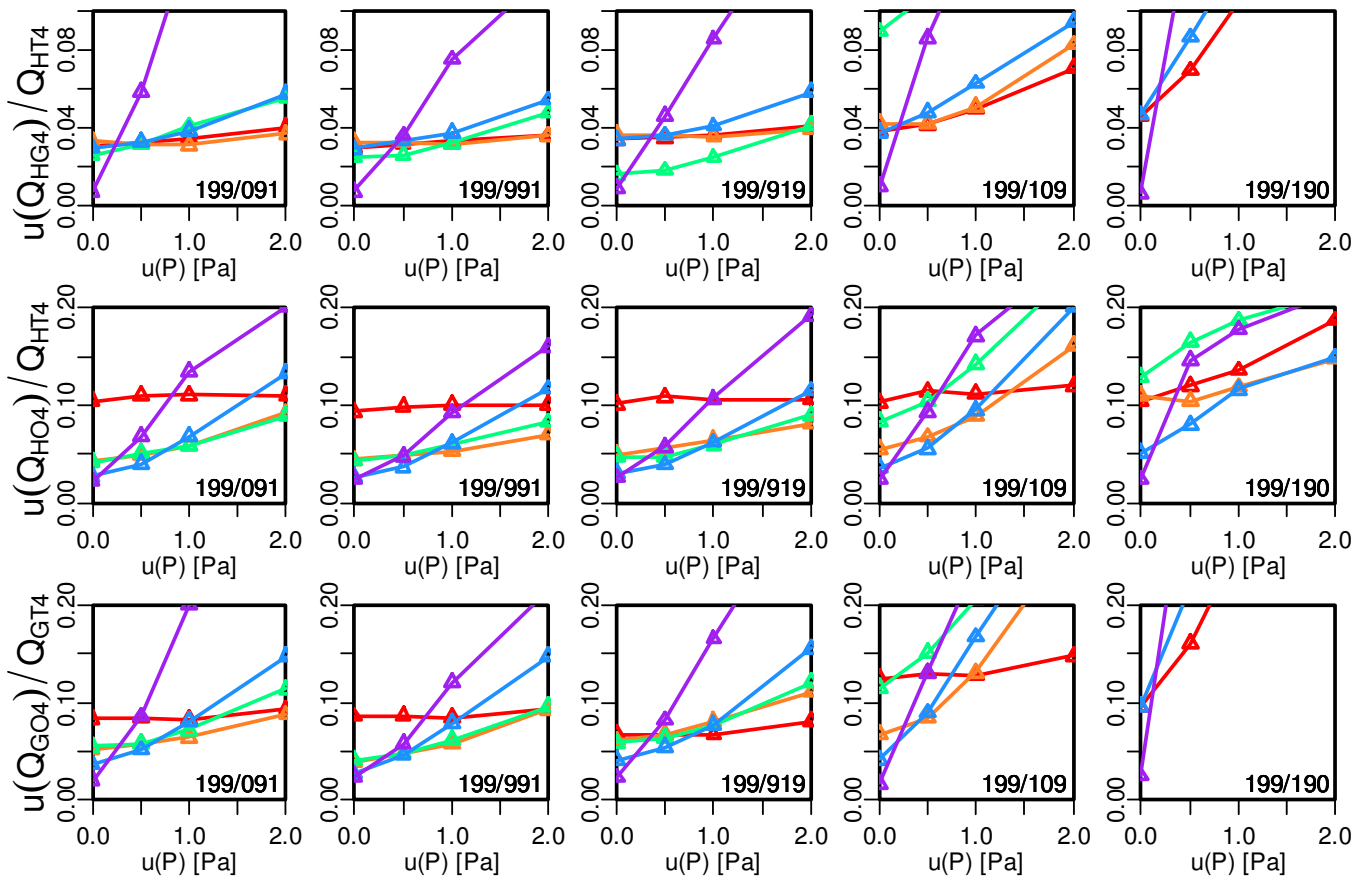


Figure 10: Uncertainty in Q_4 for leaky HG interface $C_{HG}/C_{HO}=0.3$ (differs from figure 8 where $C_{HG}/C_{HO}=0.05$), using pairs of single blower door test configurations. Each plot shows the median uncertainty as $u(P)$ is varied for the following methods: 12 parameter fit (purple), 10 parameter fit (blue), 6 parameter fit (green), 5 parameter fit (orange) and 3 parameter fit (red). The top row shows the uncertainty in Q_{HG4} , scaled by the total house zone leakage Q_{HT4} , the middle row shows the uncertainty in Q_{HO4} , scaled by Q_{HT4} , and the bottom row the uncertainty in Q_{GO4} , scaled by the total Garage zone leakage Q_{GT4} . The 84% and 16% quantiles were omitted here for clarity. $C_{GO}/C_{HO}=0.7$, 400 iterations.

While the fraction of total house leakage associated with the house-garage interface, $C_{HG}/C_{HO}=0.05$, was typical of the field measurements in this study and previous studies (Emmerich et al. 2003, Offerman

2009), there were observations for which inter-zone partition was leakier and this fraction was larger. Figure 10 has the same format as Figure 9 except the house-garage interface had a larger fraction of the total zone leakage: $C_{HG}/C_{HO}=0.3$. For the case when $C_{HG}/C_{HO}=0.3$, the same 3 test pairs (199/091, 199/991 and 199/919) had the lowest uncertainty as when $C_{HG}/C_{HO}=0.05$, although the uncertainty in Q_{HG4} was somewhat higher (about 3% of the total house leakage for the 5 parameter method). Although the 6 parameter method did have the lowest uncertainty in Q_{HG4} for the 199/919 and 199/991 methods in Figure 10, the 6 parameter method was significantly worse for the 199/109 pair (almost off the chart in Figure 9), in addition to having higher uncertainty when $C_{HG}/C_{HO}=0.05$. Thus the 5 parameter method may be a more versatile fitting method.

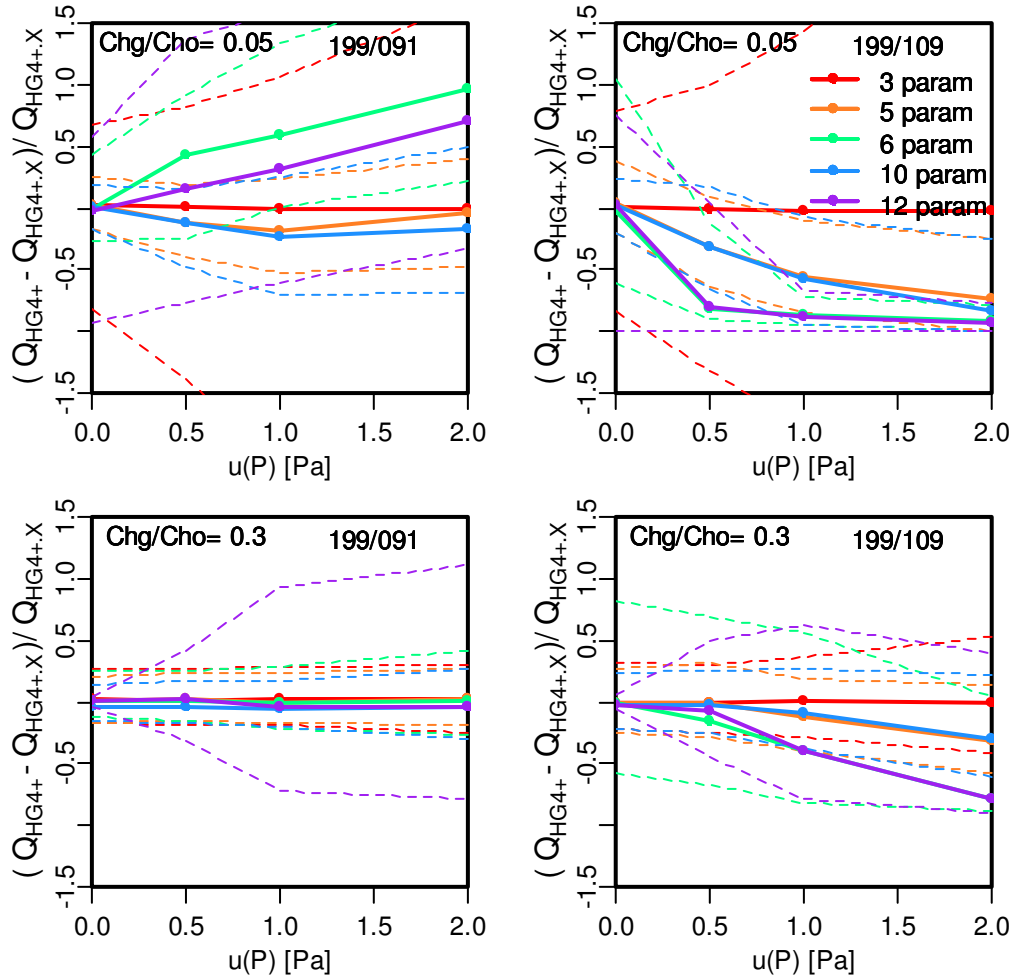


Figure 11: Bias in Q_{4HG} for 199/091 and 199/109 test configuration pairs, for $C_{HG}/C_{HO}=0.05$ (top) and $C_{HG}/C_{HO}=0.3$ (bottom). Solid lines are the median difference (0 indicates no bias) and the dashed lines show one standard deviation above and below the median (84% and 16% quantiles). $C_{GO}/C_{HO}=0.7$, 400 iterations.

While the magnitude of the uncertainty in Q_{4HG} is shown in Figure 9 and Figure 10, the difference $(Q_{HG4+}-Q_{HG4+X})$ scaled by Q_{HG4+} is shown in Figure 11 to illustrate whether there was a bias in the fitted inter-zone leakage. In some cases, there was significant bias in the uncertainty in Q_{HG4+} , but the magnitude and direction of this bias depended on the fitting method, the test configuration pair, the

magnitude of measurement fluctuations $u(P)$, as well as the ratios C_{HG}/C_{HO} and C_{GO}/C_{HO} (see also Figure 12). Because the bias depended on a range of factors, it would have been complicated to subtract this bias error from the computed results. While there was no median bias for the 3 parameter fitting method, spread of the dashed lines indicated the uncertainty magnitude is high. In general, the bias in the 6 and 12 parameter methods was greater than in the 5 and 10 parameter fitting methods.

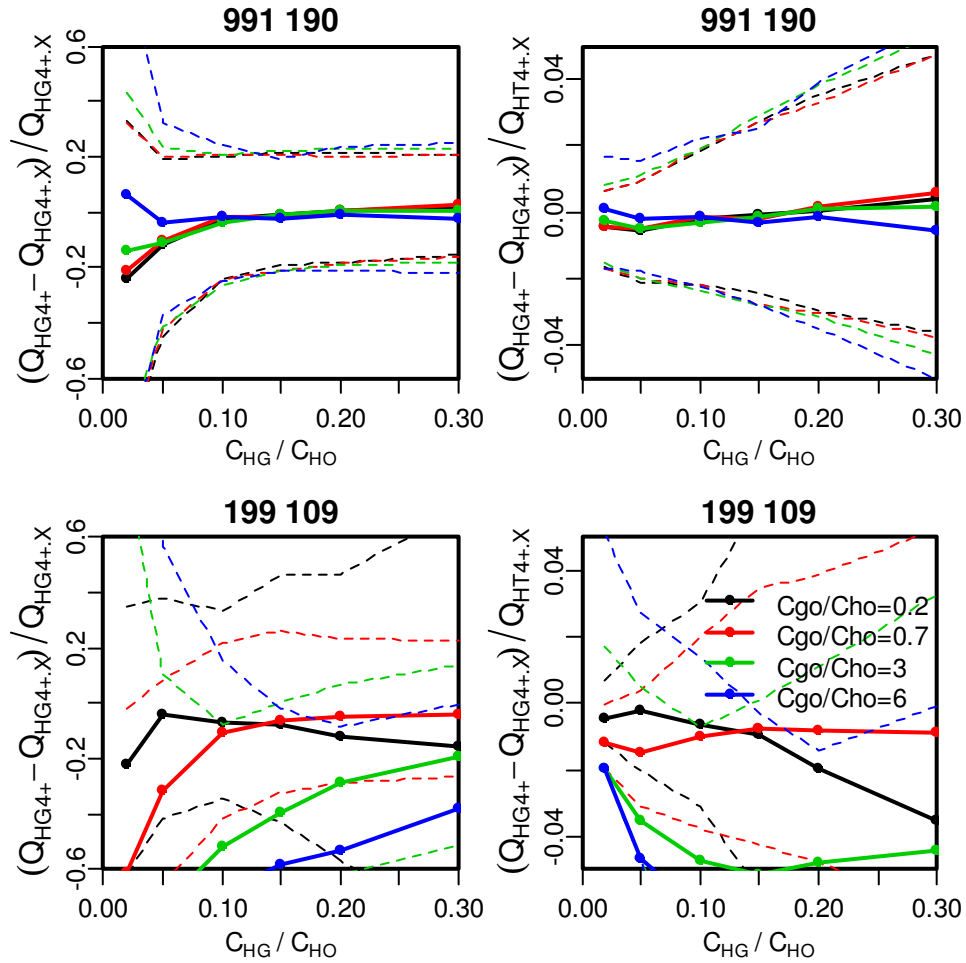


Figure 12: Bias in 991/190 and 199/109 as a function of C_{HG}/C_{HO} and C_{GO}/C_{HO} . Solid lines are the median difference (0 indicates no bias) and the dashed lines show one standard deviation above and below the median (84% and 16% quantiles). The 5 parameter fitting method was used here, $u(P)=0.5$, 1000 iterations.

The poor performance of the 10 and 12 parameter optimization method may have stemmed from the effects of error in the independent variable. The optimization function used in the analysis calculates the least squares fit to the data and one requirement of using the least squares fitting technique is that the error in the independent variables is small relative to the error in the dependent variable. Otherwise, this can lead to a bias in the fitted curves. In the linear case, the error in the independent variable will tend to decrease the slope of the fitted curve in a phenomenon known as regression dilution or attenuation. The consistent bias in the fitted curves resulting from the parameter

optimization suggests that non-linear regression dilution may be responsible. It is not clear at this point how best to remove such bias. Errors-in-variables techniques are designed to account for these effects, however there is no simple method to handle non-linear cases such as the governing system of equations in this problem. For the 12 parameter fitting method, the bias in the fitted result scaled roughly with $u(P)$ and for expected noise levels led to uncertainty of approximately a factor of 2 in $u(P)$. Evidence of the bias and is described further in Appendix C.

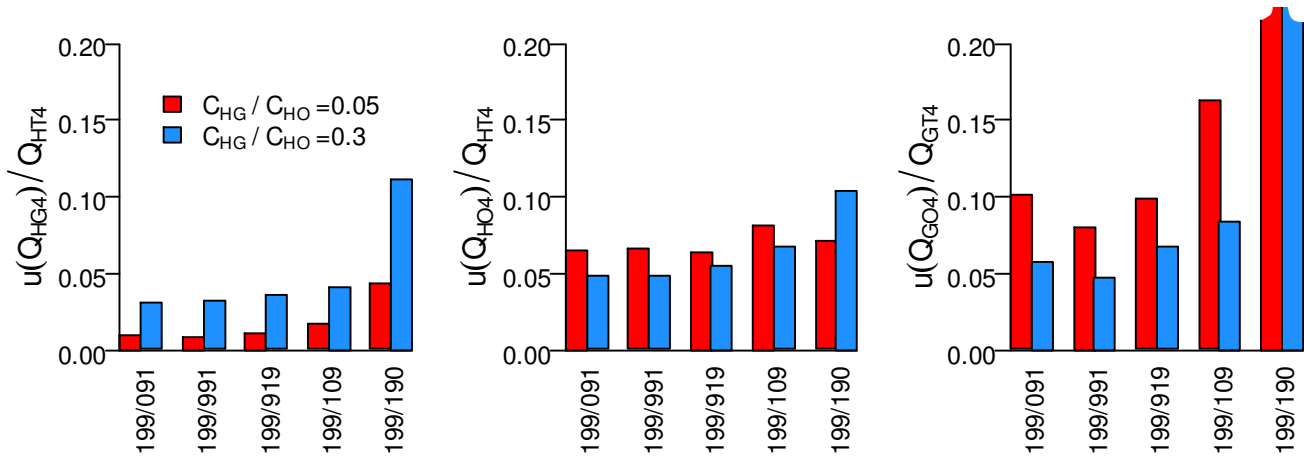


Figure 13: Uncertainty in Q_4 for a tight ($C_{HG}/C_{HO}=0.05$) and leaky ($C_{HG}/C_{HO}=0.3$) House-Garage interface using the 5 parameter fit. For $u(Q_{GO4})$ in 199/190 case, uncertainty was off the chart: 92% and 28% for $C_{HG}/C_{HO}=0.05$ and 0.3 respectively. $C_{GO}/C_{HO}=0.7$, $u(P)=0.5Pa$.

A comparison between the different test configuration pairs is provided in Figure 13, at a fixed level of pressure fluctuation, $u(P)$, and for two ratios of C_{HG}/C_{HO} . Some trends were apparent:

Test pairs 199/091, 199/991, and 199/919 had lower uncertainty than 199/109 and 199/190 for the HG, HO and GO interfaces.

The uncertainty in Q_{HG4} was generally less than in Q_{HO4} when normalized by the total House envelope leakage.

The uncertainty in the garage to outside leakage was generally higher than the house to outside leakage in this set of test pairs. This was in part due to the requirement that 199 was in each test pair. For the symmetric pair 199/991, the uncertainty for the house and garage was similar.

The analysis so far has suggested that either the three single zone method or the pairs 199/091, 199/991 or 199/919 could be used to determine Q_{HG4} to within 20% of itself as well as Q_{HO4} and Q_{GO4} to within 10% of the house and garage total leakage (respectively). There were, however, cases when C_{GO}/C_{HO} was much larger than the typical value used in this analysis. Thus far in this study, $C_{GO}/C_{HO}=0.7$ was assumed, but this ratio can be as large as 5-10, specifically if the garage space is vented to the outside (either intentionally through vents or unintentionally through large cracks, broken windows, etc.). When the garage leakage area was large relative to the leakage area in the house envelope, many methods (generally those that did not have a blower door placed in the GO interface) did not determine Q_{HG4} to within 50% or even 100% of itself.

From Figure 14, there were a range of test methods that achieved good results when $C_{GO}/C_{HO}=0.2$ and $C_{GO}/C_{HO}=0.7$ including the three single zone method and pairs of two single blower door tests. The value used was approximately the median ratio of C_{GO}/C_{HO} observed in the field data discussed later in this report and the field observations in Emmerich et al. (2003), which were 0.7 and 0.67 respectively. However, when the garage had very high leakage area relative to the house ($C_{GO}/C_{HO}=8$), it was much more difficult to resolve the inter-zone leakage. Some garages are quite leaky and others are quite tight in construction, so the ideal test method would be effective across a range of conditions.

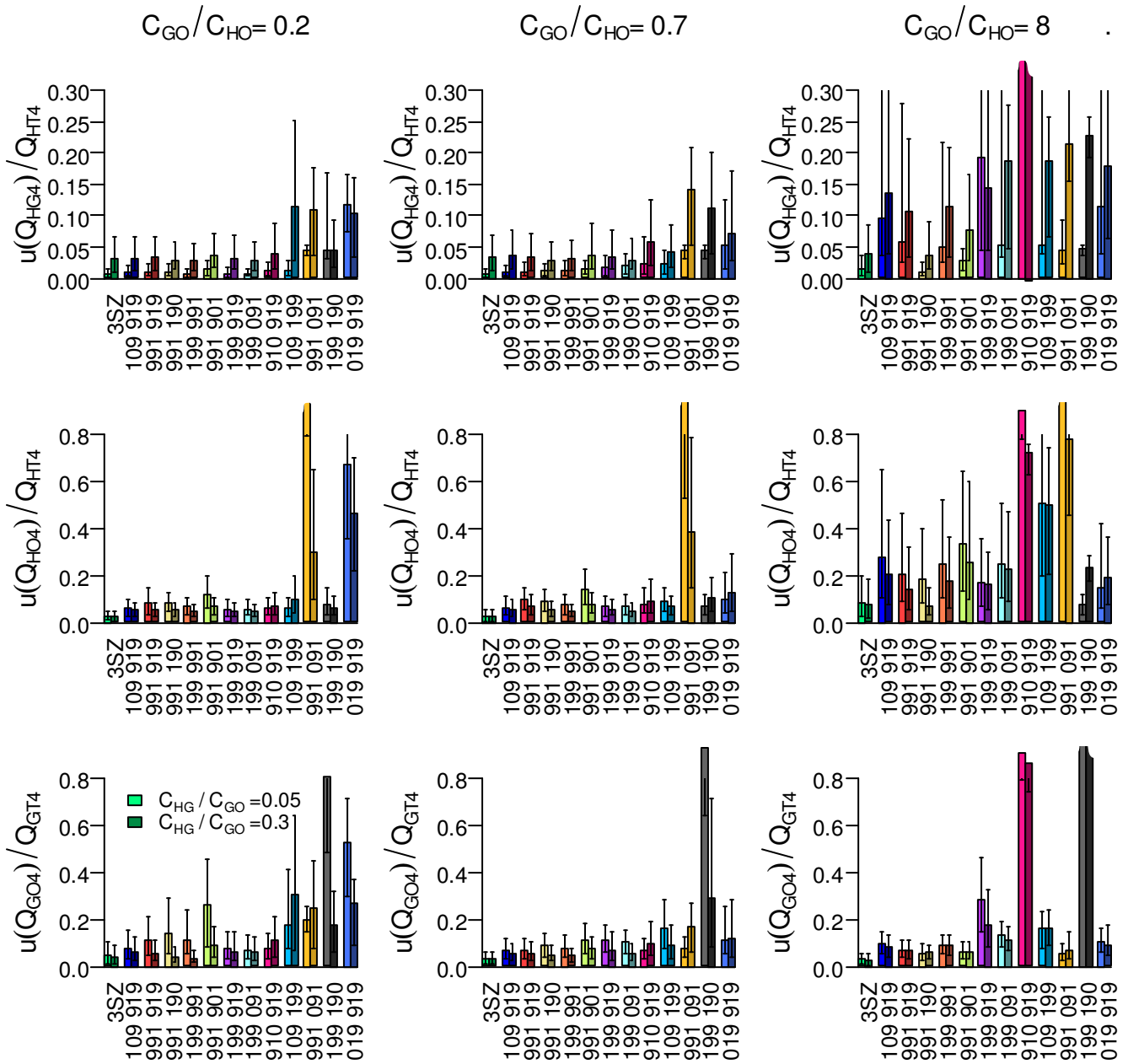


Figure 14: All single blower door test pairs as well as the three single zone method (3SZ) for the ratios of zone leakage: $C_{GO}/C_{HO}=0.2$ (left), $C_{GO}/C_{HO}=0.7$ (center), $C_{GO}/C_{HO}=8$ (right). The two columns in each cluster show tight ($C_{HG}/C_{HO}=0.05$) and leaky ($C_{HG}/C_{HO}=0.3$) House-Garage interface. Error bars show one standard deviation above and below the median uncertainty. The 5 parameter fit was used in all cases and $u(P)=0.5Pa$.

All unique pairs of single blower door configurations as well as the three single zone method are compared in Figure 14, where the rows show the uncertainty in the leakage through different segments of the envelope: HG, HO and GO. The relative leakage area between the two zones (C_{GO}/C_{HO}) was varied, with results shown in the three columns. In general, the uncertainty in Q_{HG4} was greatest when

the leakage area of one zone was much larger than the other (compare the right column of Figure 14 where $C_{GO}/C_{HO}=8$ with the left and center columns). When $C_{GO}/C_{HO}=8$, there were two methods where the median uncertainty in Q_{HG4} was less than 5% of the total house leakage: the three single zone method and the test configuration pair 991/190. Thus, these test sets are recommended as the most robust sets of single blower door tests.

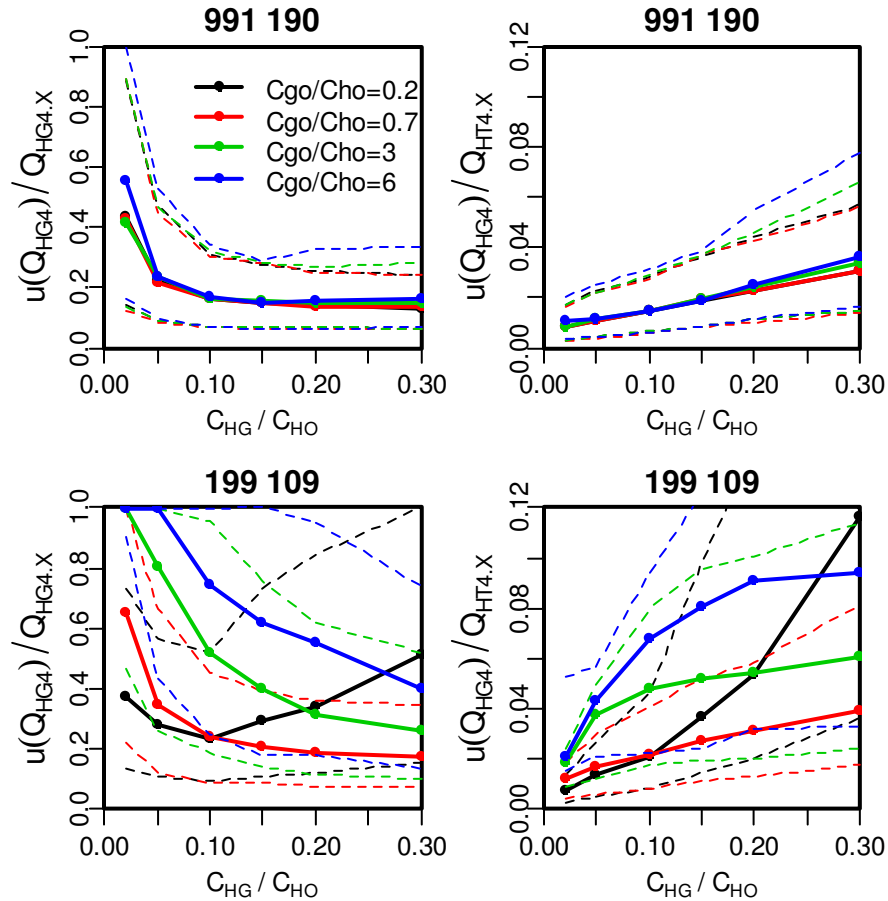


Figure 15: Uncertainty in Q_{HG4} for two different pairs of single blower door configurations: 991/190 (top) and 199/109 (bottom). Solid lines are the median uncertainties and the dashed lines show one standard deviation above and below the median (84% and 16% quantiles). Here, $u(P)=0.5Pa$ and 5 parameter fit is used. 1000 iterations.

The results from Figure 9, Figure 10, and Figure 14 suggested that factors that impacted the uncertainty in Q_{HG4} included: the uncertainty in measured quantities, scaled by $u(P)$, C_{HG}/C_{HO} , C_{GO}/C_{HO} and the analysis method (3,5,6,10,12 parameter fit). Fortunately, not all methods were sensitive to all of these parameters. From Figure 15 it is clear that the uncertainty in Q_{HG4} varied with C_{HG}/C_{HO} and C_{GO}/C_{HO} for test pair 199/109 (lower row). It is difficult to assess which test to choose when the uncertainty of the methods depend on the quantities that you are trying to compute. The results for test pair 991/190 (Figure 15 upper row), on the other hand, were largely insensitive to C_{GO}/C_{HO} . In addition, when $C_{HG}/C_{HO}>0.05$, the uncertainty in Q_{HG4} was consistently between 15 and 20% of Q_{HG4} when the test pair

991/190 was used. This provided a consistent rule of thumb for the uncertainty in Q_{HG4} using this method. The uncertainty for this method was less than 20% of the value of Q_{HG4} , which translated to less than 4% of the total house leakage (Q_{HT4}). Figure 16 shows that when C_{HG}/C_{HO} and C_{GO}/C_{HO} were varied, the results using the Three Single Zone method were very similar to the 991/190 method shown in Figure 15.

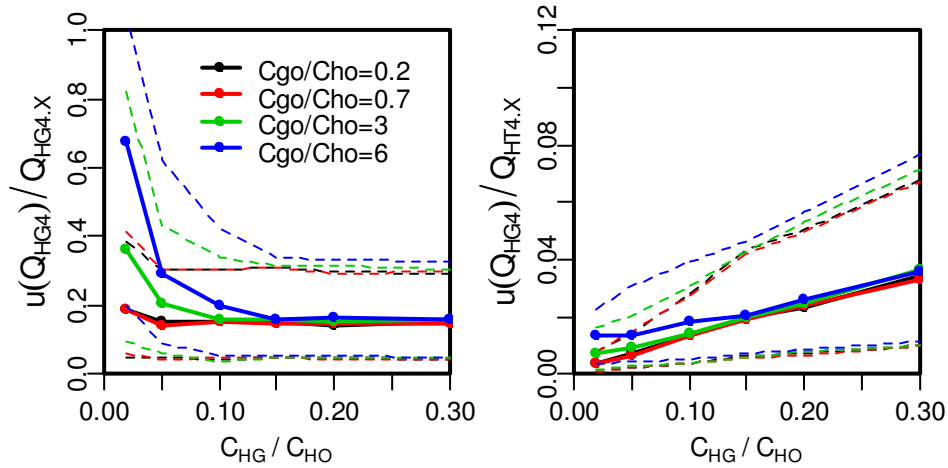


Figure 16: Three Single Zone Method, for varied C_{HG}/C_{HO} and C_{GO}/C_{HO} . Solid lines are the median uncertainties and the dashed lines show one standard deviation above and below the median (84% and 16% quantiles). Here, the 5 parameter method was used, $u(P)=0.5Pa$, 1000 iterations.

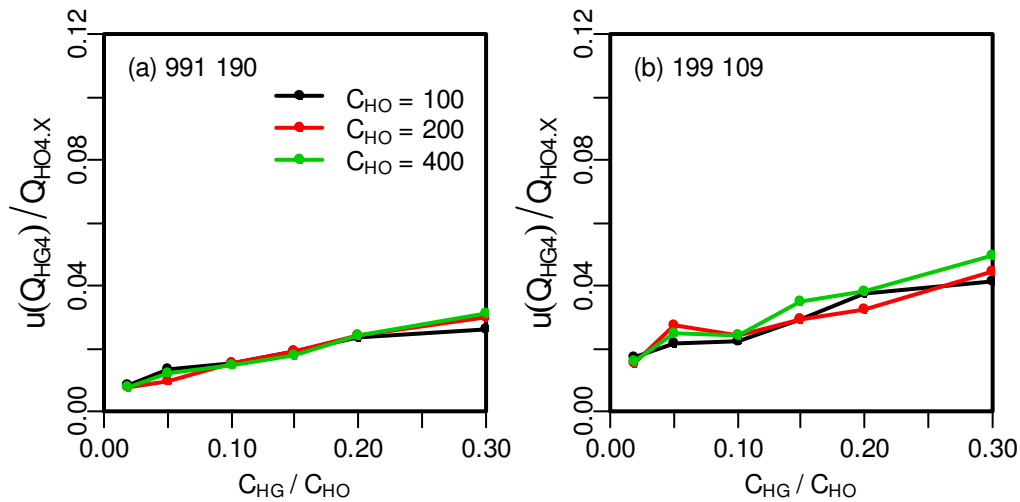


Figure 17: Impact of varying C_{HO} . The solid lines show the median uncertainty. $C_{HO}=200$ is the base case used in the rest of the analysis in this study. Here, $C_{GO}/C_{HO}=0.7$, $u(P)=0.5Pa$, 100 iterations.

The uncertainty in Q_{HG4} was found to be independent of the magnitude of the total house leakage area, as scaled by C_{HO} , for the expected range. For the two test pairs, 991/190 and 199/109, the impact of varying C_{HO} is shown in Figure 17. In this figure, C_{HG}/C_{HO} and C_{GO}/C_{HO} were held constant. Thus, for the rest of this study, C_{HO} will not be varied.

Given that both the 991/190 method and the Three Single Zone method had favorable accuracy, a number of additional factors may be considered in selecting a method for use. If the inter-zone interface was small in area, leakage around any door in this interface may be a significant portion of the HG leakage, giving an advantage to methods where the blower door is not mounted in the HG interface (such as 991/190). The choice between using the 3SZ method and 991/190 may depend on which doors are available. For example if there is no door to mount the blower door in the GO interface, but there are doorways in the HO and HG interfaces, then 991/190 cannot be performed, but 3SZ can be (using 109/190/019). On the other hand, in the testing of units in multi-family housing and the H and G zones represent two different units, then there is typically no door in the HG interface, but doors do exist in the HO and GO. This makes the 991/190 method the best single blower door method for inter-zonal testing between 2 units in a multi-family building. However, if the first zone is expected to have larger leakage area than the second, use 199/091 instead of 991/190.

When considering which test to perform, if one zone has a large leakage area (e.g., if the garage is vented to the outdoors or zones have similar construction but vastly different volumes), it is particularly important to choose one of the high performing methods (such as 991/190 or 3SZ) and to avoid 199/109.

What limits the accuracy of these methods?

In the results of this section, there was observed a certain level beneath which uncertainty could not be reduced. What limited the accuracy of these methods? For the 5 and 10 parameter methods, the uncertainty was bounded by the uncertainty introduced by assuming a fixed pressure exponent. The results in Figure 5 suggested this baseline uncertainty for the 5 and 10 parameter methods was between 12 and 15% of Q_{HG4} for the better methods. The results in this section were consistent, in that the median uncertainty in Q_{HG4} from the methods examined was never less than this baseline. For the 5 and 6 parameter methods, the uncertainty included a component associated with the mean difference between pressurization and depressurization leakage flows, given that one set of parameters was being fit to pressurization and depressurization data. The mean difference between pressurization and depressurization was 2% of the leakage flow at the reference pressure.

How do test methods fail?

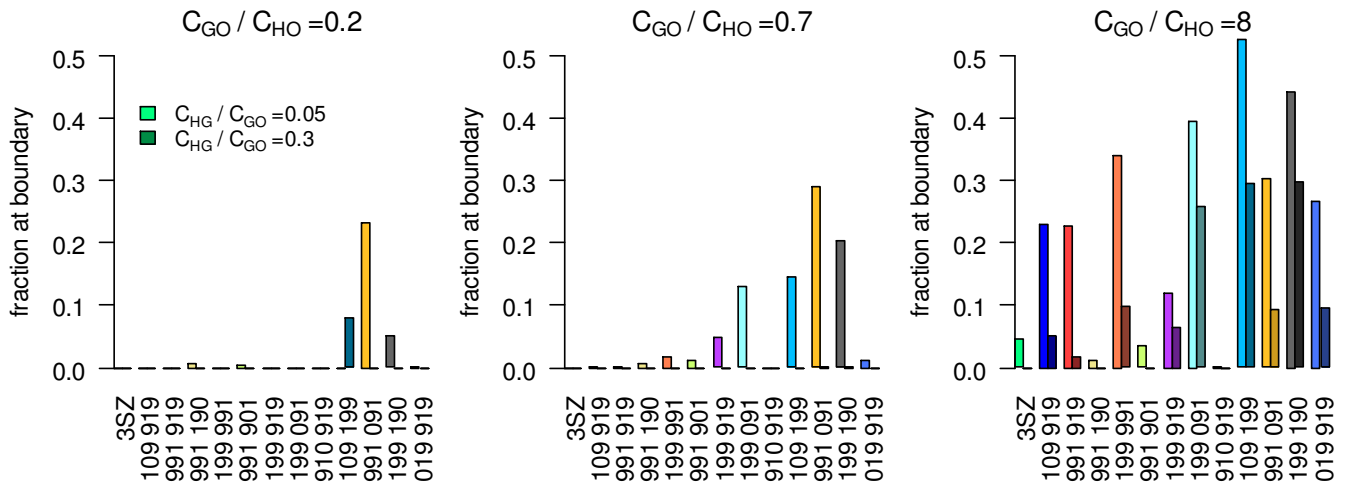


Figure 18: Fraction of simulated cases where fitted value of C_{HG} falls at constraint boundary. Data from same simulations shown in Figure 14 (5 parameter fit, $u(P)=0.5Pa$). In no cases did C_{HO} or C_{GO} fall at the constraint boundary or was C_{HG} fit to the constraint maximum.

In using an optimization routine with constraints on the fitted parameters (i.e., not the 3 parameter fit but the 5,6,10 or 12 parameter methods), it was possible that a good fit to the data was not found. One indicator of goodness of fit was whether the fitted parameter fell at the edge of the domain. Parameter constraints were specified in the *Methods* section. Because the inter-zone leakage was often small relative to the total leakage in each adjacent zone, the parameters $C_{HG(+/-)}$, and $n_{HG(+/-)}$ were the most likely to fall at the constraint boundary in the optimization process. Specifically, $C_{HG(+/-)}$ was often fit to the minimum value, here set to 0.01. When the uncertainty in Q_{HG4} in this section was described as a fraction of Q_{HT4} , this masked to some extent the impact of cases when $C_{HG}=0.01$, because the even though Q_{HG4} is 100% from the exact value, the exact value was a small fraction of the total zone leakage, Q_{HT4} . For reference, Figure 18 shows the fraction of cases when this occurred. It was not surprising that test pairs with a high fraction of cases fit at the constraint boundary tended to have high median uncertainty in Figure 14 (although some test pairs, namely 910/919, tended to overestimate Q_{HG4} and thus did not follow this trend). While one might think that the mean value of the objective function could give an indication of the typical quality of fit, this was not the case. Because the HO and GO terms tended to be of larger magnitude, the objective function value was not correlated with the uncertainty in Q_{HG4} to the extent that it could be used to differentiate between methods.

Number of pressure stations

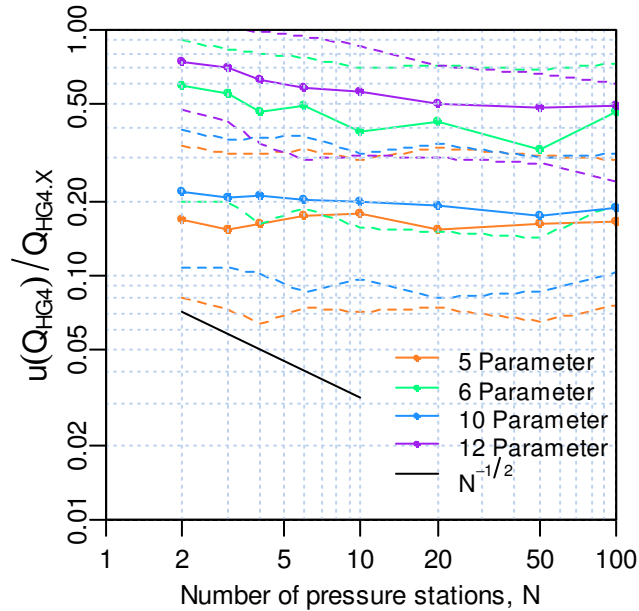


Figure 19: Uncertainty in Q_{HG4} , normalized by itself when the number of pressure stations is varied. Solid lines show the median uncertainty and dashed lines show one standard deviation above and below the median (84% and 16% quantiles). Here, the uncertainty, $u(P)$, at each station was 0.5Pa, test pair was 991/190, $C_{HG}/C_{HO}=0.10$, $C_{GO}/C_{HO}=3$, with 400 repetitions.

As the number of pressure stations is increased, we would expect that this additional information would reduce the error in the results. N here indicates the number of stations between 10Pa and 75Pa, and $2N$ stations are required for pressurization and depressurization tests. I.e., for 3 pressure stations, the stations are +/- {25, 50, 75}, and for 6 stations: +/- {12.5, 25, 37.5, 50, 67.5, 75}. Assuming the uncertainty in each pressure value was constant (i.e., independent of the number of stations), then Figure 19 shows that the Q_{HG4} error fraction did decrease with the number of pressure stations when all 12 parameters were fit (purple). The reduction in uncertainty with number of points was less than a $N^{-1/2}$ dependence. When n_{HG} was fixed, however, the uncertainty in Q_{HG4} was not strongly affected by the number of stations. This is because as the number of pressure stations is increased, the uncertainty approaches the limit of the baseline error introduced by fixing n_{HG} (Figure 5). Variability between tests (indicated by the spread of the dashed lines in Figure 19) did not decrease with the number of pressure stations when using the 5 or 10 parameter fit because the uncertainty in outlying cases was largely due to the discrepancy between the fitted and actual values of n_{HG} . It was surprising that as few as 2 stations can be used to fit the 6 pressurization parameters, and it is recommended to use at least 4 stations, as the results for less than 4 stations were not exhaustively explored.

A key result of this study was that making the assumption that n_{HG} was 0.65 (5, 10 parameter fit) was better than fitting for n_{HG} (6, 12 parameter fit) regardless of how many pressure stations were used. In the following section *Two blower door results*, the strategy of fixing $n_{HG}=0.65$ was also applied, including modifying the method of Herrlin and Modera (1988) to include this assumption.

Two blower door results

Instead of running tests using a single blower door and combining data from multiple configurations, it is possible to use two blower doors in concert to determine the house-garage leakage. With two blower doors, the pressure in each of the two zones can be controlled independently. This enables a wide range of possible test methods, including but not limited to the pressure differentials achieved in the single blower door tests. With such flexibility, one would expect that test methods using two blower doors could provide more reliable measurements than single blower door test methods.

Pressure balancing method

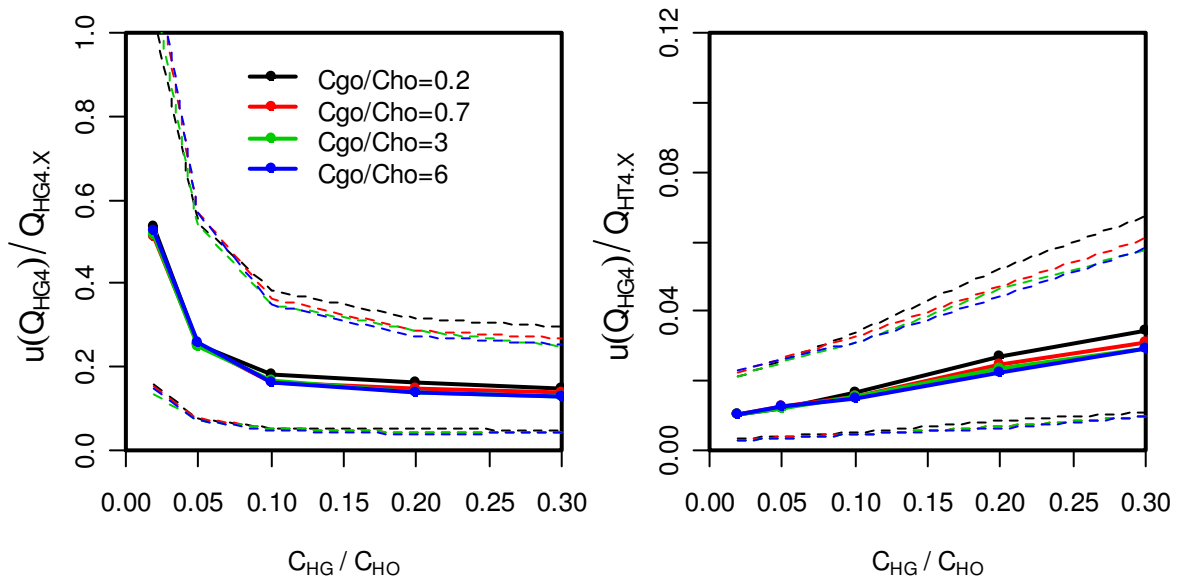


Figure 20: Uncertainty in the House-Garage leakage resulting from the Pressure-balancing method (199/192), following calculation technique used by the CMHC (2004), i.e., parameters were fit using least squares and with no optimization required. Solid lines show the median uncertainty and dashed lines show one standard deviation above and below the median (84% and 16% quantiles). Here, 6 pressure stations were used, $u(P)=0.5\text{Pa}$ 1000 iterations.

The pressure-balancing method is one method that has been used previously because it simplifies the resulting calculation of the inter-zone leakage. The method developed by Reardon et al. (1987) and used by the CMHC (2001, 2004), was used to determine the leakage between two adjacent zones, using the same assumptions applied for the single blower door analysis. Figure 20 illustrates that the pressure-balancing method gave results that were very similar to the 3SZ or 991/190 test pair. One advantage was that because the pressures in both zones were controlled explicitly, regardless of the ratio C_{GO}/C_{HO} , the curves in Figure 20 collapsed to a single curve more so than with the 3SZ method shown in Figure 16. Thus, the uncertainty was more consistent across the wide range of possible conditions that might occur when testing at a field site.

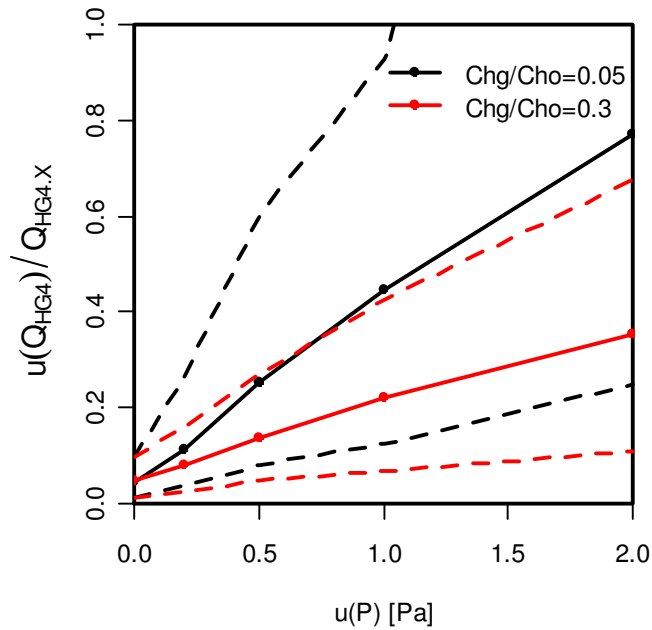


Figure 21: Impact of $u(P)$ on Pressure-Balancing Method uncertainty. Solid lines show the median uncertainty and dashed lines show one standard deviation above and below the median (84% and 16% quantiles). Here, $C_{GO}/C_{HO}=0.7$, 1000 iterations.

Figure 21 shows the sensitivity of the pressure-balancing method to uncertainty in the measured quantities, P and Q , as quantified by $u(P)$. Particularly when the inter-zone leakage is small, the uncertainty in this inter-zone leakage increases dramatically with fluctuations in the measured P and Q .

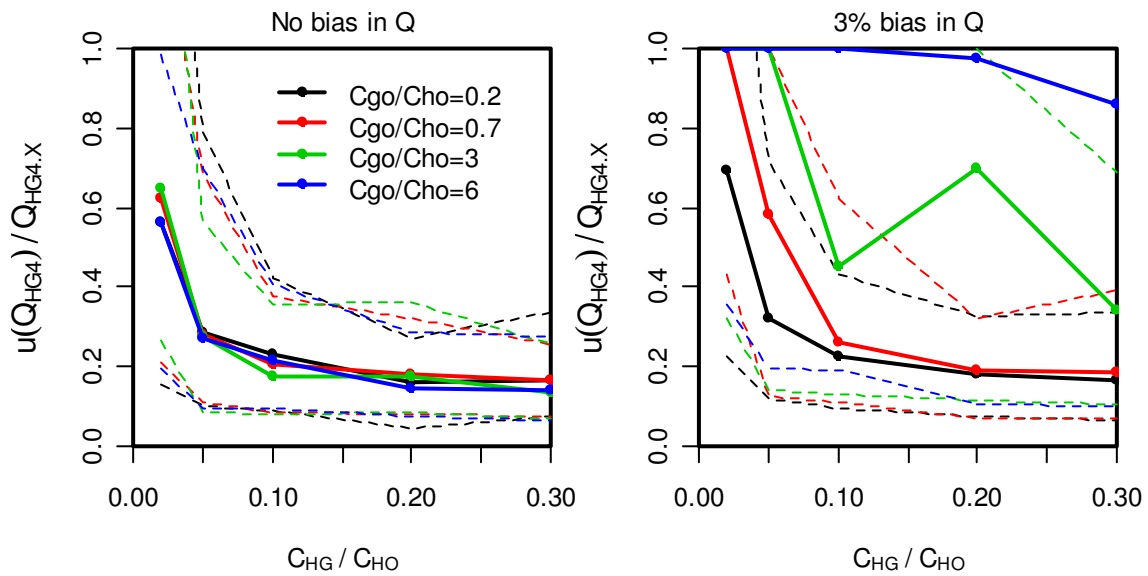


Figure 22: Impact of bias in measured flow rate for Pressure-balancing method in 129 configuration. Solid lines show the median uncertainty and dashed lines show one standard deviation above and below the median (84% and 16% quantiles). Here, $u(P)=0.5\text{Pa}$, 100 iterations.

The pressure-balancing method was also tested in the 129 configuration, rather than the 192 configuration as discussed above, but the uncertainty was significantly increased. While the pressure values for P_{HO} , P_{HG} and P_{GO} were the same for the 192 and 129 pressure-balancing routines, the main difference was that both blower doors supplied flow to the same zone. As stated previously, a 3% bias in flow rate measurements was assumed, where the sign of the bias was assigned randomly to each synthesized blower door in the testing process. Figure 22 illustrates uncertainty in Q_{HG4} if the bias in Q is not included (left) and if it is included (right). The inclusion of calibration errors in the blower door flow rate led to substantial uncertainty in Q_{HG4} , particularly when $C_{GO}/C_{HO}>1$. Unless it is possible to ensure that calibration errors for both blower doors are small, using the pressure balancing technique in the 129 configuration can introduce significant uncertainty in the results.

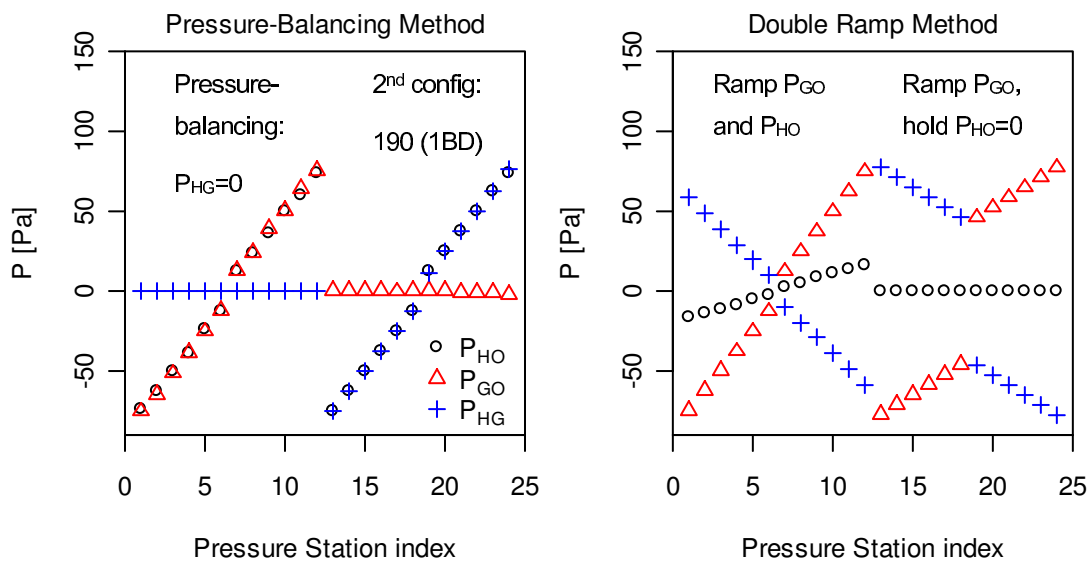


Figure 23: Pressure stations for Two Blower Door methods: Pressure-Balancing (left) and the Double Ramp Method (right). Pressure station index (order) is arbitrary.

Alternate testing methods were identified that had consistently lower uncertainty than the pressure-balancing method, as shown in Figure 23. The pressure balancing method included a 199 test (stations 1:12), and then an additional test when the pressure across the HG interface was held at zero (stations 13:24). The Double Ramp Method was developed in this study by experimenting with different sets of pressure differences in order to reduce the uncertainty in the results. The Double Ramp Method included inter-zone pressures at a range of values, but most stations had high values of P_{HG} , where the effects of fluctuations were minimized. The order of pressure stations in Figure 23 is arbitrary, but in practice, it is advantageous to run the routine in an order that minimizes the number of times that the blower door direction has to be changed.

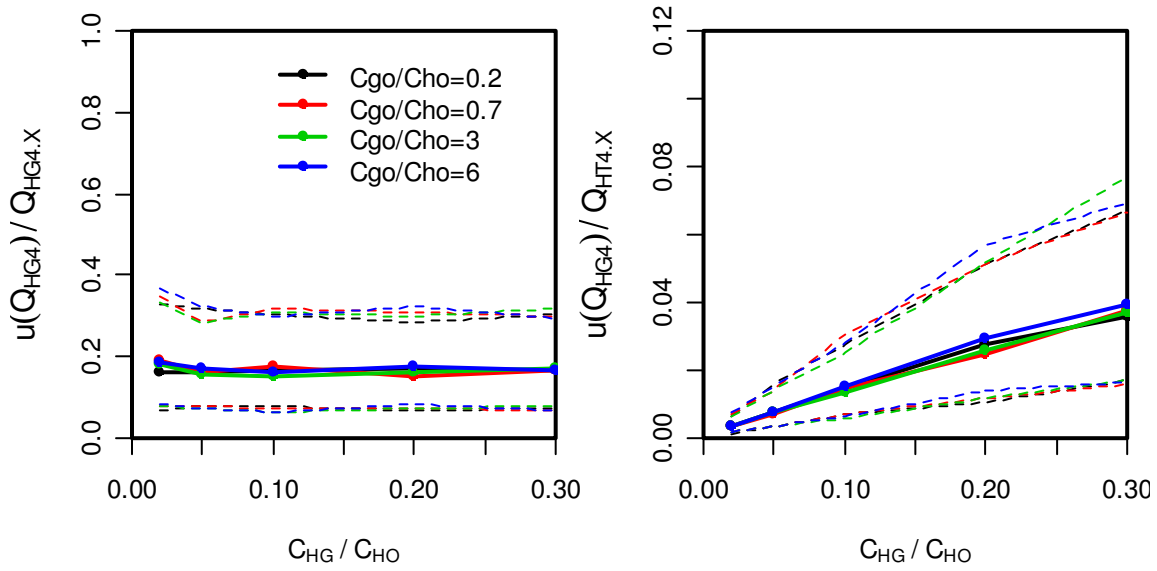


Figure 24: Double Ramp Method showing the results from the 5 parameter fit. Solid lines show the median uncertainty and dashed lines show one standard deviation above and below the median (84% and 16% quantiles). $u(P)=0.5Pa$, 1000 iterations.

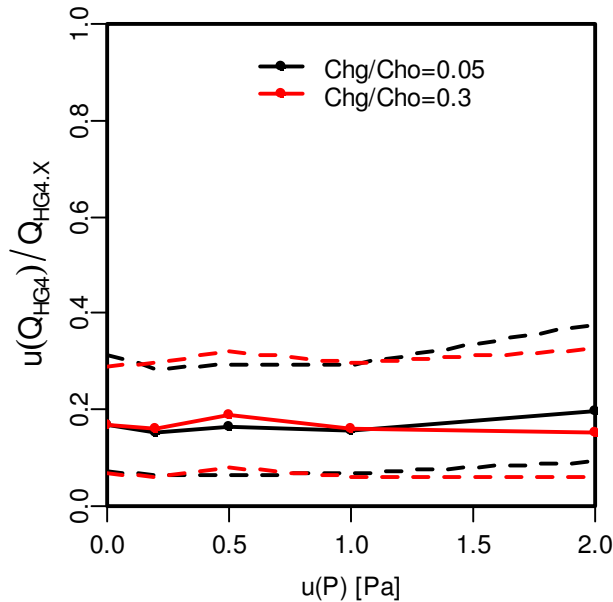


Figure 25: Double Ramp Method sensitivity to measurement uncertainty. Solid lines show the median uncertainty and dashed lines show one standard deviation above and below the median (84% and 16% quantiles). $C_{GO}/C_{HO}=0.7$.

Results from the Double Ramp Routine were shown in Figure 24 and Figure 25. In Figure 24, not only was the uncertainty consistently approximately 17% when C_{GO}/C_{HO} was varied but it was also consistent when C_{HG}/C_{HO} is varied, with only a slight increase apparent when $C_{HG}/C_{HO} = 0.02$. Thus, over the range of conditions expected in the house-garage scenario, it is expected that this testing routine

would have consistent uncertainties. The distribution of values from different test iterations was also smaller for the Double Ramp case than for the Pressure Balancing or 3SZ cases. Additionally, because the pressure difference, P_{HG} , was kept high for most of the pressure stations in the Double Ramp Routine, the sensitivity to measurement fluctuations was low, as shown in Figure 25. This routine was tested in the 192 configuration.

Table 8: Pressure Stations for Double Ramp Routine in 192 configuration. Only pressurization values are listed, but the test was designed to be performed for pressurization and depressurization. P_{HO} is controlled by adjusting Q_{HO} through door 1 in the HO interface and P_{GO} is controlled by adjusting Q_{GO} through door 2 in the GO interface.

Station index #	1	2	3	4	5	6	7	8	9	10	11	12
P_{HO} [Pa]	2.75	5.5	8.25	11	13.75	16.5	0	0	0	0	0	0
P_{GO} [Pa]	12.5	25	37.5	50	62.5	75	46	53	59	65	71	78

For reference, the pressure station values used in the Double Ramp Routine are listed in Table 8. In the Double Ramp Routine, first the pressure P_{HO} was set to 2.75 Pa and P_{GO} was set to 12.5 Pa by adjusting the flow through the blower doors in the HO and GO interfaces. Then, following the values in Table 8, the pressures P_{HO} and P_{GO} were increased, with larger increases in P_{GO} . The second part of the test required the pressure P_{HO} to be held at 0, while the pressure P_{GO} was ramped through an elevated set of pressure values. Using elevated pressures $P_{GO} > 45$ Pa reduced the impact of fluctuations in the measured pressures. Replicating these exact pressure station values was not necessary, but ramping both P_{HO} and P_{GO} led to a range of values of P_{HG} while also varying the zone pressures. This led to more consistent results than simply combining data where P_{HO} or $P_{GO} = 0$ and $P_{HO} = P_{GO}$, or than from the pressure-balancing method. From the pressure and flow rate values collected, the leakage parameters were calculated with the 5 parameter fitting method, as the single blower door data was in the previous section.

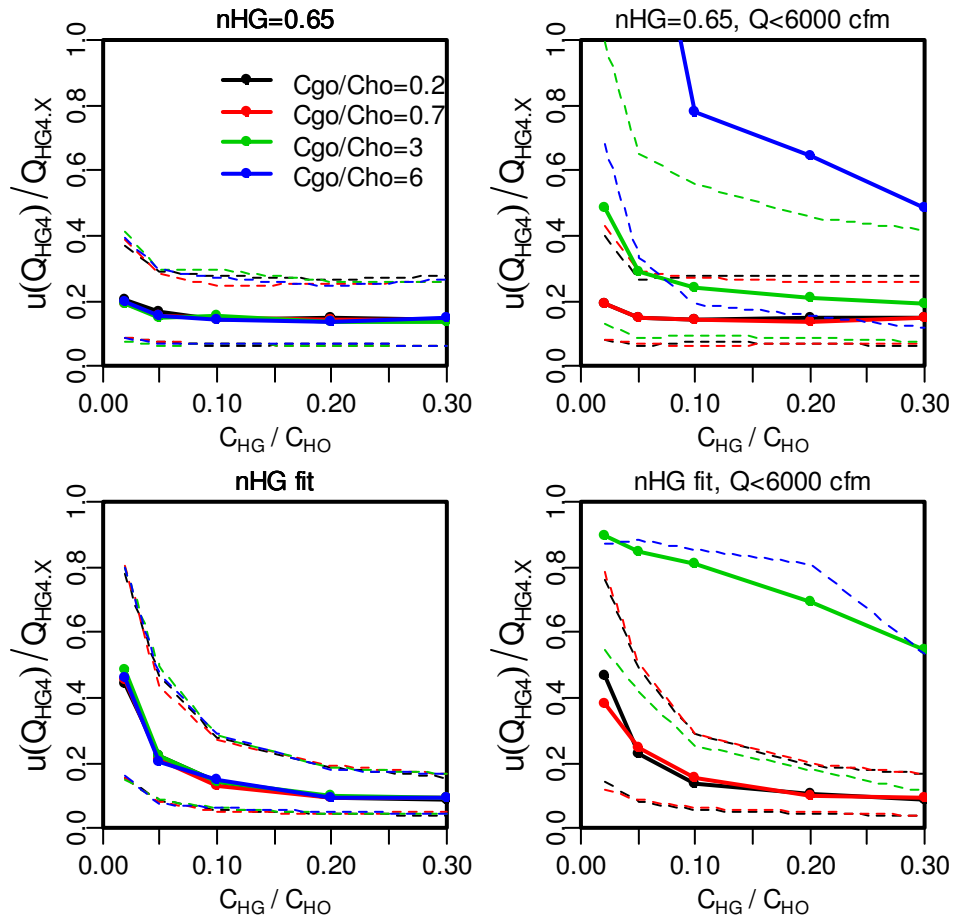


Figure 26: Uncertainty resulting from the Herrlin and Modera (1988) method to determine inter-zone leakage in the 192 configuration. In the top row, $n_{HG}=0.65$ was assumed and in the bottom row, n_{HG} was fit to the data. In the left column, pressure stations that required fan flow greater than 6000cfm were excluded. Solid lines show the median uncertainty and dashed lines show one standard deviation above and below the median (84% and 16% quantiles). $u(P)=0.5Pa$, 400 iterations.

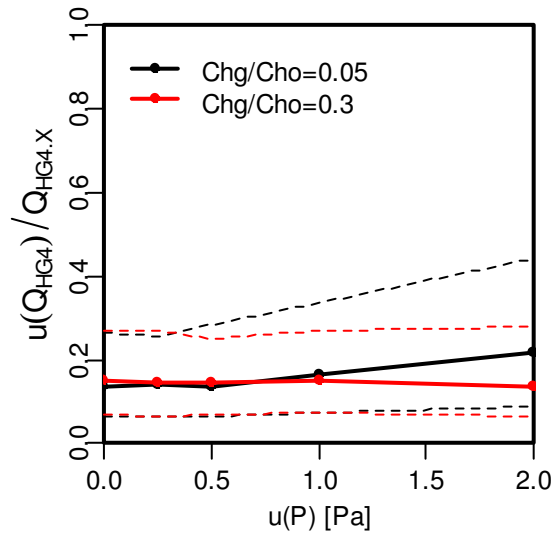


Figure 27: Sensitivity of the Herrlin and Modera (1988) method to $u(P)$. Here, $n_{HG}=0.65$ was assumed and all pressure stations were included. Solid lines show the median uncertainty and dashed lines show one standard deviation above and below the median (84% and 16% quantiles). $C_{GO}/C_{HO}=0.7$, $u(P)=0.5\text{Pa}$, 400 iterations.

The two blower door method developed by Herrlin and Modera (1988) where the first zone is held at 50Pa while the inter-zone pressure is varied was also used to determine the inter-zone leakage. This method was tested fitting both C_{HG} and n_{HG} and also fitting only C_{HG} and assuming $n_{HG}=0.65$, as shown in Figure 26. While both methods gave reasonable results when all points were included, some of these test cases included very high fan flow rates. When pressure stations drawing more than 6000 cfm through a single blower door were excluded, the method assuming $n_{HG}=0.65$ performed better. It was not surprising that if fewer pressure stations were sampled, the pressure exponent fit was less accurate. If two blower doors are available, the Herrlin and Modera method, modified to fix $n_{HG}=0.65$, can be used to determine the inter-zone leakage to within 20% across a range of conditions in the 192 configuration.

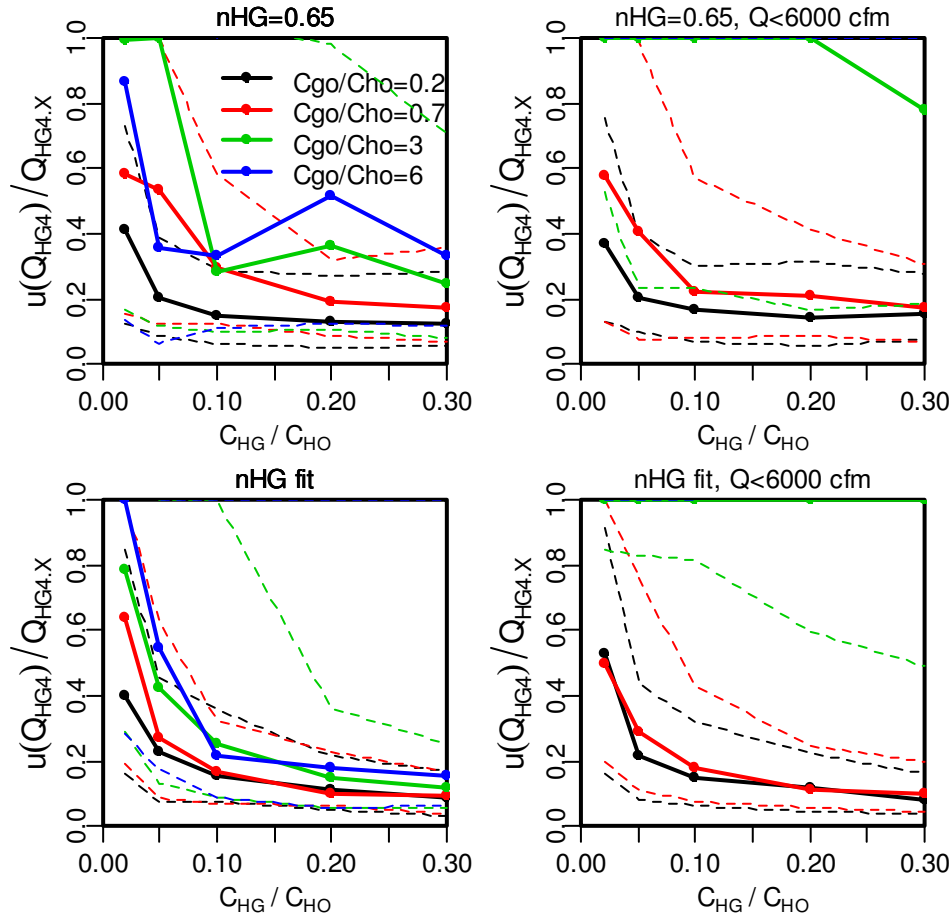
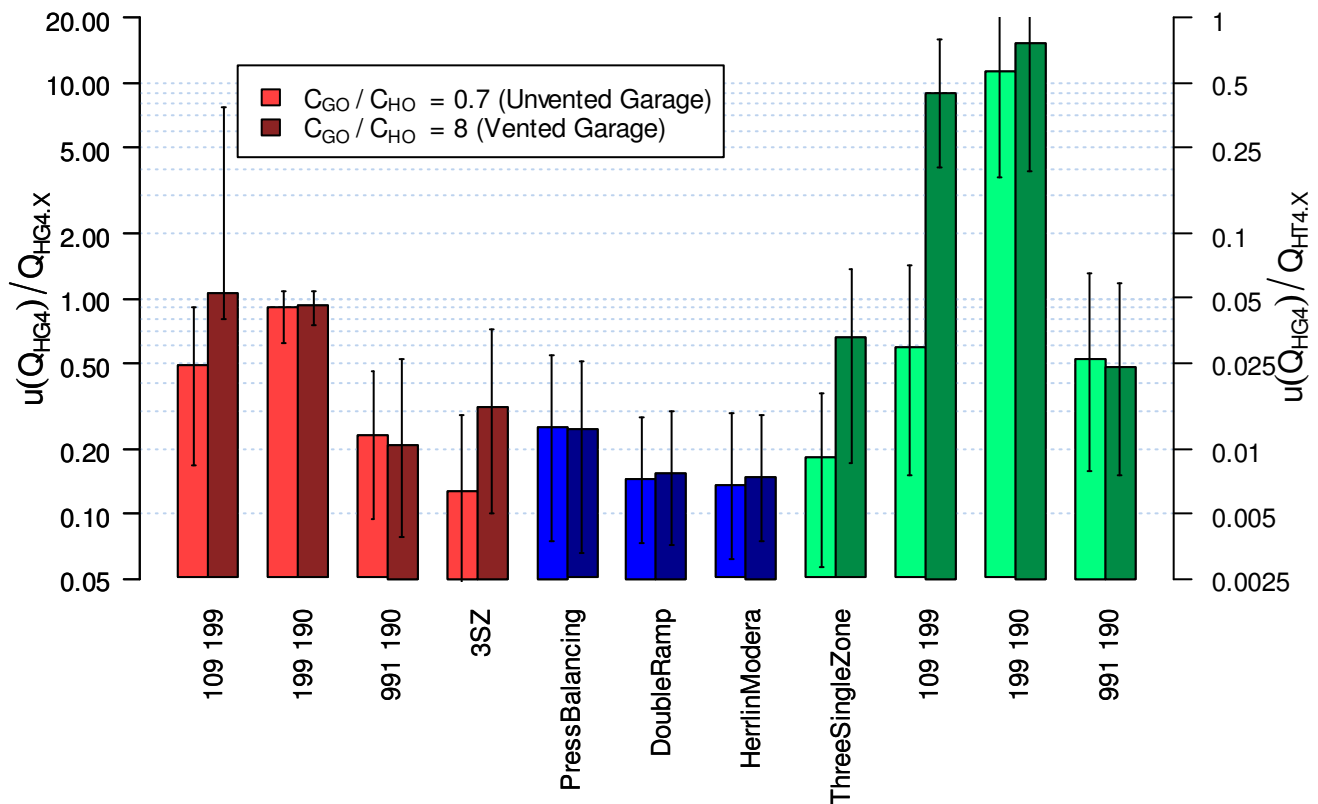


Figure 28: Using instead the 129 configuration, uncertainty resulting from the Herrlin and Modera (1988) method to determine inter-zone leakage. In the top row, $n_{HG}=0.65$ was assumed and in the bottom row, n_{HG} was fit to the data. In the left column, pressure stations that required fan flow greater than 6000cfm were excluded. Solid lines show the median uncertainty and dashed lines show one standard deviation above and below the median (84% and 16% quantiles). $u(P)=0.5Pa$, 100 iterations.

While it is possible to use the method of Herrlin and Modera in the 129 configuration instead of the 192 configuration, the required flow rates were even higher in the 129 case, making that test impractical to perform. The results for the 129 configuration test of the Herrlin and Modera method are shown in Figure 28. While the median uncertainty tended to be moderate, the dashed line showing one standard deviation above the median was quite high, suggesting that the method regularly failed to predict the leakage to within 100%. Thus, this method is not recommended for use in the 129 configuration.

In general, however, the Herrlin and Modera method provided the highest accuracy of the methods examined, with the added advantage of being relatively straightforward computationally. For these reasons, the method of Herrlin and Modera (1988) is a robust means to determine the leakage between two zones, provided two blower doors with sufficient power are available.

Summary of synthesized data analysis



Multiple Pressure, 1BD, 5Param Fit | Mult. Pres., 2BD | Single Pressure, 3Param Fit

Figure 29: Summary of the median uncertainty in Q_{HG4} , scaled by itself (left axis) and the total house leakage Q_{HT4} (right axis). Single Blower Door tests using multiple pressure stations (red) and Two Blower Door tests using multiple pressure stations (blue) use the 5 Parameter fitting method. For the single pressure station methods (green), the measurements were taken at 50 Pa and the 3 Parameter, least squares fitting method was used. The left and right bar in each cluster is characteristic of the unvented and vented garage case, respectively. The two y-axes are only equivalent when $C_{HG}/C_{HO}=0.05$ as it does here. $u(P) = 0.5Pa$.

Figure 29 summarizes the results from the synthesized data analysis. The pair of single door configurations with the lowest uncertainty was 991/190 using the multi-pressure station, 5 parameter fitting method (see Figure 15 for more detail). While other pairs of single blower door configurations had similar results when the leakage area of the two zones was comparable ($C_{GO}/C_{HO}<3$) as shown in Figure 13 and Figure 14, the pair 991/190 was more accurate when the second zone was very leaky. (199/091 is recommended if the first zone is leakier than the second). The Three Single Zone method requires an additional test but the results were excellent when the leakage area of the two zones was comparable: for $C_{GO}/C_{HO}=0.7$, the median uncertainty in Q_{HG4} was 13% of itself when multiple pressure stations are used. When the garage zone was very leaky ($C_{GO}/C_{HO}=8$), the uncertainty increased to a still

respectable 32% of Q_{HG4} . The results in Figure 29 were calculated for when $C_{HG}/C_{HO}=0.05$, and the uncertainty of the Three Single Zone method improved to less than 20% for all cases when the inter-zonal leakage as a fraction of the total house leakage was less than 0.15 as shown in Figure 8. The test configuration pair 109/199 used by Blasnik and Fitzgerald (1992) and Offerman (2009) provided relatively consistent results if the two zones had comparable leakage area (uncertainty is about 50% of Q_{HG4} at $C_{GO}/C_{HO}=0.7$), but when $C_{GO}/C_{HO}=8$, the uncertainty is near 100% of Q_{HG4} . Although this uncertainty may seem small relative to the total house leakage, the test results in this case are not terribly meaningful. Because the uncertainty introduced due to fluctuations in measured quantities was large relative to the small pressure difference associated with the inter-zone leakage, the calculation method failed in about half of cases to find a good fit for C_{HG} (see Figure 18). Because the fraction of tests that failed was still 30% even when the leakage fraction $C_{HG}/C_{HO}=0.3$, this test configuration pair is not recommended. Results for 199/190 are also included to show that the performance was also poor and should be avoided for the same reasons as 109/199.

From this analysis, it appears that Two Blower Door methods can be used to determine the inter-zone leakage to within 30%. The Double Ramp Method was used to determine Q_{HG4} to within 16%, regardless of C_{GO}/C_{HO} or C_{HG}/C_{HO} (see Figure 24). This measurement routine was also largely insensitive to fluctuations in the measured quantities (see Figure 25), making it a very robust choice if two blower doors are available for use. The Pressure Balancing Method led to uncertainty of approximately 25% of Q_{HG4} . The method developed by Herrlin and Modera (1988) led to very similar results to the Double Ramp method (for H&M, $u(Q_{HG4})/Q_{HG4} < 16\%$), but the methodology and calculations are much simpler.

The 5 Parameter fitting analysis method was found to have the lowest uncertainty compared with the 6, 10, and 12 Parameter fitting methods. I.e., fitting pressurization and depressurization conditions jointly, as well as assuming $n_{HG}=0.65$ reduced the uncertainty in Q_{HG4} . This was true for methods using one and two blower doors. In a situation where the inter-zone leakage between two zones is a large fraction of the zone leakage (such as the case of a house divided into two interior rooms), the 6 Parameter model may provide better results.

Using Single Pressure Station tests (blue bars in Figure 29), the inter-zone leakage can really only be reliably determined if C_{GO}/C_{HO} is not large (i.e., less than 3), for which conditions the Three Single Zone Method leads to an uncertainty of 20% of Q_{HG4} . Single Pressure Station methods using two single door configurations cannot be used reliably to determine Q_{HG4} . All results in Figure 29 assume $u(P)=0.5\text{Pa}$, as that was typical of the field homes surveyed. Under very calm conditions, $u(P)$ may be as low as 0.1 or 0.2Pa and this may lower the expected uncertainty slightly as shown in the previous section.

Field Testing and Evaluation

Blower door tests were completed at 7 houses in order to compare the results obtained from the various test configuration pairs. Data from House 1 was not used because at the end of the testing it was found that the attic access had blown open at some undetermined time during the testing. Field testing was completed independently from the synthesized data analysis so there are some optimal testing methods that were not used at the field sites as well as some sub-optimal methods and duplicative tests that were completed. At each site, the house to outdoors and house to garage pressure differences were

measured using a digital manometer (Energy Conservatory DG 700). Blower door tests were completed using one or two blower doors from The Energy Conservatory, controlled by a laptop computer.

Procedure

For single blower door tests, the blower door was controlled to vary the test pressure between 0 and a maximum test pressure. The pressures and flows were sampled and recorded every second. For House 2, 3, 6 and 7, each pressure station was held for 2 minutes. The pressure stations increased by 5Pa until the maximum test pressure was reached. In House 4 and House 5, the pressure was increased slowly and steadily to the maximum pressure, rather than stopping at 5Pa increments. The maximum test pressure was typically 60Pa. In some cases, a peak pressure of 60Pa could not be reached. For cases when the blower door was in the garage-outdoors interface in houses 5 and 6, the peak test pressure was only 40Pa and 20Pa respectively, due to the high garage leakage rates in those houses. For two blower door tests, a range of testing strategies were used, some of which are discussed in the analysis of the two blower door results below. The measurement data were screened to remove points where the pressure was changing quickly (i.e., the blower door was adjusting between stations). A cutoff value of 0.3Pa/s was used.

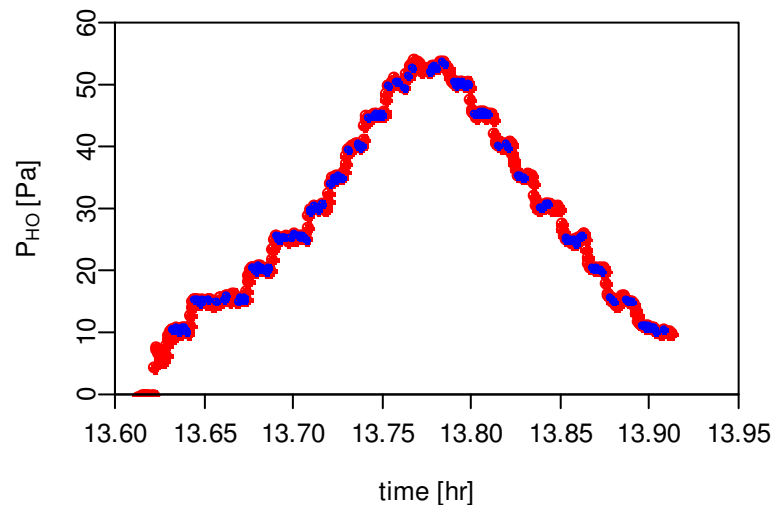


Figure 30: Data screening for PHO in 192 configuration. All pressure measurements collected are shown in red, and points used in the data analysis are shown in blue.

Data were screened to remove transition points between measurement stations as well as any outlying points that were thought to result from disturbances to the tubing, equipment or test configuration (such as a door being opened). Test pressure stations at less than 10Pa were not included in the analysis, because the measured fluctuations are large compared with the measured pressures in this regime.

To determine the mean pressure offset each pressure, P_{HO} , P_{HG} and P_{GO} , the pressure differential between the house and outside and house and garage was recorded over a 4-5 minute period. This pressure differential was measured when all doors were closed and the blower door was off

(configuration 999) and was used to calculate the mean offset value for P_{HO} and P_{GO} . This value was then subtracted from the corresponding pressure measurements at each house. These pressure offsets may not be the values that correspond to the conditions during the test but there is no way to simultaneously measure the offset while performing the test.

Table 9: Test configurations run for each house. House 7 did not have a doorway in the garage-outdoor interface. House 6 refers to House 6 as found. House 6 was also tested when the attic hatch in the garage was sealed, but only in limited configurations which are not presented here. The 999 configuration refers to all doors closed, with no blower door operation.

	House 2	House 3	House 4	House 5	House 6	House 7
999		✓	✓	✓	✓	✓
109 or 901	✓	✓	✓	✓	✓	✓
190 or 910	✓	✓	✓	✓	✓	✓
199	✓	✓	✓	✓	✓	✓
091 or 019	✓	✓	✓	✓	✓	✓
991		✓	✓	✓	✓	
919	✓	✓	✓	✓	✓	✓
192	✓	✓	✓	✓	✓	
129	✓	✓	✓	✓	✓	✓

Analysis

In the analysis of the field data, we calculated the leakage flows Q_{HG4} , Q_{HO4} and Q_{GO4} from the pressure exponents and flow coefficients fitted to the data, using various methods described in *Inter-Zone Leakage Results*. The uncertainty in these results was also estimated by interpolating from the synthesized data results to the observed conditions at the field sites. To do this interpolation, an estimate was needed of the magnitude of the fluctuations in the measured pressure differences and flow rates. It is expected that pressure fluctuations due to wind occur and that the magnitude of these fluctuations depends on the site and testing conditions. In this analysis, the magnitude of pressure fluctuations was calculated from the deviation from a curve fit in the form $Q=CP^n$, as discussed in the Methods section for the synthesized data and in Appendix A.

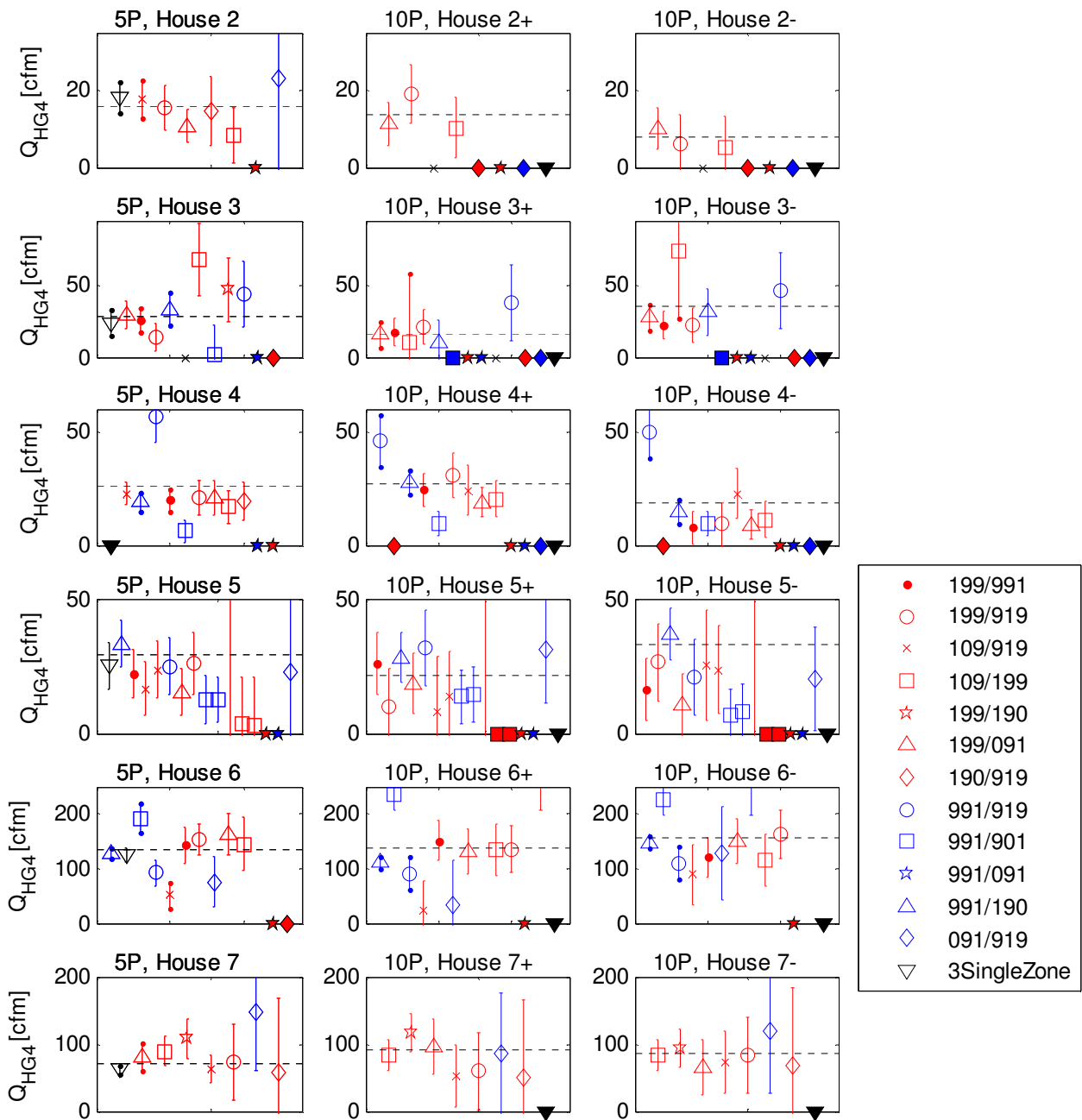


Figure 31: Q_{HG4} measured using different single blower door test configuration sets (denoted by symbol) for the 10 parameter method (pressurization in left column, depressurization in center) and 5 parameter method (right). Test configurations are ordered with increased expected uncertainty toward the left of each subplot (denoted by error bars). Uncertainty-weighted average value shown by dashed line. Solid symbols indicate tests for which a good fit was not found (i.e., one or more parameters at the boundary of range). The blue and red symbols of the same shape are symmetric test pairs.

The field data collected in various single blower door configurations were analyzed using the same tools used to analyze the synthesized data, namely the 5 and 10 Parameter fitting methods using optimization to solve for the parameters. As expected from the analysis of the synthesized data, there was variation between the results of the different test configuration pairs. The error bars in Figure 31 were interpolated from the results of the synthesized data analysis and the median error fraction for Q_{HG4} was determined for varied $u(P)$, C_{HG}/C_{HO} , and C_{GO}/C_{HO} for each test pair. Points are arranged by expected uncertainty, increasing from left to right.

The dashed line in Figure 31 shows the uncertainty-weighted average value for Q_{HG4} , defined as:

$$\bar{Q}_{HG} = \frac{\sum_{i=1}^n (Q_{HG,i} / \sigma_i^2)}{\sum_{i=1}^n (1 / \sigma_i^2)} \quad (15)$$

where σ_i^2 is the known variance in $Q_{HG,i}$, and $Q_{HG,i}$ is Q_{HG} calculated using test method i . Since $n_{HG}=0.65$ in this analysis, \bar{Q}_{HG} varies from \bar{C}_{HG} by a factor of 4^n . Leakage parameters resulting from the best set of single blower door tests are listed in Table 10 and Table 11 for the 10 and 5 Parameter fitting methods respectively. Additionally, the estimated magnitude of the measurement uncertainty $u(P)$ is listed. The ratios Q_{GO}/Q_{HO} and Q_{HG}/Q_{HO} are listed in place of ratios C_{GO}/C_{HO} and C_{HG}/C_{HO} in this section, because unlike in the synthesized data analysis, the mean pressure exponent may not be 0.65 for these houses.

Test pairs for which no solution was found are plotted on the x-axis with a solid symbol. A larger number of tests failed for houses 2, 3, 4 and 5 where the quantity C_{HG} was less than 6% of C_{HO} . At some houses, the same symbol is plotted twice—this occurs when two equivalent tests were performed (e.g., 109 and 901, enabling test pairs 109/199 and 901/199). That these tests tended to give very similar results (within 5% of Q_{HG4}) suggested that the difference in performance between non-equivalent test configurations was likely greater than the uncertainty associated with repeat testing (including blower door installation, wind variation over time, etc.). The Three Single Zone method was consistently very close to the uncertainty-weighted mean value. The exception was at House 4, but it was noted that the data obtained in the 091 configuration did not fall on a consistent P vs. Q curve, suggesting there may have been changing wind conditions with time during that test.

Table 10: Parameters calculated from 6 houses using the 10 parameter fitting method, resulting from the test configuration set of single blower door tests with the lowest uncertainty (i.e., the left-most test configuration that did not fail in the center column of Figure 31).

	House 2	House 3	House 4	House 5	House 6 (as found)	House 7
$u(P)$ [Pa]	0.61	1.42	0.46	0.49	0.35	0.78
C_{HO+} [cfm/Pa ⁿ]	197	291	122	140	129	256
C_{HO-} [cfm/Pa ⁿ]	151	283	47	157	102	254
C_{HG+} [cfm/Pa ⁿ]	4.6	6.5	18.7	10.5	45	34
C_{HG-} [cfm/Pa ⁿ]	4.1	11.3	20.1	6.7	60	34
C_{GO+} [cfm/Pa ⁿ]	148	40	100	687	1224	157
C_{GO-} [cfm/Pa ⁿ]	133	53	36	578	880	162
n_{HO+}	0.63	0.65	0.73	0.78	0.63	0.64
n_{HO-}	0.69	0.80	0.98	0.72	0.64	0.61
n_{GO+}	0.58	0.73	0.40	0.58	0.53	0.56
n_{GO-}	0.69	0.77	0.85	0.61	0.62	0.56
Q_{GO}/Q_{HO}	0.80	0.17	0.57	3.4	8.3	0.57
Q_{HG}/Q_{HO}	0.025	0.028	0.20	0.051	0.48	0.14

Table 11: Parameters calculated from 6 houses, resulting from the test configuration set of single blower door tests with the lowest uncertainty (i.e., the left-most test configuration that did not fail in the first column of Figure 31). The values were calculated using 5 parameter fitting method using multiple pressure stations.

	House 2	House 3	House 4	House 5	House 6 (as found)	House 7
$u(P)$ [Pa]	0.61	1.42	0.46	0.49	0.35	0.78
C_{HO} [cfm/Pa ⁿ]	211	585	146	239	119	273
C_{HG} [cfm/Pa ⁿ]	7.3	9.8	9.2	10.2	52	25
C_{GO} [cfm/Pa ⁿ]	160	117	102	771	1129	166
n_{HO}	0.60	0.50	0.67	0.60	0.63	0.62
n_{GO}	0.60	0.49	0.57	0.53	0.55	0.51
Q_{GO}/Q_{HO}	0.76	0.20	0.60	2.9	8.5	0.53
Q_{HG}/Q_{HO}	0.037	0.021	0.061	0.046	0.45	0.096

There are three main factors that have a major impact on the uncertainty of the house-garage leakage: the magnitude of pressure fluctuations $u(P)$, the relative leakiness of the two zones C_{GO}/C_{HO} , and the magnitude of the interface leakage C_{HG}/C_{HO} . Although wind speed was not measured directly, based on observations of the conditions and calculated fluctuations in the measured pressures, one house had windy conditions (House 3) and the other 5 houses had light wind (House 2, 4, 5 and 6). Two houses had high leakage in the Garage zone with $Q_{GO}/Q_{HO} > 2$ (House 5 and 6), and three houses had a very tight house-garage interface wall with $Q_{HG}/Q_{HO} < 5\%$ (House 2, House 3 and House 5). Also, House 6 had an attic hatch connecting the garage and house, hence the large interface leakage flow in that case.

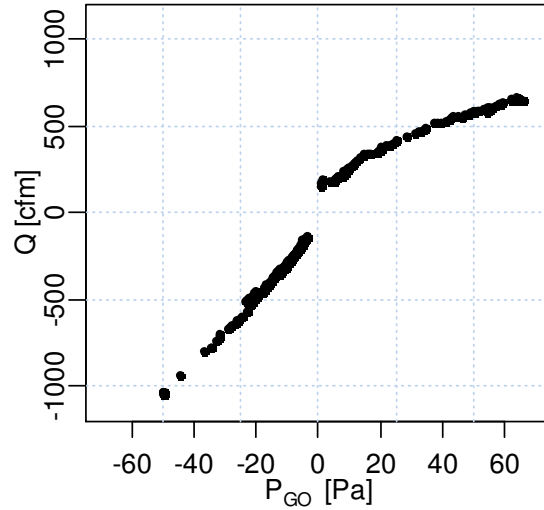


Figure 32: Flow rate measured in the 991 configuration at House 4 versus, illustrating the difference between leakage under pressurization ($P_{GO}>0$) and depressurization ($P_{GO}<0$).

The attached garage in House 4 showed remarkably different leakage behavior under pressurization and depressurization conditions as shown in Figure 32. Q_{GO+} is 60% higher than Q_{GO-} (see C_{GO} and n_{GO} in Table 10) whereas it was assumed in the synthesized data analysis that Q_{+} exceeds Q_{-} by $2\% \pm 11$ percentage points (Sherman and Dickerhoff 1998). The large difference between pressurization and depressurization leakage may have increased the error in the results for House 4 above the expected uncertainty, particularly when the 5 parameter fitting method was used.

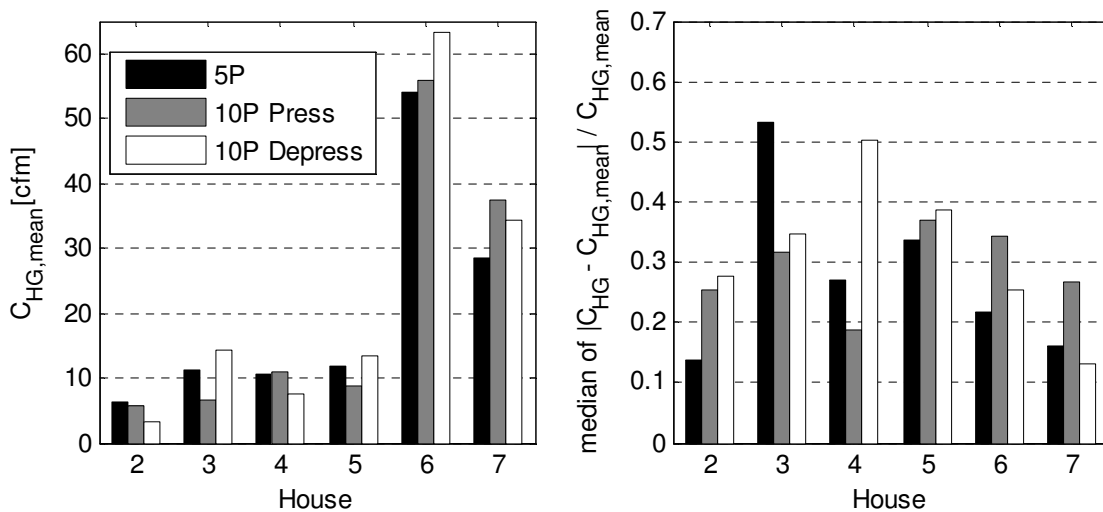


Figure 33: Uncertainty-weighted mean value of C_{HG} for each house (left). On the right, the median deviation from that mean value from the set of all test pairs available at that house. The test pairs where no solution was found were omitted.

In general, the uncertainty shown by the error bars seemed to account for the scatter in the test results. Comparing the results for the 5 Parameter and the 10 Parameter methods, there were definitely fewer failed tests when the 5 Parameter fit was used (10 for the 5 Parameter method versus 19 for the 10

Parameter case). Based on the synthesized data analysis, the 5 Parameter method was expected to give slightly more consistent results than the 10 Parameter method. Besides the reduction in failed curve fits, the two methods showed similar variability in the results, as shown in Figure 33. The deviations shown in Figure 33 were not consistently lower for the 5 Parameter method than for 10 Parameter fitting, in fact the variability at House 3 and 5 was higher for the 5 Parameter fit. Although the houses had a wide range of values for $u(P)$, C_{HG}/C_{HO} , and C_{GO}/C_{HO} , the variation between tests pairs was relatively consistent between houses, as quantified by the median value of $|C_{HG}-C_{HG,mean}|/C_{HG,mean}$. Overall, 50% of the values were typically within 35% of best guess using the 5 or 10 Parameter fitting method. Omission of cases where no good solution was found biased this result somewhat low. Additionally, proximity to the mean in this situation does not necessarily indicate accuracy—it is possible that many tests may have biased the result in the same direction.

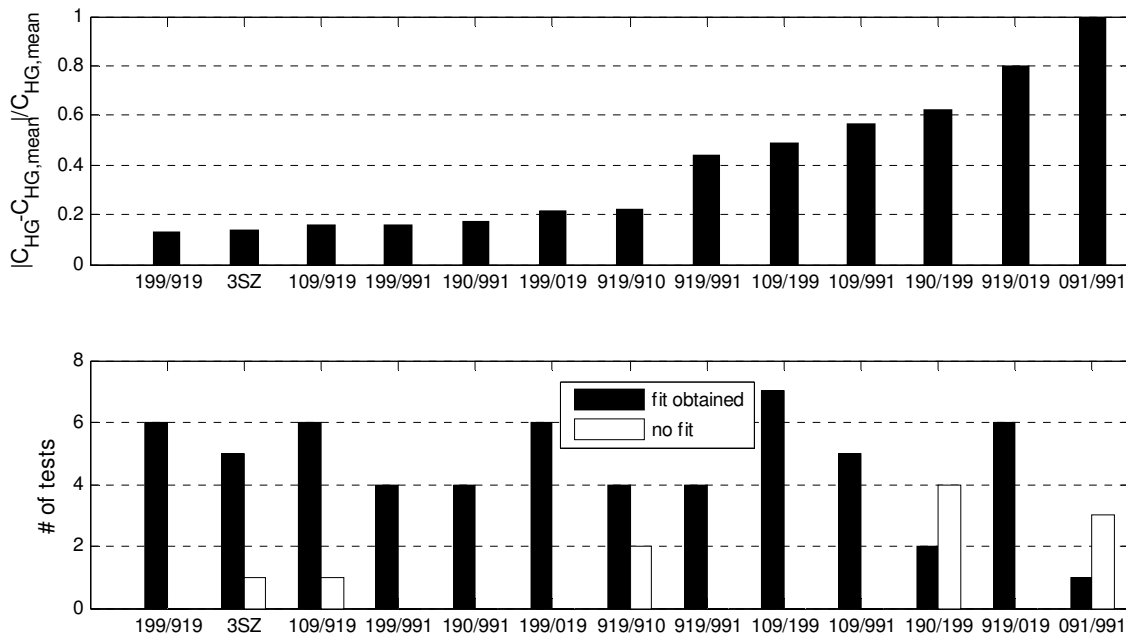


Figure 34: Median deviation from the house mean value for C_{HG} by test configuration pair (top) and number of test sets completed (bottom), separated by whether or not a good fit was found.

Although the variation between test set results was consistent between houses, the same could not be said for the results from a particular test set. Figure 34 confirms that some sets showed much more consistent results than others, as seen in the analysis of the synthesized data. Assuming the uncertainty-weighted mean value of C_{HG} for all of the sets of single blower door tests provided a good estimate of the true value, the test sets that were most consistently close to this best estimate were: 199/919, the Three Single Zone Method, 109/919, 199/991, 190/991, and 199/091. The most versatile pair of single blower door tests identified in the synthesized data analysis, 190/991, had among the lowest deviations from the mean. The magnitude of the deviations shown in Figure 34 was also consistent with the uncertainties reported in the synthesized data analysis of about 20% for the best methods. The

number of tests that failed to find a good fit should also be taken into consideration when comparing the test pairs. For example, 919/910 had moderate performance, but 33% of tests were unsuccessful at finding a good fit, suggesting this pair may not be very robust. The pairs 190/199, 091/991 and 109/919 also showed elevated failure rates in the synthesized data analysis. The test pair 919/910 failed in 2/6 cases when applied to the field data, but almost never failed in the synthesized data analysis. While this pair did not trigger a 'fail' flag in the synthesized data analysis because the parameters were not at a boundary constraint, this method consistently overestimated Q_{HG4} by a large margin, so it is not recommended.

Expected vs. Observed variability in test results

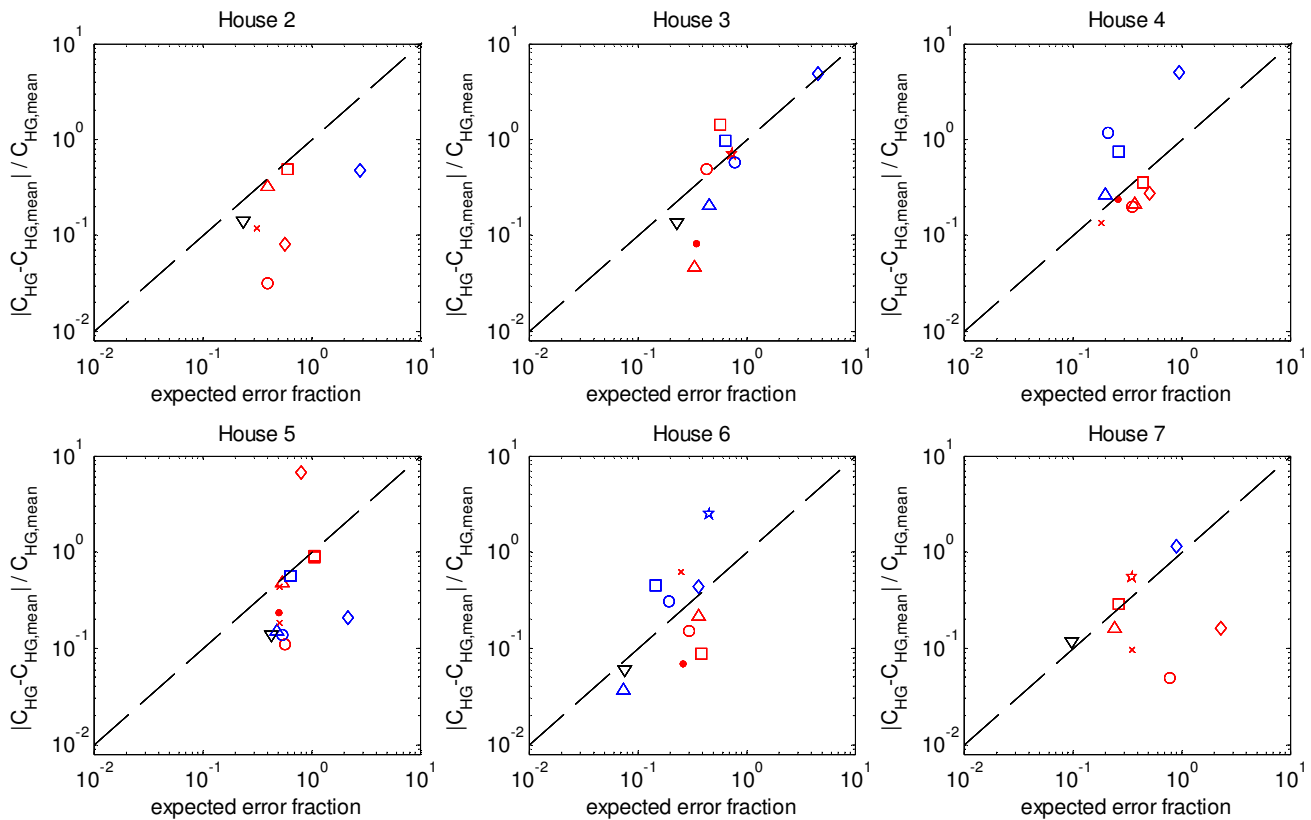


Figure 35: Deviation of individual test results relative to the median value for C_{HG} compared with the expected error fraction for 5 Parameter fitting method. The expected error fraction is the median fractional uncertainty in Q_{HG4} , interpolated from the synthesized data analysis for the values of $u(P)$, C_{GO}/C_{HO} and C_{HG}/C_{HO} specific to the house. For symbols, see legend in Figure 31.

One objective of the synthesized data analysis was to estimate the expected uncertainty for different test methods. To determine how well the expected error fraction compares with the observed variability in the field data results, the normalized difference between C_{HG} and the weighted mean C_{HG} for all tests at that house is plotted in Figure 35 versus the normalized expected error. If the expected error accurately describes the median error, we would expect half the points above the unity line (dashed) and half below. For most houses (3,4, 5 and 6), the dashed line fell near the center of the cluster, thus the expected error predicted reasonably well the variability between tests.

At two houses, House 2 and House 7, the points followed the same trend as the line, but fell slightly below the curve. This suggests that the uncertainty analysis captured the functional dependence of factors causing uncertainty, but was overly conservative in predicting the magnitude of the uncertainty. In these two cases, measurements of the pressures P_{HO} and P_{HG} when all doors were closed (999 configuration) had very small fluctuations, suggesting that there were very low wind fluctuations at the time of the tests at these houses. The method described in the synthesized data analysis to quantify the uncertainty in the measured quantities by looking at the deviation of points from a fitted curve may have led to an overestimate of the measurement uncertainty in these two cases. The argument against using the fluctuations in P_{HO} and P_{HG} in the 999 configuration to estimate wind fluctuations is that some of these pressure fluctuations would be balanced by correlated fluctuations in Q . However, the deviations calculated from the fitted curve were, in some cases, larger than the magnitude of fluctuations observed in the 999 configuration. This may have been due to time variability in the wind conditions. It may be that the minimum of these two metrics is a better metric for the measurement uncertainty.

Two Blower Door Field Tests

As discussed in the analysis of the synthesized data, there are a wide range of pressure station sets that can be tested using two blower doors simultaneously. Because the field data was completed independently from the synthesized data analysis, it was not possible to apply all of the two blower door methods discussed in the synthesized data analysis to the field data. However, two blower door field data was collected using a range of strategies and the results are presented here.

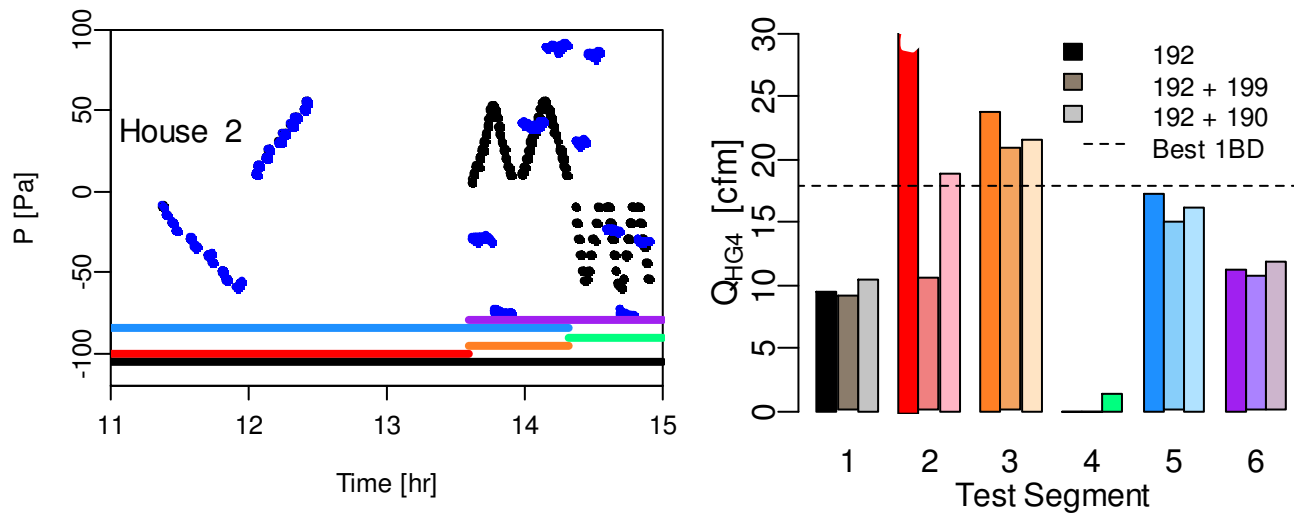


Figure 36: Two Blower Door tests in the 192 configuration for House 2. The left panel shows the pressures established for P_{HO} (black) and P_{GO} (blue). The stripes along the bottom of the left panel demarcate which test data corresponds to the calculated leakage flow in the right panel. Q_{HG4} was calculated using just the 192 segment, as well as by combining the 192 segment with 199 or 190 test data (shown by the three bars in each cluster). The right panel also shows the value for the best of the single blower door tests. 5 Parameter fitting was used.

In Figure 36, the pressure stations are shown for tests performed on House 2, as well as the corresponding inter-zone leakage calculated using different portions of that test data. Other subsets are also possible. Test Segment 1 in the right panel corresponds with the values calculated when all data was used in the parameter optimization, and it was expected that this would provide the best estimate of Q_{HG4} . Although this estimate was about 30% less than the leakage flow found from the best set of single blower door tests, there was significant variability in the single blower door results (Q_{HG4} was between 8 and 23 cfm). In Figure 31, the median leakage value from the 10 Parameter method was closer to 10 cfm. Test Segment 2 corresponds with the first tests shown in the left panel. The strategy used here was the pressure-balancing method: data was collected where P_{HO} was increased with P_{GO} to minimize leakage across the HG interface. While it was not expected that the 192 pressure-balancing data alone would give an accurate determination of the HG leakage (first column of red cluster), when combined with the 190 test data, the result was consistent with the best 1BD test. Test segments 5 and 6 used larger subsets of the 192 data and gave slightly higher estimates of Q_{HG4} . The data in Test Segment 4 did not give a good fit for the HG leakage flow. One reason that the results that used Segments 3 and 4 may have been poorly constrained is that P_{HO} was only positive for Segment 3 and only negative for Segment 4. It may be that sampling positive and negative pressure stations and then fitting pressurization and depressurization parameters jointly using the 5 Parameter method leads certain errors to be reduced. This may be why Segment 6 (which was Segment 3 + Segment 4) was more consistent with the other results than Segment 4 alone.

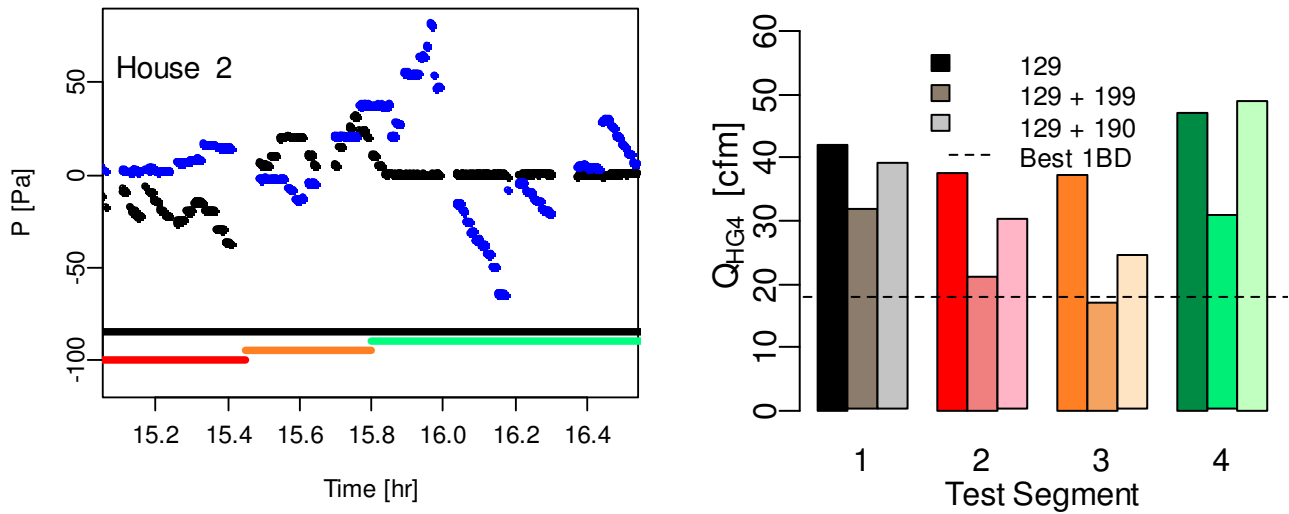


Figure 37: Two Blower Door tests in the 129 configuration for House 2. The left panel shows the pressures established for P_{HO} (black) and P_{GO} (blue). The stripes along the bottom of the left panel demarcate which test data corresponds to the calculated leakage flow in the right panel. Q_{HG4} was calculated using just the 129 segment, as well as by combining the 129 segment with 199 or 190 test data (shown by the three bars in each cluster). The right panel also shows the value for the best of the single blower door tests. 5 Parameter fitting was used.

Although the 129 test data was not expected to provide as consistent results based on the synthesized data analysis, the results of 129 testing is presented for House 2 in Figure 37 for comparison with the 192 and single blower door testing results. While including 199 or 190 test data in the analysis led to similar results for the 192 configuration, with the 129 configuration this was not the case. When the 199 test data was included, the leakage flow calculated from the 129 data was lower and more consistent with the 1BD and 192 results. It is not clear why the 129 configuration lead to higher estimates of Q_{HG4} than the 192 configuration, but may have been caused by calibration error in the blower doors. As discussed in the synthesized data analysis section, the uncertainty in the 129 configuration is strongly dependent on bias error in the flow rate measurements.

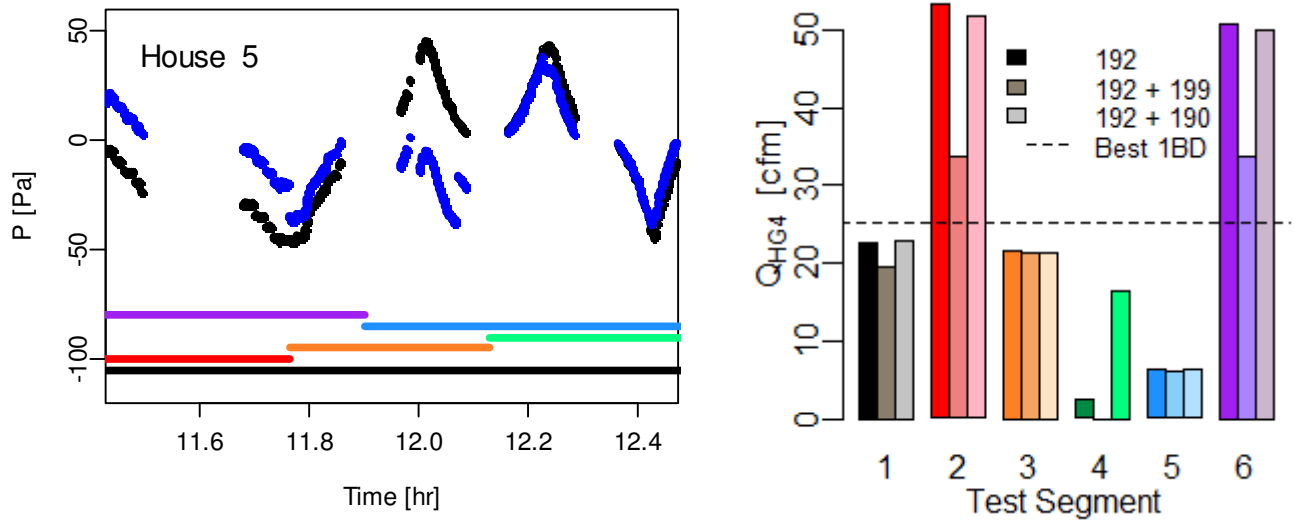


Figure 38: Two Blower Door tests for House 5. The left panel shows the pressures established for P_{HO} (black) and P_{GO} (blue) in the 192 configuration. The stripes along the bottom of the left panel demarcate which test data corresponds to the calculated leakage flow in the right panel. Q_{HG4} was calculated using just the 192 segment, as well as by combining the 192 segment with 199 or 190 test data (shown by the three bars in each cluster). The right panel also shows the value for the best of the single blower door tests. 5 Parameter fitting was used.

The Two Blower Door tests in the 192 performed on House 5 had more variation than those completed at House 2, as shown in Figure 38. The result for all 192 configuration data, Test Segment 1, was only 8% less than the best Single Blower Door value for Q_{HG4} , and Segment 3 had similar results. One strategy used here was to establish a large pressure difference across the HG interface during the testing, as shown in Test Segments 2 and 3 in Figure 38. Increasing the pressure difference across the HG interface increases the pressure measurement signal relative to random noise that may be present in the signal. However, it appears that taking measurements over a range of pressures P_{HG} provides for a more robust fit (in Segment 2, P_{HG} was approximately constant). For example, Segment 4 included points where P_{HO} and P_{GO} were equal (pressure-balancing) as well as points where they were offset by 10Pa to give $P_{HG}=10$ Pa. As at House 2, the pressure-balancing data combined with 190 test data lead to a value of Q_{HG4} more consistent with other strategies. Test Segment 3 included points where P_{HO} and P_{GO} were offset from each other, but by different amounts, and for this segment, the results were consistent with the 1BD methods.

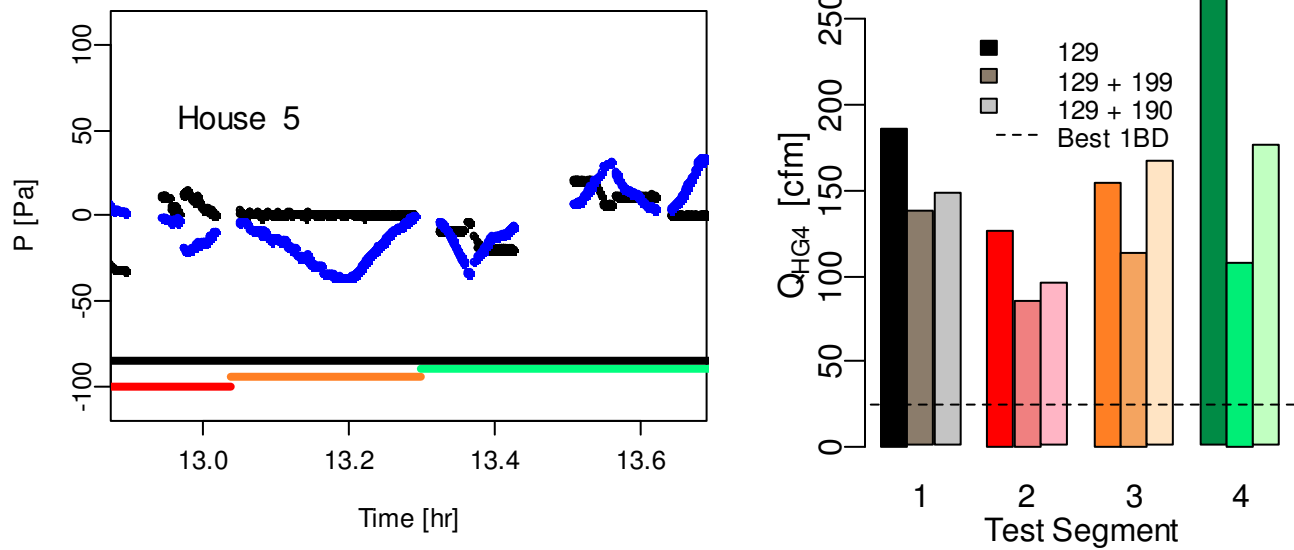


Figure 39: Two Blower Door tests in the 129 configuration for House 5. The left panel shows the pressures established for P_{HO} (black) and P_{GO} (blue). The stripes along the bottom of the left panel demarcate which test data corresponds to the calculated leakage flow in the right panel. Q_{HG4} was calculated using just the 129 segment, as well as by combining the 129 segment with 199 or 190 test data (shown by the three bars in each cluster). The right panel also shows the value for the best of the single blower door tests. 5 Parameter fitting was used.

As for House 2, the 129 configuration test values of Q_{HG4} were higher than the 192 or single blower door test results for House 5, shown in Figure 39. The 129 estimates for House 5 were in fact much higher than the results from other methods. If this is the result of bias in the measured flow rate, it may be possible to estimate and correct for the bias if test data is obtained in multiple configurations, however, this was not done for this study. Because of the uncertainty observed in the 129 testing in the synthesized data analysis as well as the variability of 129 test results in the field testing, testing in the 129 configuration does not appear to be very robust and is not recommended.

In general, there were testing methods using two blower doors that provided good results, but also many possibilities that did not. One should not assume that because the pressure difference P_{HG} is large that C_{HG} (and therefore Q_{HG4}) will be well determined.

Conclusions

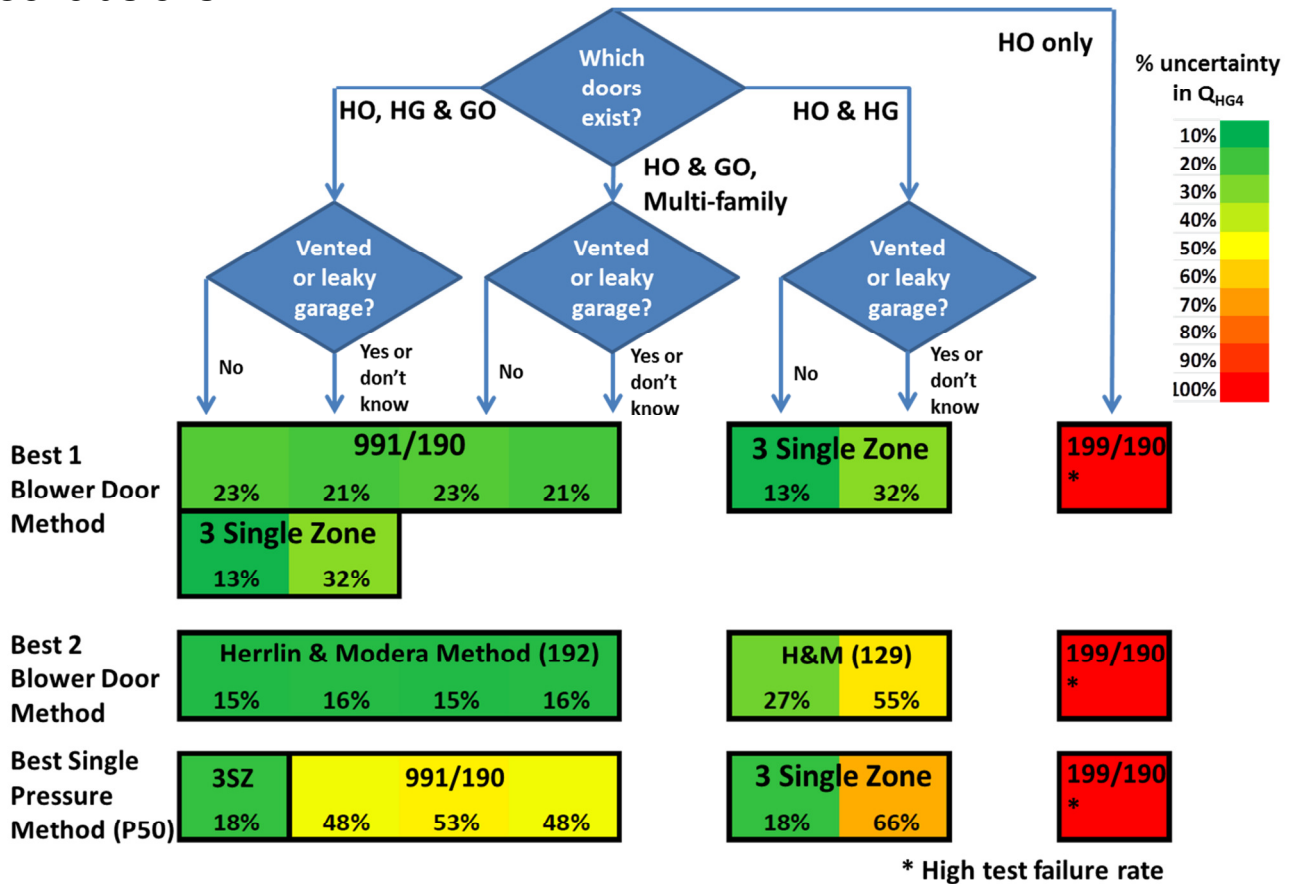


Figure 40: Decision tree for choosing single door testing configurations and method. The terms HO, HG, and GO refer to whether doors exist in the house-outdoors, house-garage, and garage-outdoors interfaces. Shading refers to median Q_{HG4} uncertainty from synthesized data analysis, assuming $u(P)=0.5Pa$, $C_{HG}/C_{HO}=0.05$, for the unvented garage case, $C_{GO}/C_{HO} = 0.7$ and for the vented garage case, $C_{GO}/C_{HO} = 8$.

Figure 40 provides a starting point for choosing a testing method, showing the expected uncertainty for each approach. The goal is to guide towards the best choices and give an indication of the impact of making worse choices. This chart does not include the effects of wind, instead using the assumption of $u(P)=0.5Pa$, because the best test choices are not strongly affected by the magnitude of the fluctuations. Walking through the decision chart, the first question to consider in choosing a testing strategy is where it is possible to mount the blower door. Some homes will have doors in the HO, GO, and HG interfaces, but some homes will only have some of these doorways. If it is known that the garage is vented directly to the outdoors (through intentional or unintentional means), this can significantly increase the uncertainty of the best test options. If it is not known whether the garage zone is vented or leaky, it should be assumed that it is. If all doorways are available, the best test option is the 3 Single Zone Method followed by 991/190 if a contractor prefers to only run two test configurations rather than 3. If higher accuracy is desired, or if high fluctuations due to wind are expected, it may desirable to use the Herrlin and Modera (1988) Method. The uncertainty for single pressure station methods are listed

for reference to show the increased uncertainty in results when these tests are used. The chart can be followed the same way if there are HO and HG doorways or HO and GO doorways present. If there is only a doorway in the HO interface to mount the blower door, the only test configuration pair possible is 199/190 which cannot be reliably used to determine the house garage leakage.

In practice, it is difficult to obtain accurate results when the leakage area of one zone is much greater than the other, both because larger uncertainties tend to occur in this scenario and because it is difficult to establish high pressures in the leaky zone. In the discussion of how to determine the leakage between a house and a vented attic, Blasnik and Fitzgerald (1992) suggest temporarily sealing attic vents during testing to improve accuracy. This strategy would also be a quick and straightforward means to improve the accuracy when testing leakage between a house and vented garage, provided the vents are accessible.

In addition to the house-garage leakage question, it is also of interest what is the best method to determine leakage between homes in a multi-family unit or row of townhouses. Using the same type of analysis discussed in this report, the leakage between multiple units could be determined using a single blower door in a series of different configurations. For two connected units with a single shared interface, there are typically doors available connecting each zone to the outside, but not connecting the two units to each other. Thus 991/190 method (or 199/991 if zones are of comparable leakage area) is likely to be the best choice if only one blower door is available.

Key findings are listed below:

The best of the measurement and analysis methods was the method developed by Herrlin and Modera (1988) which uses two blower doors simultaneously to determine the inter-zone leakage to within 16% of Q_{HG4} , over the range of expected conditions for a house and attached garage ($0.05 < C_{HG}/C_{HO} < 0.3$, $0.2 < C_{GO}/C_{HO} < 8$, $0 < u(P) < 2\text{Pa}$).

While there are methods using two blower doors that obtain consistently accurate results, there are also many possible tests that do not give accurate results, so care should be taken to follow recommended testing procedures.

The best methods to determine inter-zone leakage using a single blower door were the 991/190 method and the 3 Single Zone method, which can be used to determine Q_{HG4} to within 30% of its value.

The test configuration selected can have a large impact on the uncertainty of the results. Some pairs performed very poorly and should definitely be avoided. For example, the 991/190 test configuration pair outperforms the 109/199 when the leakage area of the second zone is large ($C_{GO}/C_{HO} > 1$).

The choice of analysis method can reduce uncertainty in the calculation of house-garage leakage significantly. The most rigorous analysis method found was to sample over a range of pressure stations, and then fit C_{HG} , C_{HO} , C_{GO} , n_{HO} , and n_{GO} , while assuming a fixed value for n_{HG} (rather than fitting n_{HG} directly). This assumption allows for good fits for the zone pressure exponents n_{HO} and n_{GO} while requiring a physically reasonable value for the pressure exponent for the relatively smaller inter-zone leakage flow. Making the assumption that n_{HG} is 0.65 (as is done in the 5 and 10 parameter fit) is better than fitting for n_{HG} (6, 12 parameter fit) regardless of how many pressure stations are used. Additionally, the uncertainty can be reduced by fitting a single set of parameters to both pressurization and depressurization data.

The single pressure station approach cannot reliably be used to determine inter-zone leakage due to uncertainty in measured quantities and the pressure exponents in the different interfaces. If the

objective is simply to identify which inter-zone partitions may have the highest leakage flows for air-sealing purposes, using single point testing may be sufficient (Blasnik and Fitzgerald 1992).

Analysis of field data sets confirm a similar level of variation between test methods as was expected from the analysis of synthesized data sets and confirm the assertion that some test pairs provide more consistent results than others.

Limitations and future work

In synthetic data analysis, limitations on blower door power (flow rate) are not considered. In some cases, a more powerful blower door can be used to reach specified pressures, but this equipment is not always available. Some methods will be compromised when tested only over a limited range of pressure stations.

The effect of a mean (or time-varying) pressure offset is not tested in the synthetic data analysis. The authors experience suggests that fitting pressurization and depressurization parameters jointly (or averaging leakage quantities for pressurization and depressurization conditions) tends to reduce the impact of a pressure offset in the data. This has not been explored in this study.

On a related note, the impact of adding the same fluctuations to the pressure differences P_{HO} and P_{HG} was not explored (correlated noise, versus the uncorrelated noise used in the synthesized data analysis).

The methods used here to optimize leakage parameters associated with different wall interfaces could be used to test leakage between more than two zones using multiple configurations of single blower door tests, but this has not been explored in this study.

One of the outcomes of this study was that typically fitting n_{HG} from the data available introduces more uncertainty than assuming $n_{HG}=0.65$. Rather than assuming $n_{HG}=0.65$, it may be more accurate to assume that $n_{HG}=n_{HO}$. Because there are not data available to assess how much n_{HG} typically varies from n_{HO} , it was not possible to explore this hypothesis in this study.

The methods were evaluated here assuming the leakage area associated with the inter-zone partition was a small fraction of the leakage of either zone (here $0.02 < C_{HG}/C_{HO} < 0.3$). If the inter-zone leakage is a larger fraction of the zone leakage, there would likely be less benefit to fixing the pressure exponent of the inter-zone leakage term.

References

- ASHRAE, Standard 62.2-2007: "Ventilation and Acceptable Indoor Air Quality in Low-Rise Residential Buildings", American Society of Heating, Refrigerating and Air-conditioning Engineers, 2007.
- ASTM , Standard E1554 -07 "Standard Test Methods for Determining Air Leakage of Air Distribution Systems by Fan Pressurization", ASTM Book of Standards, American Society of Testing and Materials, 2007.
- ASTM , Standard E1827 - 11 "Standard Test Methods for Determining Airtightness of Buildings Using an Orifice Blower Door", ASTM Book of Standards, American Society of Testing and Materials, 2011.

- ASTM, Standard E779-10, "Test Method for Determining Air Leakage by Fan Pressurization", ASTM Book of Standards, American Society of Testing and Materials, Vol. 4 (11), 2010. .
- ASTM, Standard E779-99, "Test Method for Determining Air Leakage by Fan Pressurization", ASTM Book of Standards, American Society of Testing and Materials, 2000.
- American Lung Association, "Health House Builder Guidelines", St. Paul, Minnesota, 2006. Accessed 30 March 2012, <www.healthhouse.org/build/2007-2008HHbuilderguidelines.pdf>.
- Batterman, S., C. Jia, G. Hatzivasilis, "Migration of volatile organic compounds from attached garages to residences: A major exposure source", *Environmental Research*, Vol. 104(2), pp. 224-240, 2007.
- Blasnik, M. and J. Fitzgerald, "In Search of the Missing Leak", *Home Energy*, Vol. 9(6), Nov/Dec 1992.
- BPI, "Envelope Professional Standard", Building Performance Institute, Inc, BPI 104, 2011. Accessed 20 July 2012, <<http://www.bpi.org/>>.
- CMHC, "Air infiltration from attached garages in Canadian Houses", Canada Mortgage and Housing Corporation, Research Highlight Technical Series 01-122, 2001.
- CMHC, "Garage performance testing", Canada Mortgage and Housing Corporation, Research Highlight Technical Series 04-108, 2004.
- Emmerich, S.J., J.E. Gorfain and C. Howard-Reed, "Air and Pollutant Transport from Attached Garages to Residential Living Spaces – Literature Review and Field Tests", *International Journal of Ventilation*. Vol. 2(3), 2003.
- Feustel, H.E., "Measurements of Air Permeability in Multizone Buildings", *Energy and Buildings*, Vol. 14, 1990.
- Finch, G., J. Straube and C. Genge, "Air Leakage Within Multi-Unit Residential Buildings: Testing and Implications for Building Performance", In *Proceedings of the 12th Canadian Conference on Building Science and Technology*, Montreal, Quebec, pp. 529-544, 2009.
- Gay, D.M, "Usage Summary for Selected Optimization Routines", Bell Labs Computing Science Technical Report No. 15, 1990.
- Graham, L.A., L. Noseworthy, D. Fugler, K. O'Leary, D. Karman, and C. Grande, "Contribution of vehicle emissions from an attached garage to residential indoor air pollution levels", *Journal of the Air & Waste Management Association*, Vol. 54(5), 2004.
- Herrlin, M.K. and M.P. Modera, "Analysis of errors for a fan-pressurization technique for measuring inter-zonal air leakage", In *Proceedings of the 9th AIVC Conference: Effective Ventilation*, Vol. 1, pp. 215-232, 1988, LBL-24193.
- Love, J.A. and R.S. Passmore, "Air leakage in existing town houses", Alberta Department of Housing Report, 1985.
- Love, J.A., and R.S. Passmore, "Airtightness testing methods for row housing", *ASHRAE Transactions*, Vol. 93(1), 1987.

- Modera, M.P., R.C. Diamond and J.T. Brunsell, "Improving diagnostics and energy analysis for multifamily buildings: a case study", LBNL Report, LBL-20247, 1986.
- Moore, G. and P. Kaluza, "Indoor air quality & ventilation strategies in new homes in Alaska", Alaska Building Science Network, Anchorage, Alaska, 2002.
- Nylund, P.O. "Tightness and its testing in single and terraced housing." Air Infiltration Instrumentation and Measuring Techniques (proceedings of the First Air Infiltration Centre Conference), 1981.
- NYSERDA, "Simplified Multizone Blower Door Techniques for Multifamily Buildings" New York State Energy Research and Development Authority, Report 95-16, 1995.
- Offermann, F. J., "Ventilation and Indoor Air Quality in New Homes", California Air Resources Board and California Energy Commission, PIER Energy-Related Environmental Research Program. Collaborative Report. CEC-500-2009-085, 2009.
- Orme, M., M.W. Liddament and A. Wilson, "An analysis and data summary of the AIVC's numerical database", Air Infiltration and Ventilation Centre Report, Technical Note AIVC 44, 1994.
- Proskiw, G., "An innovative airtightness test procedure for separating envelope air leakage from interior partition air leakage in multi-zone buildings", Master's Thesis, Concordia University, Montreal, Quebec, Canada, 2007.
- Proskiw, G. and A. Parekh, "A proposed test procedure for separating exterior envelope air leakage from interior partition air leakage", in proceedings: Performance of Exterior Envelopes of Whole Buildings VIII, 2001.
- Reardon, J.T., A.K. Kim, and C.Y. Shaw, "Balanced fan depressurization method for measuring component and overall air leakage in single- and multifamily dwellings", ASHRAE Transactions, Vol. 93(2), 1987.
- RESNET, "RESNET Standard for Performance Testing and Work", Chapter 8, RESNET Standards, 2011. 20 July 2012, <<http://www1.resnet.us/>>.
- Shaw, C.Y., "Methods for conducting small-scale pressurization tests and air leakage data of multi-storey apartment buildings", ASHRAE Transactions, Vol. 86(1), pp. 241-250, 1980.
- Sherman, M., "A Power-Law Formulation of Laminar Flow in Short Pipes", Journal of Fluids Engineering, Vol. 114(4), 1992.
- Sherman M and D. Dickerhoff, "Airtightness of U.S. dwellings", Lawrence Berkeley Laboratory Report, LBL-35700, 1998.
- Sherman, M.H., and W.R. Chan, "Building Airtightness: Research and Practice", LBNL Report No. LBL-53356, 2003.
- Thomas, K.W., E.D. Pellizzari, C.A. Clayton, R.L. Perritt, R.N. Dietz, R.W. Goodrich, W.C. Nelson and L.A. Wallace, "Temporal variability of benzene exposures for residents in several New Jersey homes with attached garages or tobacco smoke", Journal of Exposure Analysis and Environmental Epidemiology, Vol. 3(1), 1993.

- Tsai, P.-Y. and C.P. Weisel, "Penetration of evaporative emissions into a home from an M85-fueled vehicle parked in an attached garage", *Journal of the Air and Waste Management Association*, Vol. 50(3), pp 371-377, 2000.
- Walker, I.S., M.H. Sherman, J. Joh, W. R. Chan, "Applying Large Datasets to Developing a Better Understanding of Air Leakage Measurement in Homes", (in press).
- Wouters, P., D. L'Heureux, P. Voordecker, "Advanced Single Fan Pressurization", AIVC Measurement Techniques Workshop, Koge, Denmark, 1988.

Appendices

Appendix A: Uncertainty in pressure and flow rate measurements

Pressure fluctuations due primarily to wind can have a substantial impact on the ability to use blower door tests to determine the air leakage through the interface between adjacent zones. Local air speed fluctuations can also affect the measured pressure differences and the reference pressure for the calculation of the pressure drop across the blower door fan used to determine the flow rate. In this study, we will assume that there is no mean pressure differences measured, only fluctuations with zero mean (or that any mean pressure difference is subtracted before any calculations). Generally, blower door operators attempt to place the reference pressure measurement in a sheltered location that will minimize fluctuations in the measured pressure difference. While this leads to measurements with less apparent noise, this does not necessarily mean that the measured pressure more accurately represents the mean pressure difference across the building envelope.

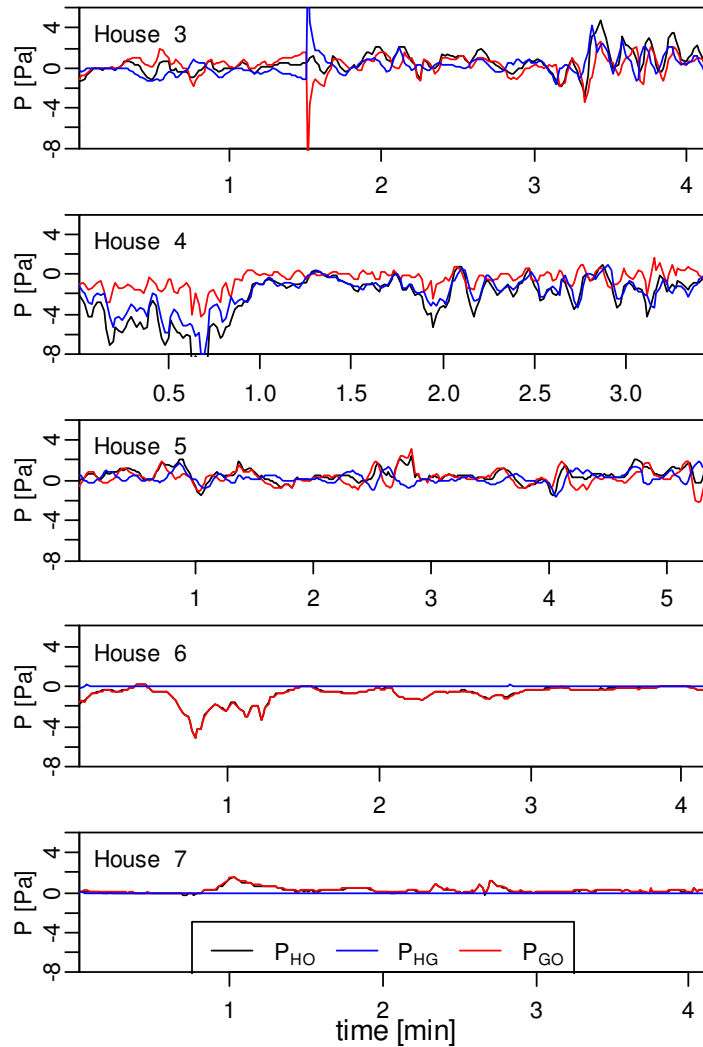


Figure 41: Measured pressure in the house relative to outdoors (P_{HO}) and in the house relative to the garage (P_{HG}), with all doors and windows closed (999 configuration). The calculated pressure difference $P_{GO}=P_{HO}-P_{HG}$ is also shown.

Although the blower door and pressure manometers used are quite accurate under ideal conditions, the interpretation of the measurements obtained can introduce additional uncertainty into the analysis. The pressure across the building envelope can vary substantially due to largely to wind, and because the manometer measures the pressure difference between two points, this measured pressure difference may not be representative of the pressure difference across cracks in the envelope that leads to leakage. Typical pressure fluctuations between the house and outside and house and garage pressure measurement locations can be recorded while all doors are closed and the blower door is off, and this may give an indication of the relative amount of wind present at a particular field site. Such pressure measurements are displayed in Figure 41 for Houses 3-7 from the field data section of this study. Such measured fluctuations are very sensitive to where the outdoor pressure measurement is taken, i.e., what side of the house is it on, how sheltered is the location. Reducing the magnitude of fluctuations in the P_{HO} measurement by choosing a sheltered location for the measurement may or may

not give you more accurate results, as the pressure at the sheltered location may be less representative of the pressure at the outside of the cracks in the building envelope. Fluctuations in the pressure and flow rate introduce noise in the data, however these fluctuations typically correspond with real changes in the local pressure differences between the measurement points. The important question is to what extent does the measured pressure difference between two locations correspond with the effective pressure difference across the leakage between the zones.

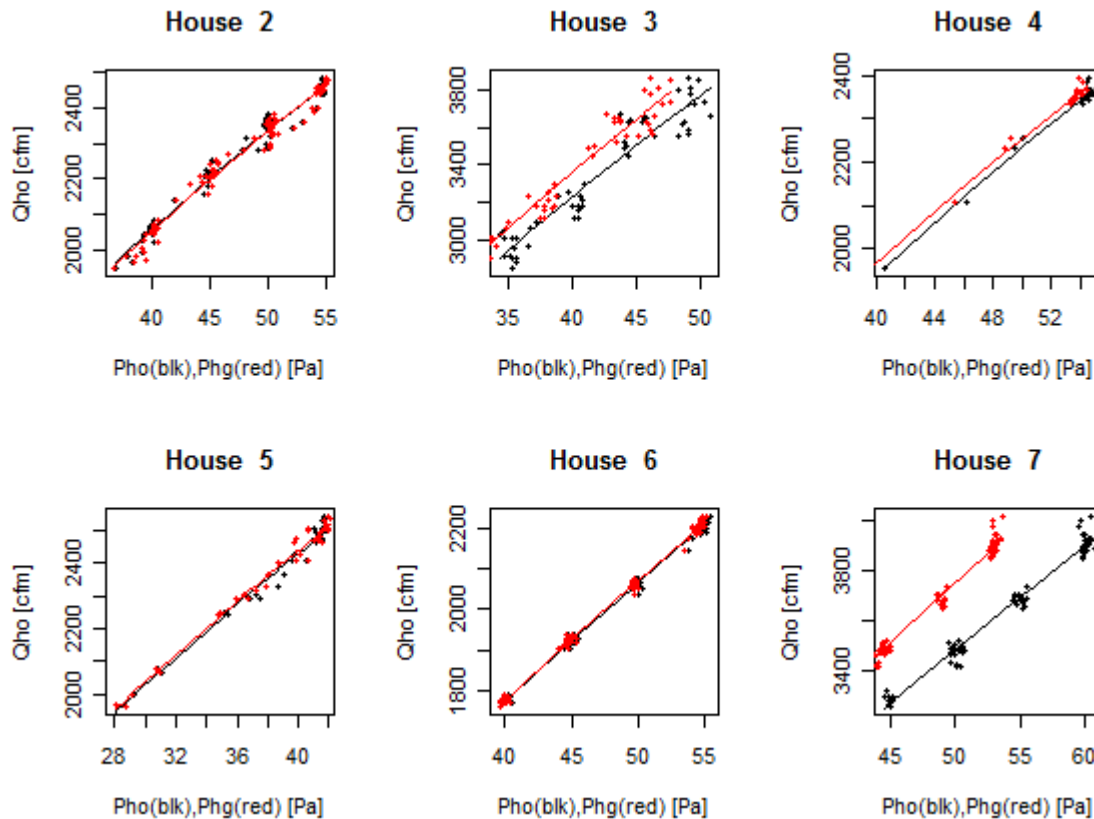


Figure 42: Pressure vs. flow rate measurements for pressurization in configuration 199 used to estimate the fluctuations in P or Q for each field site house. Curves in the form $Q=CP^n$ are fit to the data, and then the distance from the fitted curve is used to estimate the fluctuation of the quantity. Thus fluctuations in P that are correlated with a fluctuation in Q do not contribute to the magnitude of dP estimated with this method.

One method to estimate the impact of pressure and flow rate fluctuations on the uncertainty of the leakage is to look at the correlation between pressure and flow rate measurements. For a single zone, if the model, $Q=CP^n$ is reasonable, then measured points would be expected to fall along this curve (see Figure 42). If such a curve is fitted to measured points over a range of pressures, P, then the average distance from the curve gives an estimate of the variability in the measured values. If a puff of wind comes along and increases the pressure difference P_{HO} , but the blower door also responds to this puff of wind by increasing the flow Q_{HO} , then the resulting data point would still fall on the curve. By limiting the range of measured values of P that the curve is fitted to, the effect of poor model choice or changing pressure exponent is reduced. While the deviation from the model curve is due both to fluctuations in

Q and P, it is difficult to determine the contribution of each, and for now, we will assume that the deviation is due either entirely due fluctuations in P or in Q. While this approach does not make it easy to identify bias error in Q or P due to consistent wind, it does give an indication of the extent to which the measured quantities deviate from the expected form where flow rate is proportional to the pressure difference raised to a power between 0.5 and 1.

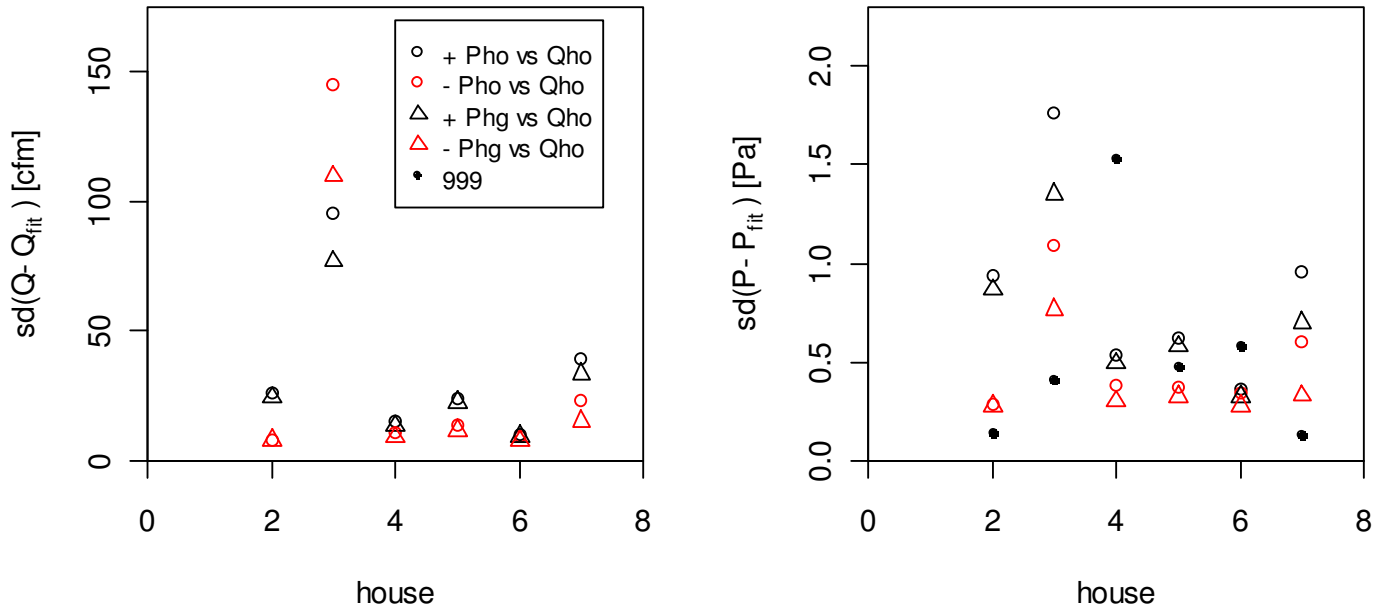


Figure 43: Deviation of measured points from fitted model curve. Left: assuming deviation is entirely due to fluctuations in measured flow rate, Q_{HO} . Right: assuming deviations are entirely due to fluctuations in P_{HO} (or P_{HG}).

The standard deviation of the measured points from a fitted curve is shown in Figure 43 for each of 6 houses. If the fluctuations are attributed to the flow rate measurement, the standard deviation from the model is less than 40cfm (or about 1% of Q_{HO}) for all houses except for House 3 where the wind was high. If the fluctuations are attributed to pressure fluctuations, the standard deviation for P_{HO} is between 0.3Pa and 1Pa, and is typically 10-30% lower for P_{HG} (again excluding House 3).

The difference between pressurization and depressurization test data was used to help partition the fluctuations between the pressure and flow rate measurements. The standard deviation of measurements from the fitted curve for House to Outdoor quantities was typically 1.5 times higher during pressurization tests than in depressurization tests. This difference was likely due to the fact that during pressurization, the reference pressure measurement for the blower door was placed outside of the house, where there is typically more local variation in the pressure due to wind, compared to depressurization tests where the reference pressure was measured indoors. Thus the magnitude of the difference between pressurization and depressurization was attributed to fluctuations in the flow rate measurement. This fluctuation was typically about 0.5% of Q_{HO} in the results shown in Figure 43. The pressure fluctuations measured for P_{HO} with all doors closed and the blower door off (999 configuration) is also shown in Figure 42.

The standard deviation of P_{HO} in the 999 configuration was not necessarily of the same order as the deviation of P from the model curve. These quantities were quite different at Houses 2, 3, 4 and 7, which could either be due to wind speeds and directions changing between when the 999 and 199 data were taken or due to the fact that the location of the pressure measurements was less representative of pressure difference across cracks in the envelope in these cases. From this analysis, it was estimated that about 1/3 of the variability in the measured data comes from fluctuations in Q and 2/3 from fluctuations in P . Deviations in pressure for pressurization tests were between 0.25Pa for the most calm conditions observed and 1.2Pa for the windiest conditions. Based on this partitioning, deviations in the flow rate Q led to uncertainty between 0.2 and 0.8% of the measured flow. The deviations calculated were for data collected at 1s intervals in time. Repeated measurements may reduce the uncertainty, provided the interval between measurements is long relative to the correlation time scale of the wind. The pressure data collected in this study suggested that measurements every 15s could be considered independent. However, the longer the full test took to complete, the more likely it is that there were substantial changes in the wind speed and/or direction. Because a change in the mean wind speed can introduce additional uncertainty, increasing sampling time is unlikely to significantly reduce the overall uncertainty.

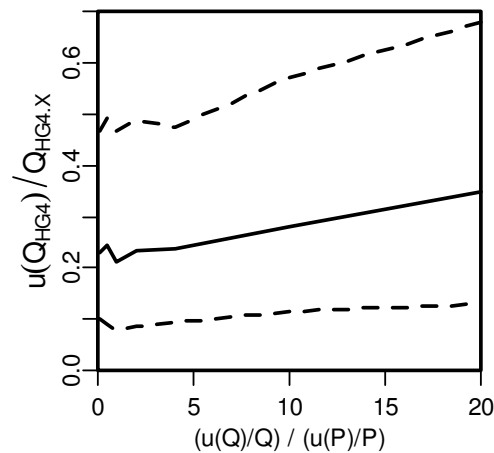


Figure 44: Sensitivity of $u(Q_{HG4})$ to $u(Q)$. Here, $u(P)=0.5$ Pa, and the magnitude of $u(Q)/Q$ relative to $u(P)/P$ was varied between 0.1 and 20. This is using the 190/991 test pair configuration with 5 parameter fitting, $C_{HG}/C_{HO}=0.05$, $C_{GO}/C_{HO}=0.7$, 400 iterations.

It turns out that the overall uncertainty in Q_{HG4} was not very sensitive to $u(Q)$. In Figure 44, the quantity $u(P)$ was held constant, while $u(Q)$ was varied over two orders of magnitude. When the relative magnitude of $u(Q)$ was increased by an order of magnitude from 50% of $u(P)/P$ to 5 times $u(P)/P$, the effect on $u(Q_{HG4})$ was negligible. The dependence of $u(Q_{HG4})$ on $u(P)$ tends to be more pronounced (e.g., Figure 9), so it is important that the assumption for the magnitude of $u(P)$ is reasonable in this type of analysis. However, the estimate of $u(Q)$ appears to be less critical.

Appendix B: Optimization Function

To verify the effectiveness of the optimization routine, the zero-noise limit was tested. With no noise added to the pressure or flow rate synthesized data, the optimization routine identified the 12 parameters used to generate the cases to a very high degree of accuracy (Q_{HG4} accurate to within 10^{-4} to 10^{-6} times the value of Q_{HG4} , for 6 pressure stations, $C_{HG}/C_{HO} = 5\%$, or Q_{HG4} accurate to within 3% of Q_{HG4} for $C_{HG}/C_{HO} = 1\%$, both for the less accurate 199/190 test pair). The choice of optimization function, however, can derail this result. For example, if we minimize the less smooth optimization function:

$$\sum_{i=1}^N |Q_{m,i} - Q_{c,i}| \quad (16)$$

in place of the optimization function in Equation (14), the optimization routine does not determine the original parameters very accurately. In addition to the optimization function, the scaling factors for the optimization of the various parameters affected whether or not an accurate solution was found for a wide range of initial guesses. These scaling factors are used to adjust the step size taken such that incrementally changing each parameter has roughly a unit change in the optimization function. For more information on the optimization method, see Gay (1990). The function call for the optimization routine is provided here:

```
opt =nlminb(parms,Ofun,lower=c(rep(.01, 6),rep(0.4,6)),upper=c(rep(4000,6),rep(1.2,6)),
scale=c(c(.05,.05,.05,.05,.05,.05),rep(100,6)),control=list(abs.tol=1e-12,iter.max=4000,
x.tol=1e-10,rel.tol=1e-12,eval.max=30000,trace=0))}
```

where 'parms' is the vector of 12 parameters: $\{C_{HO+}, C_{HO-}, C_{HG+}, C_{HG-}, C_{GO+}, C_{GO-}, n_{HO+}, n_{HO-}, n_{HG+}, n_{HG-}, n_{GO+}, n_{GO-}\}$, for the 12 Parameter fitting case. 'Ofun' is the optimization function. For the 'nlminb' optimization routine, the most effective scaling parameters were found to be 0.05 for the flow coefficients C_{xy} and 100 for the flow coefficients n_{xy} . To identify these optimal scaling parameters, the zero noise case was run for a range of 27 unique initial guess scenarios (low, intermediate and high initial guesses for C_{HO} , C_{HG} , and C_{GO}).

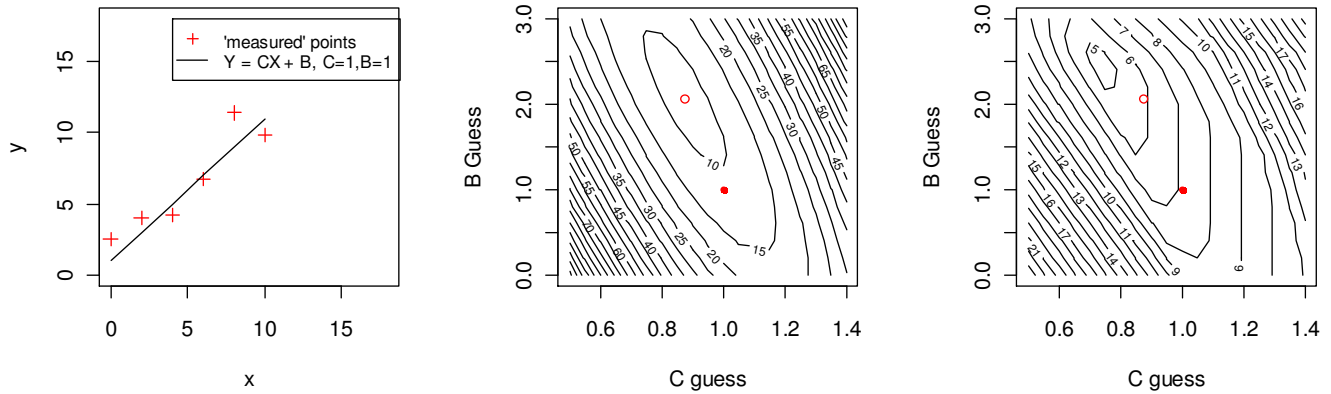


Figure 45: Illustration of how optimization function can affect the smoothness of the parameter space. The left plot shows the equation $Y=X+1$ along with some simulated measured data in which random noise has been added to y to give 'measured' points (x,y) . To find the optimal parameters C and B for a line of form $Y=CX+B$ fitted to the 'measured' data, one can guess values of C and B and calculate the resulting value of the optimization function. In the center plot the optimization function is $f(C,B) = \Sigma(Cx_{\text{measured}}+B - y_{\text{measured}})^2$. This function is calculated over the range C and B . The values of C and B that minimize the optimization function are the parameters that best fit the 'measured' data, according to this optimization function. The right plot uses $f(C,B) = \Sigma|Cx_{\text{measured}}+B - y_{\text{measured}}|$ as the optimization function to minimize. Because of the discontinuity in the function that results as a point crosses from one side of the fitted line to the other, this optimization function produces a less smooth field. While there is still a clear minimum in this simple example, differentiability or smoothness of the optimization function becomes more important as the form of the optimization function becomes more complex and more parameters are fitted.

Appendix C: Bias associated with least squares fitting in a non-linear system

As mentioned in the text, it is suspected that non-linear regression dilution may have contributed to the bias error observed in the results from the multiple pressure station parameter fitting method.

Regression dilution refers to the phenomenon when least-squares fitting is used when the error in the independent variable is large relative to the error in the dependent variable. If this is the case, least squares will tend to under-predict the slope for a linear relationship between x and y . It is relatively straightforward to remove this effect in the linear case, but the effect can be quite difficult to remove in a non-linear case, such as the inter-zone leakage problem.

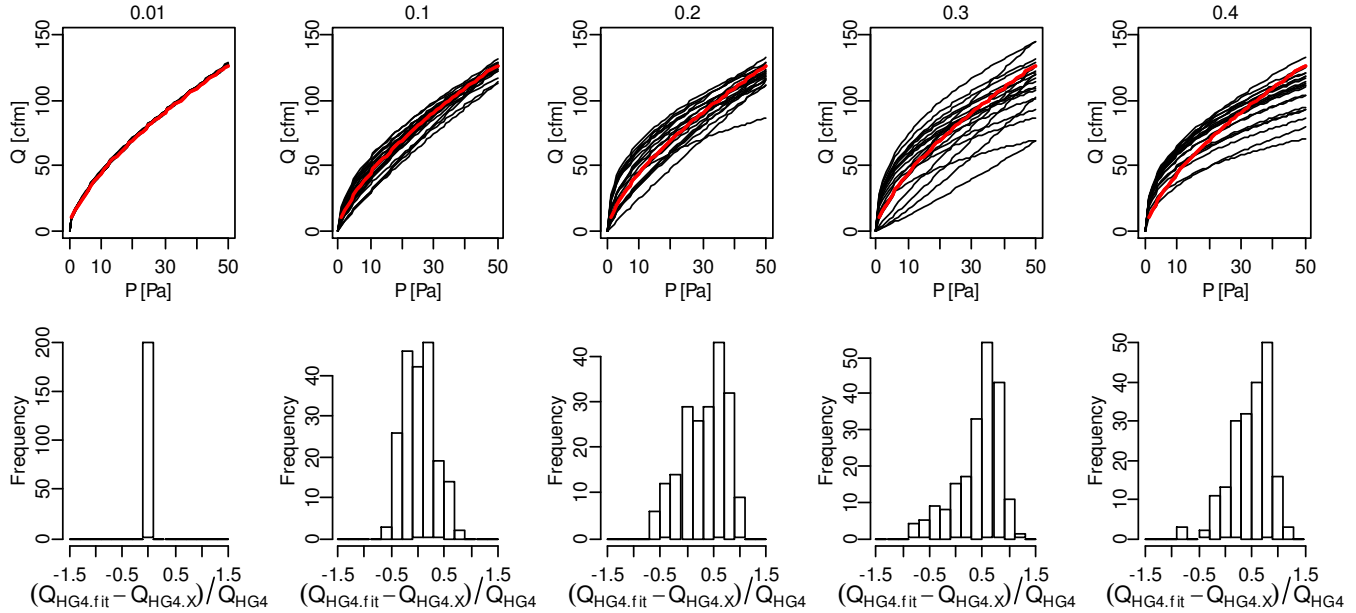


Figure 46: Fitted curves for HG leakage (black) versus actual HG leakage (red), with $u(P)$ and $u(Q)$ as the only sources of uncertainty, with parameters fit using the 6 parameter method. The top row shows the curves fit in 20 iterations and the bottom row shows a histogram of the % difference between the fitted and exact values of Q_{HG4} from 200 iterations. Here, $C_{HG}/C_{HO}=0.05$, $C_{GO}/C_{HO}=0.7$, and the test pair is 991/190.

To demonstrate this effect for the inter-zone leakage case, simulations were performed where there was no difference between the exact parameters specified for pressurization and depressurization conditions and there was bias included for measurements of P and Q . The only source of uncertainty was the random fluctuations added to P and Q . In the limit of no noise added, the exact solution was found. As the noise level was increased, there was increased variability in the results, but there was also a bias in the difference between the fitted and exact leakage flow. Figure 46 shows that as the uncertainty in P is increased, the fitted curve systematically over-predicts the exact curve. Simulations with large numbers of pressure stations confirm this result. This is consistent with the effects of regression dilution. The direction of the shift depends on the test configurations used. At noise levels of interest, i.e., $0.1 < u(P) < 1$, the bias error is of the order of the variation between iterations, suggesting that if we can remove the bias, we may be able to reduce uncertainty by about a factor of 2. While this effect is clearly visible, it is not clear how to correct the analysis for this effect.

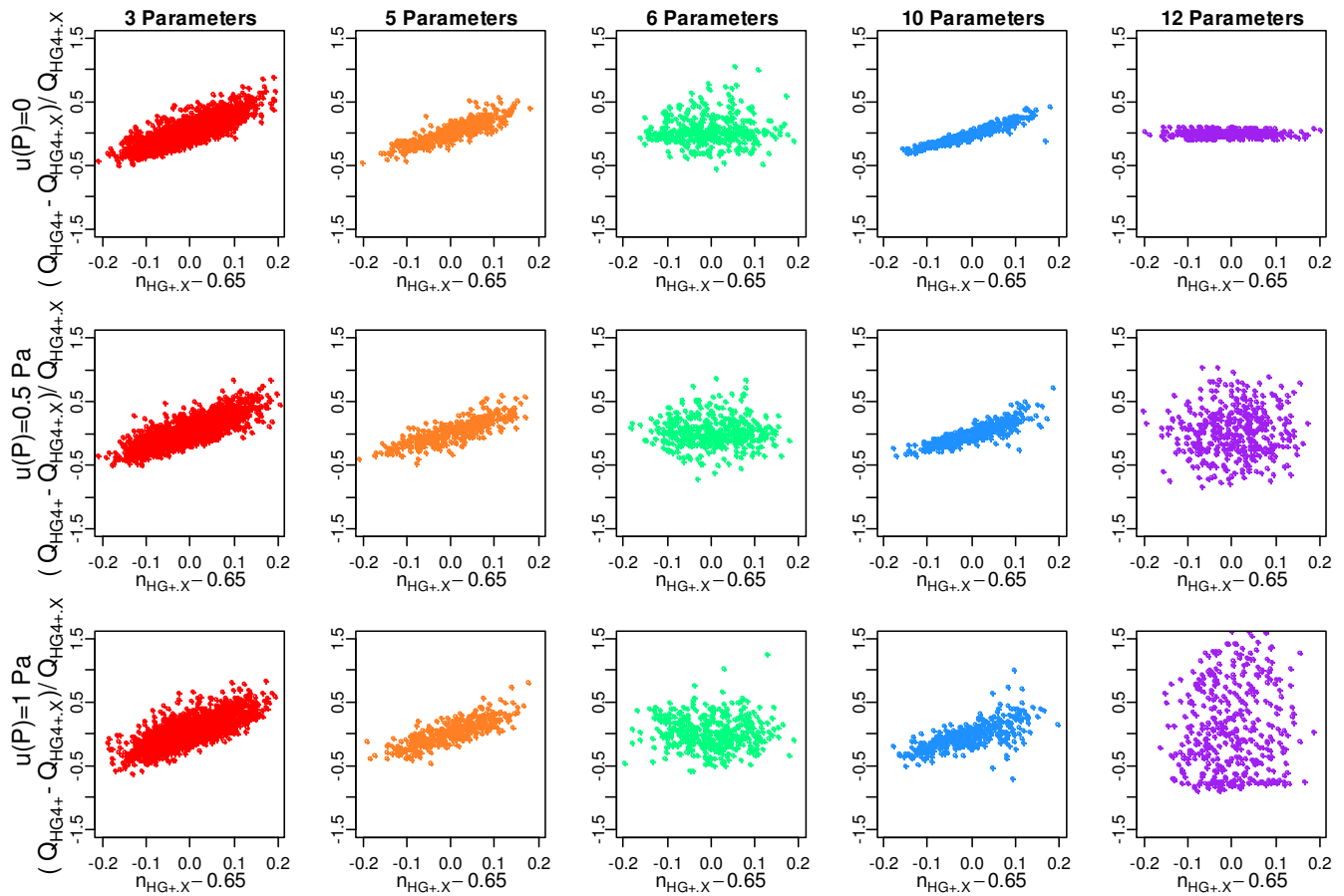


Figure 47: Correlation between the offset in the pressure exponent and the difference between the fitted and exact leakage $Q_{HG4+} - Q_{HG4+X}$. The value of $u(P)$ is 0 for the top row, 0.5Pa for the middle row and 1Pa for the bottom row. $C_{HG}/C_{HO}=0.3$ and $C_{GO}/C_{HO}=0.7$ for test configuration pair 199/091.

The effect of regression dilution is clear when the random fluctuations are the only source of uncertainty included, but it is also possible to see this effect under the standard set of assumptions used in the synthesized data analysis.

When a fixed value is assumed for n_{HG} (typically 0.65), this assumption can introduce uncertainty if the exact value of n_{HG} is not 0.65. Figure 47 shows that the difference between the fitted and exact leakage was correlated with the offset the exact value of n_{HG} for pressurization and 0.65. These quantities were correlated here for the 3, 5 and 10 parameter fitting methods where $n_{HG}=0.65$ was assumed and uncorrelated for the 6 and 12 parameter fitting methods where n_{HG} is fit directly. When the $u(P)$ increases, there was more scatter in the data, although the trend was still apparent. Even when $u(P)=1Pa$, the offset in n_{HG} was the dominant source of uncertainty in Q_{HG4} . Bias in the result due to regression dilution was not significant relative to these other sources of uncertainty.

When the inter-zone leakage becomes smaller, the magnitude of the fluctuation $u(P)$ becomes larger relative to critical pressure differences in the problem. For example in the 199 test, as C_{HG}/C_{HO} becomes

small, P_{HG} approaches P_{HO} , and thus the fluctuations $u(P)$ make the inter-zone leakage parameters increasingly difficult to resolve.

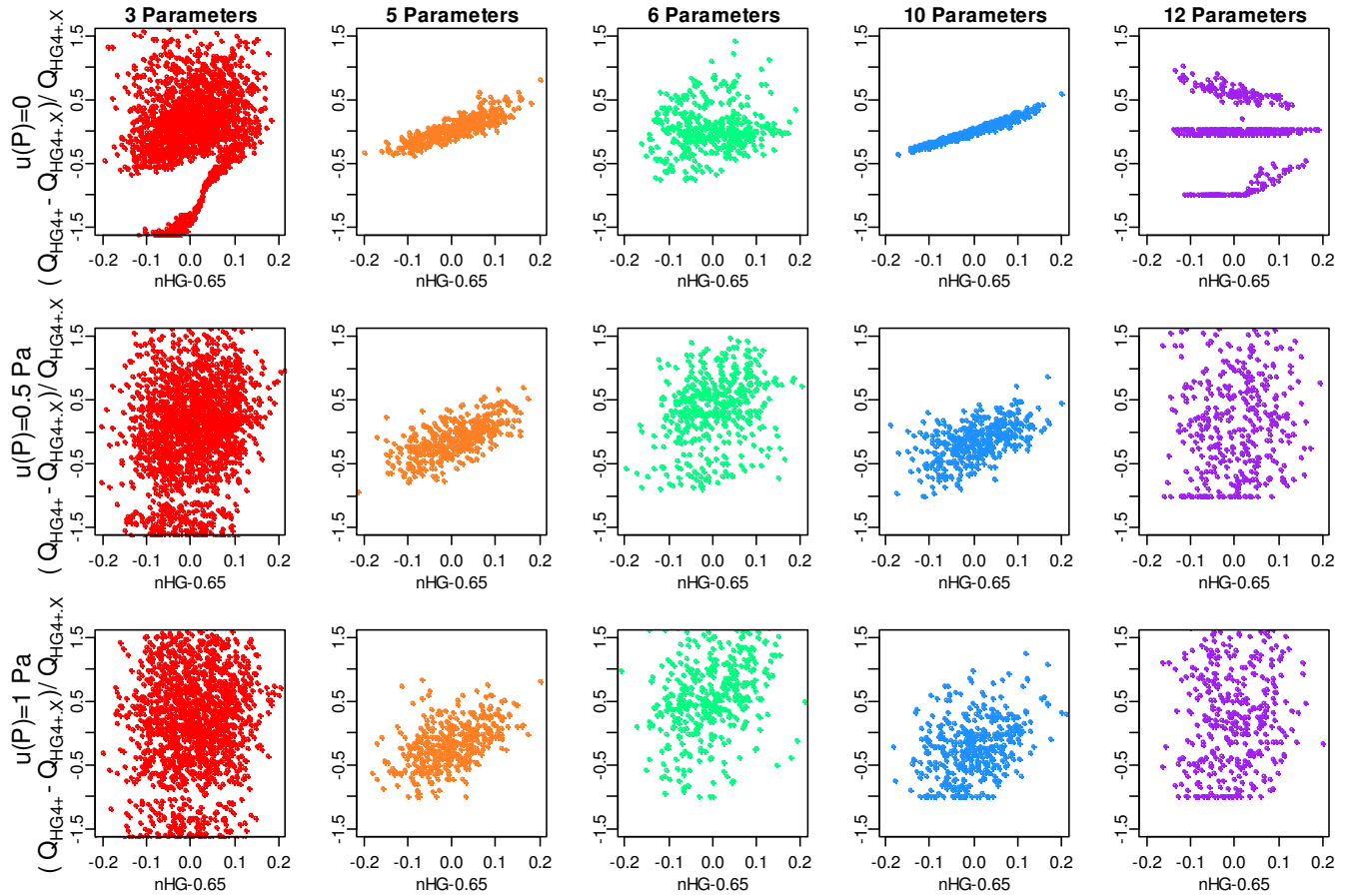


Figure 48: Case from Figure 47 except $C_{HG}/C_{HO}=0.05$. Correlation between the offset in the pressure exponent and the difference between the fitted and exact leakage $Q_{HG4+}-Q_{HG4+.X}$. The value of $u(P)$ is 0 for the top row, 0.5Pa for the middle row and 1Pa for the bottom row. $C_{GO}/C_{HO}=0.7$ for test configuration pair 199/091.

Figure 48 shows the results for the same scenario as in Figure 47, except the inter-zone leakage was reduced: $C_{HG}/C_{HO}=0.05$. In this case, the fluctuations in the pressure were large relative to the pressure differences of interest in the 199 testing. In this case, the variation between tests was large relative to the trend with $n_{HG}-0.65$ when $u(P) \geq 0.5$. For the 6 and 12 parameter fitting methods especially, the cluster of points shifted up as $u(P)$ increased, consistent with the regression dilution effect discussed earlier. This effect was much less pronounced with the 5 and 10 parameter methods, so even with the additional uncertainty introduced by assuming $n_{HG}=0.65$, the overall uncertainty is reduced for these methods.

Appendix D: Leakage testing in Under-Floor Air Distribution Systems

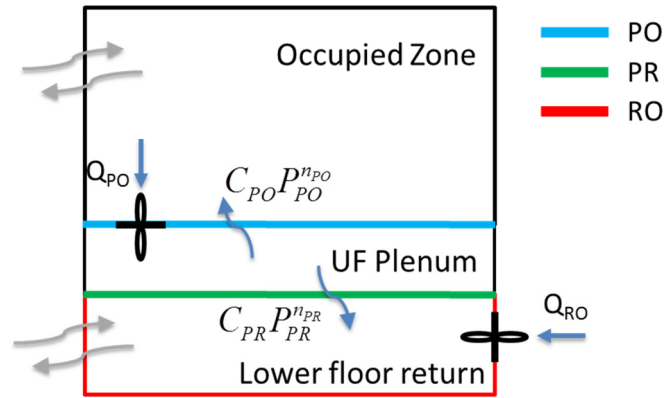


Figure 49: Schematic of fan pressurization testing of an under-floor air distribution system.

Similar methods to those outlined in the main text can be applied to determine the leakage from the under-floor plenum in an under-air distribution (UFAD) system. To test the leakage from the under-floor plenum, vents between the plenum and the occupied zones are sealed and then the plenum zone is pressurized using a blower door. As illustrated in Figure 49, the dominant leakage paths from the plenum are thought to be from the plenum to the occupied zone (PO) and from the plenum to the lower floor return duct below (PR), and leakage from the plenum to the outdoors is thought to be minimal. Here, the plenum can be pressurized using a blower door and the lower floor return pressure can be altered by turning off or on the return duct fan. This leads to testing conditions analogous to the 192 configuration, where the objective is to determine the leakage between the plenum and the occupied zone as well as the leakage between the plenum and the lower floor return. Because the under-floor plenum is largely removed from the influence of outdoor wind fluctuations, the magnitude of fluctuations in the measured pressure is likely to be smaller in the UFAD case (perhaps 0.2 Pa or less), compared with the single family house case.

By applying control volume analysis to the plenum zone, the resulting equation is:

$$Q_{PO} = C_{PO}P_{PO}^{n_{PO}} + C_{PR}P_{PR}^{n_{PR}} \quad (17)$$

By varying P_{PO} and P_{PR} , the leakage parameters for the PO and PR interface can be determined. In field testing of UFAD systems, the pressure, P_{PO} was pressurized to between 0 and 50 Pa, and the pressure between the lower floor return (P_{RO}) was either 0 Pa or 10Pa, as shown in Figure 50(a). Unlike in the 192 configuration testing of the house-garage system, the control volume equation applied to the second zone is not included here, because the leakage between the lower floor return and the occupied zone below is not of concern.

To quantify the uncertainty associated with testing the UFAD plenum in this way, the synthesized data analysis developed in the main text was applied, using typical parameters for this case. Here, pressurization conditions only were tested, as the plenum is typically only pressurized during operation. Because neither the PO or PR leakage is necessarily much smaller than the other in this case, both pressure exponents n_{PO} and n_{PR} were fit directly in the simulations (rather than assuming $n=0.65$).

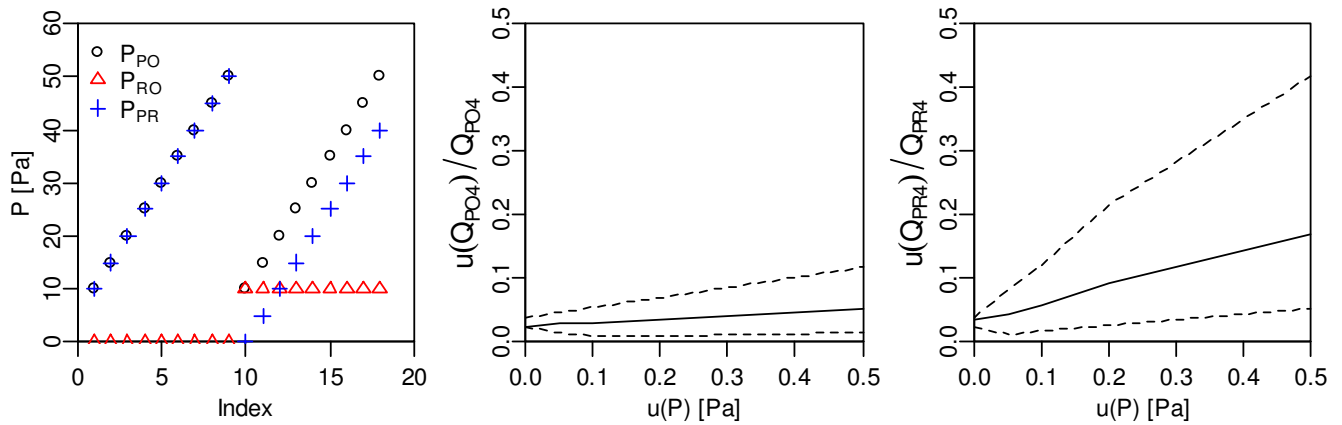


Figure 50: In (a), pressures tested, (b) & (c): uncertainty in the leakage from plenum to occupied zone and plenum to return duct. Here exact leakage parameters were based on field test data: $C_{PO} = 600$, $C_{PR}/C_{PO} = 0.3$, $n_{\text{mean}}=0.65$, 1000 iterations.

The results from the synthesized data analysis for parameters typical of a UFAD system are shown in Figure 50(b) and (c). Even though the pressure in the second zone, P_{RO} only had two values, the uncertainty resulting from this testing method is quite low: 10% or less at the expected noise level of $u(P)=0.2$ Pa. The uncertainty is greater for the pathway from the plenum with smaller leakage area (in this example, that is from the plenum to the lower floor return). If one leakage path from the plenum is much smaller than the other, it may be advantageous to fix the pressure exponent for the smaller leakage path in the parameter fitting. Leakage to flow paths not included in the model described here could lead to additional uncertainty. In general, it appeared that this testing method provided an accurate method to test the leakage from the under-floor plenum.